UTILITY OF PHOSPHATIDYLINOSITOL 3-KINASE INHIBITORS IN GASTROINTESTINAL CANCER

CHONG MEI LING

NATIONAL UNIVERSITY OF SINGAPORE

2014

UTILITY OF PHOSPHATIDYLINOSITOL 3-KINASE INHIBITORS IN GASTROINTESTINAL CANCER

CHONG MEI LING

(B.Sc, HONS.), University of Auckland

A THESIS SUBMITTED

FOR THE DEGREE OF DOCTOR OF PHILOSOPHY

NUS GRADUATE SCHOOL FOR INTEGRATIVE SCIENCES AND ENGINEERING

NATIONAL UNIVERSITY OF SINGAPORE

2014

Declaration

I hereby declare that this thesis is my original work and it has been written by me in its entirety.

I have duly acknowledged all the sources of information which have been used in the thesis.

This thesis has also not been submitted for any degree in any university previously.

_____

Chong Mei Ling

January 30, 2015

ACKNOWLEDGEMENTS

My greatest gratitude goes to my supervisors, A/Prof Richie Soong who has given me much freedom to pursue various ideologies throughout the course of my PhD. It is only with their full support that I am able to complete my PhD with ease. I have to thank them for constantly reviewing my work progressively and giving critical advice throughout the whole course of study.

I would also like to take this opportunity to thank W/Prof Barry Iacopetta for his constant encouragement and advice. I thank him not only for sharing his ideas and experiences academically but also for his help in reviewing my thesis.

I would also like to specially thank my co-supervisor, Prof. Yoshiaki Ito for his advice and support. My greatest appreciation goes to NGS for providing me the scholarship throughout my PhD. Also, I would like to thank my thesis committee member, A/Prof Lim Yoon Pin and Dr Koichi Okumura for their support throughout my PhD study.

In addition, I would like to express my sincere thanks to Dr Bhaskar Bhattacharya for always sharing constructive advice and experiences with me. I thank him for his guidance and assistance throughout my PhD. I would also like to thank to Bayer HealthCare for providing PI3K inhibitors.

Many thanks go to all my fellow colleagues and friends at CSI for their continuous support and assistance both academically and emotionally through this course. I truly appreciate the close friendship I have built with them thus far.

Lastly, it would not be possible if not for the emotional care and moral support that I have received from my beloved family members. It is with their utmost trust and personal sacrifices that made it possible to reach the endpoint of my PhD. I truly believe I am always in their prayers and they are also in mine.

Table of Contents

STATEMENT OF CANDIDATE CONTRIBUTION

The thesis contains published work and/or work prepared for publication, some of which has been co-authored. The bibliographical details of the work and where it appears in the thesis are outlined below.

Chong, M. L., Loh, M., Thakkar, B., Pang, B., Iacopetta, B. and Soong, R. (2014). Phosphatidylinositol-3-kinase pathway aberrations in gastric and colorectal cancer: Meta-analysis, co-occurrence and ethnic variation. Int J Cancer 134(5): 1232-8.

Chong ML performed all experimental works using clinical samples, drafted the manuscript, analysed and interpreted the data.

Chong, M.L., Bhattacharya, B. and Soong, R. Identification of potential biomarkers for PI3K inhibitors in GC and CRC cell lines (in preparation for publication).

Chong ML performed the IC_{50} screening, executed functional analysis, analysed and interpreted the data.

Other publications during PhD candidature are outlined below.

Davids, M. S., Charlton, A., Ng, S. S., Chong, M. L., Laubscher, K., Dar, M., et al. (2009). Response to a novel multitargeted tyrosine kinase inhibitor pazopanib in metastatic Merkel cell carcinoma. J Clin Oncol 27(26): e97-100.

Dickgreber, N., Farrand, K. J., van Panhuys, N., Knight, D. A., McKee, S. J., Chong, M. L., et al. (2012). Immature murine NKT cells pass through a stage of developmentally programmed innate IL-4 secretion. J Leukoc Biol 92(5): 999-1009.

Pang, B., Ong, C. W., Chong, M. L., Muliana-Ismail, T., Soong, R. and Salto-Tellez, M. (2012). KRAS mutation analysis in a complex molecular diagnostic referral practice: the need for test redundancy. Pathology 44(7): 655-7.

Chong ML, Ku CS, Wu MC, Soong R. Characterising Somatic Mutations in Cancer Genome by Means of Next-generation Sequencing (2012). eLS book chapter (a0023379).

SUMMARY

Gastric cancer (GC) and colorectal cancer (CRC) are two of the top ten cancers and leading causes of death worldwide, and in Singapore. Inhibition of the phosphatidylinositol-3-kinase (PI3K) signalling pathway is a cancer treatment strategy that has entered into clinical trials for GC and CRC patients. Based on previous experience in targeted therapy development, ethnic differences, co-occurrence pattern of pathway aberrations and predictive biomarkers are important in determining the success of drug therapy. The aims of this study were 1) to characterise inter-ethnic frequencies and co-occurrence patterns of prominent PI3K pathway aberrations in GC and CRC, and 2) to identify predictive biomarkers for PI3K inhibitors in GC and CRC cells.

A meta-analysis was first performed on the frequency of genetic (*PIK3CA* mutation, *PIK3CA* amplification, *PTEN* deletion) and protein expression (high PI3K, PTEN loss, high pAkt) aberrations in the PI3K pathway in GC and CRC. Sanger sequencing, quantitative PCR (qPCR) and immunohistochemistry were also performed to investigate the co-occurrence of these aberrations. OncoCarta analysis and RNA-sequencing were used to identify potential predictive biomarkers for PI3K inhibitors. *In-vitro* manipulations and interrogations were performed to investigate the role of candidates in determining PI3K inhibitor sensitivity.

The meta-analysis indicated that East Asian and Caucasian GC patients differ significantly in the frequencies of *PIK3CA* exon 9 and exon 20 mutations

(7% vs. 15% respectively), *PTEN* deletion (21% vs. 4%) and PTEN loss (47% vs 78%), while CRC patients differed for PTEN loss (57% vs. 26%). High study heterogeneity (I^2>80) was observed for all aberrations except *PIK3CA* mutations. Analysis of tumours from East Asian patients revealed significant differences between GC (n=79) and CRC (n=116) for the frequencies of *PIK3CA* amplification (46% vs. 4%) and PTEN loss (54% vs. 78%). The incidence of GC cases with 0, 1, 2 and 3 concurrent aberrations was 14%, 52%, 27% and 8% respectively, while for CRC it was 10%, 60%, 25% and 4% respectively. OncoCarta analysis revealed that *PIK3CA* mutation (p=0.001) was associated with increased sensitivity to PI3K inhibitors, and *KRAS* (G12V) mutation (p=0.004) was associated with decreased sensitivity to PI3K inhibitor in CRC cell lines. To identify biomarkers for *PIK3CA* wildtype cell lines, RNA-sequencing was performed and high expression of *IGFBP3* was identified as a top candidate associated with increased sensitivity to PI3K inhibitors. siRNA experiments confirmed the role of *IGFBP3* in mediating sensitivity to PI3K inhibition.

In conclusion, this study consolidates knowledge on the frequency, co-occurrence and clinical relevance of PI3K pathway aberrations in GC and CRC. Up to 86% of GC and 90% of CRC have at least one aberration in the PI3K pathway, and there are significant differences in the frequencies of these aberrations according to cancer type and ethnicity. Moreover, this study has helped to reveal novel candidate biomarkers for GC and CRC that could assist in improving the efficacy of PI3K inhibitors.

LIST OF TABLES

LIST OF FIGURES

LIST OF ABBREVIATIONS

5-FU	5-fluorouracil
ABD	Adaptor binding domain
ACTB	Beta-actin
AKT	v-akt murine thymoma viral oncogene homolog
ALL	Acute lymphoblastic leukemia
AML	Acute myeloid leukemia
APC	Adenomatous polyposis coli
ATCC	American Type Culture Collection
ATP	Adenosyl-triphosphate
Bcr-Abl	Breakpoint cluster region-c-abl oncogene
BRAF	v-raf murine sarcoma viral oncogene homolog B
C2	Complement component 2
CDH1	E-cadherin
CDH3	P-cadherin
CDK	Cyclin-dependent kinase
cDNA	Complementary DNA
CLDN1	Claudin 1
CLL	Chronic lymphocytic leukemia
CLS	Cell lines Service GmbH
CML	Chronic myeloid leukemia
CRC	Colorectal cancer
CTNNB1	Catenin (cadherin-associated protein), beta 1
DAVID	Database for Annotation, Visualization and Integrated Discovery
EBER1	EBV-encoded small ribonucleic acid 1
EBV	Epstein-Barr virus
EGF	Epidermal growth factor
EGFR	Epidermal growth factor receptor
ENHO	Energy homeostasis associated
ERK	Extracellular signal-regulated kinases
FBX4	F-box protein 4
FBXW7	F-box and WD repeat domain containing 7
FFPE	Formalin-fixed and paraffin embedded
FGFR2	Fibroblast growth factor receptor 2
FISH	Fluorescent *in situ* hybridization
FLT3	Fms-related tyrosine kinase 3
GAB1	GRB2-associated binding protein 1
GAB2	GRB2-associated binding protein 2
GAP	GTPase-activating protein

GAPDH	Glyceraldehyde-3-phosphate dehydrogenase
GBM	Glioblastoma multiforme
GC	Gastric cancer
GIST	Gastrointestinal stromal tumour
GNAQ	Guanine nucleotide binding protein (G protein)
GSK3	Glycogen synthase kinase-3
GDP	Guanosine-5'-diphosphate
GTP	Guanosine-5'-triphosphate
H.pylori	*Helicobacter pylori*
HER2	Human epidermal growth factor receptor 2
HLA-DRB1	Major histocompatibility complex, class II, DR beta 1
HRAS	v-Ha-ras Harvey rat sarcoma viral oncogene homolog
ICAM1	Intercellular adhesion molecule 1
IGF	Insulin-like growth factor
IGFBP1	Insulin-like growth factor binding protein 1
IGFBP3	Insulin-like growth factor binding protein 3
IGFBP4	Insulin-like growth factor binding protein 4
IGF-IR	Insulin-like growth factor-I receptor
IR	Insulin receptor
IRS	Insulin receptor substrate
ISH	*in situ* hybridization
iSH2	Inter-SH2
JAK2	Janus kinase 2
JCRB	Japanese Collection of Research Bioresources
KEGG	Kyoto Encyclopedia of Genes and Genomes
KIT	v-*kit* Hardy-Zuckerman 4 feline sarcoma viral oncogene homolog
KRAS	v-Ki-ras2 Kirsten rat sarcoma viral oncogene homolog
MALDI-TOF	Matrix-assisted laser desorption/ionization-time of flight
MAP2K1	Mitogen-activated protein kinase kinase 1
MAP2K2	Mitogen-activated protein kinase kinase 2
MCL	Mantle cell lymphoma
MEK	Mitogen-activated protein kinase kinase
MET	Met proto-oncogene
mTORC2	Mammalian target of rapamycin mTOR complex 2
NHLs	Non-Hodgkin lymphomas
NRAS	Neuroblastoma RAS viral (v-ras) oncogene homolog
NSCLC	Non-small cell lung cancer
PAK1	p21-activated kinase 1
PDGF	Platelet derived growth factor
PDK1	Serine/threonine kinases 3-phosphoinositide-dependent kinase 1
PH	Pleckstrin-homology
PI3K	Phosphoinositide 3-kinase
PIK3CA	Phosphatidylinositol-4,5-bisphosphate 3-kinase, catalytic subunit alpha

PIK3CB	Phosphatidylinositol-4,5-bisphosphate 3-kinase, catalytic subunit beta
PIK3CD	Phosphatidylinositol-4,5-bisphosphate 3-kinase, catalytic subunit delta
PIK3CG	Phosphatidylinositol-4,5-bisphosphate 3-kinase, catalytic subunit gamma
PIK3R1	Phosphoinositide-3-kinase, regulatory subunit 1 (alpha)
PIP_2	Phosphatidylinositol-4,5-biphosphate
PIP_3	Phosphatidylinositol (3,4,5)-triphosphate
PKB	Protein kinase B
pNET	Pancreatic neuroendocrine tumours
PTEN	Phosphatase and tensin homolog
PTPN11	Protein tyrosine phosphatase, non-receptor type 11
qPCR	Quantitative-PCR
RBD	Ras-binding domain
RCC	Renal cell carcinoma
RET	Ret proto-oncogene
RIN	RNA integrity number
SAP	Shrimp alkaline phosphatase
SCCHN	Squamous cell carcinoma head and neck cancers
SDC1	Syndecan 1
SH3	Src homology 3
SOS1	Son Of Sevenless Homolog 1
TCC	Transitional cell carcinoma
TP53	Tumor protein p53
VEGF-A	Vascular endothelial growth factor-A
Yonsei CC	Yonsei Cancer Centre

1 Introduction

1.1 Gastric cancer

Gastric cancer (GC) is the third leading cause of cancer death in the world (GLOBOCAN 2012: Estimated Cancer Incidence, Mortality and Prevalence Worldwide in 2012). Almost one million new cases of GC were estimated to have occurred in 2012 (952,000 cases, 6.8% of the total), making it the fifth most common malignancy in the world, after cancers of the lung, breast, colorectum and prostate. More than 70% of cases (677,000 cases) occur in developing countries (456,000 in men, 221,000 in women), and half the world total occurs in Eastern Asia (mainly in China). In Singapore, between 2009 to 2013, GC was the fourth most common cause of cancer death in men (913, 6.7% of the total) and the fifth most common cause of cancer death in women (690, 6.1% of the total) (Singapore Cancer Registry Interim Annual Registry Report Trends in Cancer Incidence in Singapore 2009-2013). It is estimated that there will be 22,200 new cases in the U.S. in 2014 and 10,990 GC-related deaths in the same year (SEER Stat Fact Sheets: Stomach Cancer).

The majority of GCs are adenocarcinomas which can be divided histologically into an intestinal or diffuse type and anatomically into cardia or noncardia cancers. Pathogenesis and prognosis differ based on GC subtype. Intestinal-type GC, for example, is more common in Asia and tends to be associated with *Helicobacter pylori* (*H.pylori*) infection (Yakirevich and Resnick, 2013). *H.pylori*, which colonizes the human stomach, is the strongest known risk

factor for gastric malignancies, in particular non-cardia gastric adenocarcinoma (cancer in all areas of the stomach, except for the top portion where it joins the oesophagus) and mucosa-associated lymphoid tissue lymphoma (Israel and Peek, 2010). It is also estimated that *H.pylori* accounts for ~80% of non-cardia GC which is potentially preventable (Helicobacter and Cancer Collaborative, 2001).

Epstein–Barr virus (EBV) is a herpes virus that infects most humans in adulthood. EBV is associated with several human malignancies, such as Burkitt's lymphoma, Hodgkin's lymphoma, nasopharyngeal carcinoma and GC. In 1990, EBV genomes were detected in GCs using polymerase chain reaction (Burke *et al.*, 1990) and *in situ* hybridization (ISH) for EBV-encoded small ribonucleic acid 1 (EBER1) (Liu *et al.*, 1995). It is estimated that EBV-associated gastric cancer comprises about 1.3–20.7% of all GCs worldwide (Shibata and Weiss, 1992; Hsieh *et al.*, 1998; Morewaya *et al.*, 2004). A characteristic feature of EBV-associated gastric cancer is lymphoepithelioma-like carcinoma, which presents as diffuse-type histology with lymphoid infiltration. Diffuse-type GC seems to have a worse prognosis (Miyahara *et al.*, 2007; Yamashita *et al.*, 2009).

Currently, there is no optimal treatment for advanced GC. In order to improve outcomes, it is critical to understand the molecular pathogenesis of GC (Wong and Yau, 2012) and to identify biomarkers of prognostic or predictive significance. Ideally, physicians will be able to tailor therapy toward individual patients according to biomarkers suggesting increased likelihood of response, thus improving outcomes for those with GC and sparing patients without these predictive biomarkers from the toxicities of ineffective therapies.

1.2 Colorectal Cancer

Colorectal cancer (CRC) is now the third most common malignant disease in both men and women in Asia. In the Asia-Pacific region, the incidence varies between regions, with high incidence in Australia and Eastern Asia. GLOBOCAN estimation project for 2012 indicated that, the age-specific rates (ASR) incidence for Asia was 13.7 and ASR mortality was 7.2 per 100,000 (GLOBOCAN 2012: Estimated Cancer Incidence, Mortality and Prevalence Worldwide in 2012). Although the incidence and mortality rates of this cancer are still higher in the western world, the ratio of mortality/incidence for Asian regions are higher, indicating poorer survival in Asian countries.

CRC is a heterogeneous disease with three different, but partly overlapping, molecular phenotypes reflecting different forms of DNA instability. The chromosomal instability pathway (CIN) is the most common phenotype, accounting for ~85% of all sporadic CRCs (Lengauer *et al.*, 1997; Hermsen *et al.*, 2002; Nowak *et al.*, 2002). The malignant cells in CIN tumors are typically aneuploid and reveal large-scale chromosomal rearrangements. The microsatellite instability (MSI) phenotype represents ~15% of all CRCs and is caused by various deficiencies in the DNA mismatch-repair system, leading to a large increase in the mutation rate (Shibata *et al.*, 1994; Lothe, 1997). Cancers with the CpG island methylator phenotype (CIMP) exhibit aberrant DNA methylation, leading to concordant promoter hypermethylation of multiple genes (Issa, 2004).

Despite the established relationship between *H.pylori* and GC, the association between *H.pylori* and CRC is much less clear. Using PCR, one study

found that 1.2% of malignant colorectal tissues were positive for *H.pylori*, whereas 6.0% of normal tissues were positive (Bulajic *et al.,* 2007). Therefore, the authors concluded that *H.pylori* are not important in the pathogenesis of CRC. However, two other studies that used PCR to detect *H.pylori* in colorectal neoplasms indicated that a much greater proportion of these tissues were positive for *H.pylori*: one study detected *H.pylori* DNA in 27% of colorectal adenocarcinoma tissues (Grahn *et al.,* 2005) and another found that detection of *H.pylori* DNA in colorectal tissue was associated with an increased risk of colorectal adenocarcinomas (Jones *et al.,* 2007).

1.3 Molecular aberrations and targeted therapies in GC and CRC

Although surgery and cytotoxic chemotherapy are the main treatment modalities for GC and CRC, drug resistance and lack of specificity are major problems. The past two decades have seen some progress towards the development of "targeted therapies". These therapies are designed to exploit the dependency, or "addiction", of cancer cells on specific signaling pathways or oncogenes. By specifically inhibiting the pathways on which tumour cells are dependent for survival, normal tissues may thus be spared. This should be associated with less side effects and better overall better drug efficacy (Zhukov and Tjulandin, 2008).

A number of molecularly targeted drugs have been developed as a consequence of improved understanding of the molecular aberration in GC and CRC (Figure 1.1). For instance, epidermal growth factor receptor 2 (HER2)

amplification or overexpression is observed in 10-38% (Wong and Yau, 2013) of GC tumour samples and HER2 inhibitors have been developed for GC treatment such as trastuzumab and pertuzumab (Yamashita-Kashima *et al.*, 2011). In the clinic, the combination of trastuzumab and chemotherapy is the standard of care in first line therapy for HER2 positive GC patients (De Vita *et al.*, 2012). Overexpression of epidermal growth factor receptor (EGFR) has also been observed in GC and CRC (Spano *et al.*, 2005; Galizia *et al.*, 2007). Inhibitors that target EGFR (cetuximab and panitumumab) have been approved for the treatment of metastatic colorectal cancer (Bartlett and Chu, 2012). However, EGFR inhibitors are still in clinical trials for GC treatment (Wong and Yau, 2013).

Amplification of met proto-oncogene (*MET*) and fibroblast growth factor receptor 2 (*FGFR2*), mutation of v-raf murine sarcoma viral oncogene homolog B (*BRAF*) and Kirsten rat sarcoma viral oncogene homolog (*KRAS*) have also been reported in GC and CRC (Di Nicolantonio *et al.*, 2010; Deng *et al.*, 2012). Several inhibitors that target MET, FGFR and BRAF are being studied in clinical trials or are in preclinical testing (Mao *et al.*, 2013; Wong and Yau, 2013). Moreover, therapeutics targeting the phosphoinositide 3-kinase (PI3K) pathway are being developed rapidly due to the fact that PI3K is a major downstream effector of receptor tyrosine kinases (RTKs), and the PI3K pathway is activated in GC and CRC (Engelman, 2009).

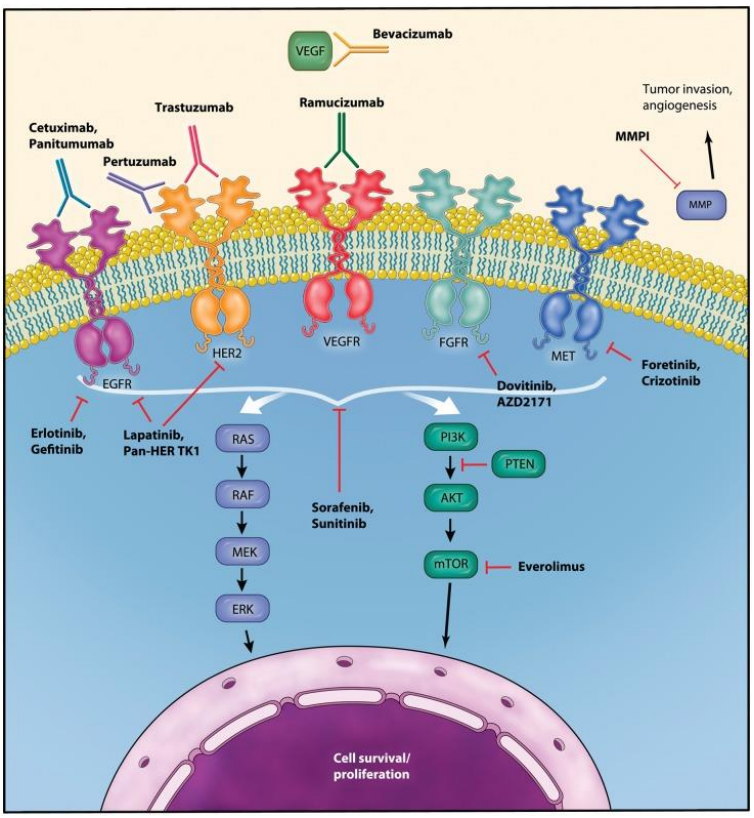

Figure 1.1. Schematic diagram of molecular aberrations and targeted therapies in GC and CRC (Wong and Yau, 2013).

1.1 The phosphoinositide 3-kinase family: structure and function

PI3K is a lipid kinase that phosphorylates phosphatidylinositol (4,5)-biphosphate (PIP_2) to phosphatidylinositol (3,4,5)-triphosphate (PIP_3) (Chalhoub and Baker, 2009). PI3Ks are subdivided into four different classes based on their subunit composition and the substrate specificity for phosphoinositides (Vanhaesebroeck *et al.*, 2001). Class I PI3Ks are further divided into IA and IB on the basis of their mechanism of activation (Stein and Waterfield, 2000).

The class IA group forms a heterodimeric complex consisting of a 110 kDa catalytic subunit and a regulatory subunit. The three catalytic subunits

(p110α, p110β, p110δ) are encoded by *PIK3CA*, *PIK3CB* and *PIK3CD*, respectively. p110α and p110β isoforms are ubiquitously expressed among tissues, whereas p110δ is more restricted to hematopoietic cells (Bader *et al.*, 2005). All class IA PI3Ks contain an N-terminal adaptor binding domain (ABD) followed by a Ras-binding domain (RBD), a C2 domain, a helical domain and a catalytic kinase domain. There are five isoforms of the regulatory subunits of class IA PI3Ks: p85α, p85β, p55γ, p55α and p50α (Foukas and Shepherd, 2004).

Class IB PI3K proteins consist of a catalytic subunit, p110γ (encoded by *PIK3CG*) and a regulatory subunit of which p101 is the most common. Its expression is largely confined to leukocytes (Foukas and Shepherd, 2004). The p110γ subunit is activated by G-protein βγ subunit following stimulation of G-protein coupled receptors (Walker *et al.*, 2000; Shepherd, 2005).

Class II kinase is a large protein (170-210 kDa) characterised by the presence of an N-terminal RBD, a C2 domain, a helical domain, a catalytic domain, a PX domain and a C-terminal C2 domain (Katso *et al.*, 2001). There are three isoforms in mammals and these are products of separate genes: PI3K-C2 α, ß and γ. No regulatory subunits have been identified to date.

The biological function of class III PI3Ks is less well established, although it is thought they can be activated by RTKs such as EGFR and insulin receptor (IR). Moreover, they play an important role in clathrin-mediated vessel trafficking (Williams *et al.*, 2009).

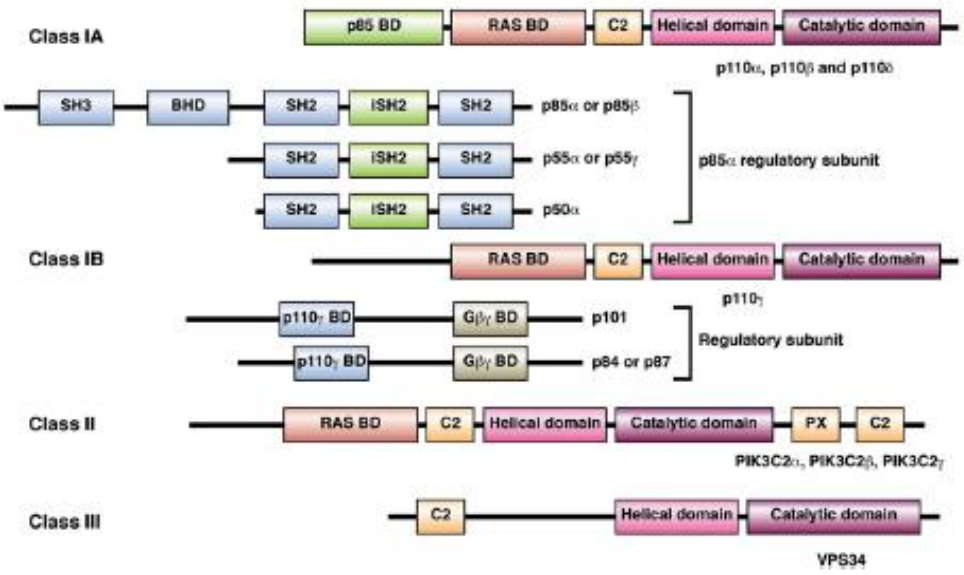

Figure 1.2. Substrate specificity and domain structure of different classes of PI3Ks (Zhang *et al*., 2011)**.**

1.2 RAS/RAF/MEK and PI3K/AKT signalling pathways

RAS is activated in human cancer by a number of different mechanisms, such as mutations in RAS, loss of GTPase-activating protein (GAP) or overexpression of RTKs (Downward, 2003). RAS protein signals through direct interaction with a number of effector enzymes. RAS/RAF/MEK pathway was the first RAS-effector pathway identified. RAS fluctuates between an inactive guanosine-5'-diphosphate (GDP)-bound state and an active guanosine-5'-triphosphate (GTP)-bound state (McCubrey *et al.*, 2007). The RAF family of proteins (Raf-1, A-Raf and B-Raf) are serine/threonine kinases that bind to the effector region of RAS-GTP, thus inducing translocation of the protein to the plasma membrane. RAF proteins are phosphorylated by protein kinases such as protein kinase C (PKC) and bind to 14-3-3 proteins (Fabian *et al.*, 1994; Morrison, 1994; Marais *et al.*, 1995; Avruch *et*

al., 2001). Active RAF phosphorylates MEK which in turn phosphorylates extracellular signal regulated kinases 1 and 2 (ERK1/2) (Crews and Erikson, 1993). ERK phosphorylation promotes homodimerization and translocation of ERK to the nucleus, where they stimulate the activity of different transcription factors, such as p62/Elk-1 and Ets-2 (Marais *et al.*, 1993; Treisman, 1996; Khokhlatchev *et al.*, 1998).

PI3K is another well-characterized downstream effector of RAS. PI3K can also be activated by RTKs. A model for PI3K signalling is shown in Figure 1.3. Binding of ligands such as insulin, platelet derived growth factor (PDGF) and epidermal growth factor (EGF) to RTKs initiates the dimerization of RTKs which then leads to their auto-phosphorylation at tyrosine residues. This allows them to activate class IA PI3K through interaction with the SH2 domain in the regulatory subunit (Cully *et al.*, 2006). Apart from membrane-bound receptors, substrates of RTKs such as insulin receptor substrate (IRS) and GRB2-associated binding protein 1/ GRB2-associated binding protein 2 (GAB1/GAB2) can lead to activation of PI3K. Moreover, class I PI3Ks can be activated by direct binding of p110 to activated RAS, allowing its localization to the membrane and activation of its lipid kinase activity (Rodriguez-Viciana *et al.*, 1994; Katso *et al.*, 2001).

Activated PI3K transduces signals by generating intracellular PIP_3 second messenger. The tumour suppressor, phosphatase and tensin homolog (PTEN), antagonises this reaction by dephosphorylating the 3' position of PIP_3 (Cully *et al.*, 2006). PIP_3 signals are largely localized to the inner leaflet of the plasma membrane (Shepherd, 2005). This allows recruitment of signalling proteins with

pleckstrin-homology (PH) domains to the membrane by directly binding to PIP_3, including serine/threonine kinases 3-phosphoinositide-dependent kinase 1 (PDK1) and v-AKT murine thymoma viral oncogene homolog (AKT), also known as protein kinase B (PKB) (Meili *et al.*, 1999). Subsequently, AKT is phosphorylated at two sites, Thr308 and Ser473 by PDK1 and mammalian target of rapamycin mTOR complex 2 (mTORC2) respectively (Sarbassov *et al.*, 2005). Phosphorylation of both Thr308 and Ser473 is required for full activation of AKT (Andjelkovic *et al.*, 1997). The biological function of AKT became apparent when it was revealed to be a major downstream effector of the PI3K pathway. AKT activates a wide range of substrates to mediate cell proliferation, growth, metabolism, survival and angiogenesis (Stauffer *et al.*, 2005). For instance, phosphorylation of glycogen synthase kinase-3 (GSK3) leads to the phosphorylation of transcription factors such as v-myc myelocytomatosis viral oncogene homolog (Myc) and jun (Jun) oncogenes, as well as the cell cycle regulators cyclin D and p21 (de Groot *et al.*, 1993; Nikolakaki *et al.*, 1993; Sears *et al.*, 2000; Rossig *et al.*, 2002; Gregory *et al.*, 2003; Wei *et al.*, 2005). Activated AKT also phosphorylates tuberous sclerosis 2 (TSC2) at multiple sites, which in turn relieves the inhibitory effects of the TSC1/TSC2 complex on Ras homolog enriched in brain (Rheb), thereby activating mTORC1 in response to growth factors (Kovacina *et al.*, 2003). mTORC1 stimulates protein synthesis by phosphorylating proteins such as p70S6 kinase (p70S6K) and eukaryotic translational initiation factor binding proteins 1 (4E-BP1) (Ruggero and Pandolfi, 2003; Bjornsti and Houghton, 2004).

Activated AKT also suppresses apoptosis via the regulation of forkhead box O transcription factor (FOXO) or BCL-2 antagonist of death (BAD). Phosphorylated FOXO forms a complex with the 14-3-3 family of proteins in the cytosol, which in turns inhibits the transcription of anti-apoptotic genes such as p27 and p21 (Cardone *et al.*, 1998). AKT negatively regulates the pro-apoptotic protein BAD by generating binding sites for 14-3-3 proteins. This prevents BAD from interacting with B-cell CLL/lymphoma 2 (BCL2) family members and allows them to proceed with cell survival (Datta *et al.*, 1997).

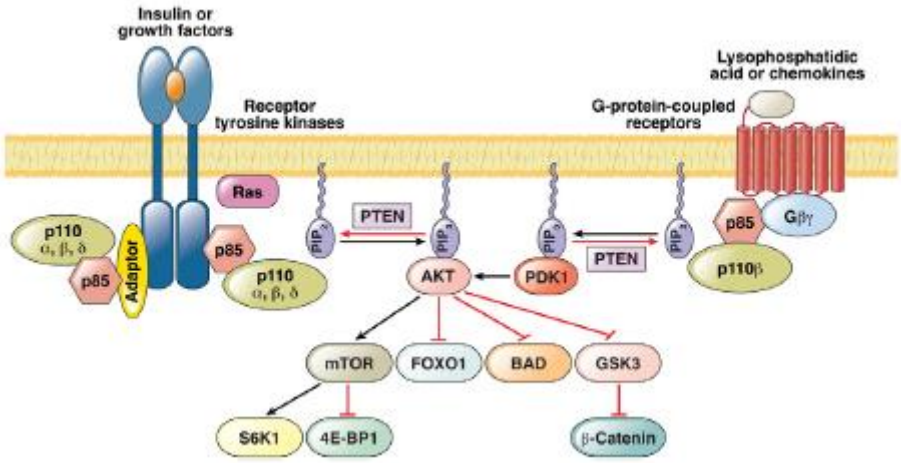

Figure 1.3. Model for regulation of the PI3K/AKT signalling pathway. Upstream activation of PI3K by RTK or GPCR leads to activation of PI3K, resulting in generation of PIP_3. Membrane bound PIP_3 recruits AKT and PDK1, which in turn leads to activation of AKT and its downstream effectors (Zhang *et al.*, 2011).

1.3 PI3K pathway aberrations in human cancer

Deregulation of the PI3K/AKT pathway has been directly implicated in several human cancers (Samuels and Velculescu, 2004). In 2004, Samuels *et al.* sequenced the kinase domains of eight PI3K genes in 35 primary colorectal carcinomas and found that only *PIK3CA*, the gene encoding p110α, harboured somatic mutations. Full exon sequencing of *PIK3CA* in an additional 199 CRC showed that most of the mutations were predominantly located within the kinase and helical domains (Samuels *et al.*, 2004). Three hot spot mutations occur within the kinase and helical domains: E542K, E545K and H1047R. Further investigation of *PIK3CA* mutation in additional tumour types reveals this gene is mutated in approximately 15% of human cancers (Karakas *et al.*, 2006). Expression of *PIK3CA* containing the hot spot mutations in chicken embryo fibroblasts induced oncogenic transformation and elevated lipid kinase activity (Samuels and Velculescu, 2004; Kang *et al.*, 2005). Several studies have reported that *PIK3CA* mutations found in human cancer increase the lipid kinase activity of PI3K by several fold.

Transformed cells with *PIK3CA* hot spot mutations are also tumourigenic in animal models. For example, transgenic expression of the H1047R mutation induces lung adenocarcinoma (Engelman *et al.*, 2008). Moreover, Gymnopolous *et al*. (2007) showed that 14 out of 15 rarer *PIK3CA* mutations found in human cancers were gain of function mutations. However, these rarer mutations were associated with lower levels of lipid kinase activity than the three hot spot mutations. Figure 1.4 summarizes the various *PIK3CA* mutations that have been

reported in studies to date. Although all the three hot spot mutations are gain of function mutations, the activity of helical domain mutations (E542K and E545K) are dependent on Ras activation but independent of binding to p85. In contrast, the activity of the kinase domain hot spot mutation (H1047R) is highly dependent on the interaction with p85 but independent of RAS-GTP binding (Zhao and Vogt, 2008).

Mutations in *PIK3R1* coding for p85 have been identified in ovarian and colon tumours (Philp *et al.*, 2001). Several *PIK3R1* mutations in the inter-SH2 (iSH2) domain have been shown to enhance the PI3K signaling pathway through activation of AKT, leading to stimulation of cell replication and oncogenic transformation (Jaiswal *et al.*, 2009). Mutations in the iSH2 domain disrupt the inhibitory contact of p85α with p110 (Jaiswal *et al.*, 2009; Wu *et al.*, 2009).

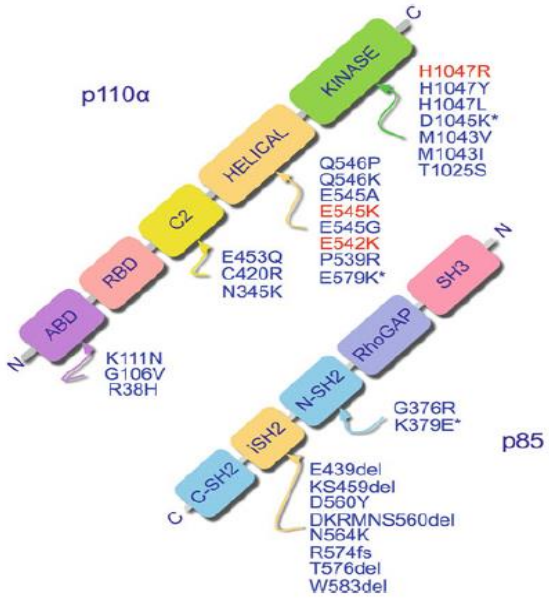

Figure 1.4. Gain of function mutations in *PIK3CA* (coding for p110α) and *PIK3R1* (coding for p85α). The three hot spot mutations are in red, rarer mutations in blue and engineered gain of function mutations are marked by an asterisk (Christian Rommel, 2011).

Although few cancer-specific mutations have been observed in other isoforms of class I PI3Ks, differential expression of other isoforms has been reported in human cancers (Benistant *et al.*, 2000; Jiang *et al.*). Wildtype non-α isoforms have the ability to induce oncogenic transformation when overexpressed in cell culture, whereas wildtype p110α lacks this ability (Kang *et al.*, 2006). This suggests the oncogenic potential of non-α isoforms may correlate with their expression levels.

Aberrations of upstream or downstream effectors of the PI3K pathway have been reported in human cancers. For example, the mutation, amplification and overexpression of EGFR and HER2 occur in breast, lung and gastric cancer (Press *et al.*, 1997; Selvaggi *et al.*, 2004; Tanner *et al.*, 2005). *PTEN* is also frequently mutated in various tumours including prostate cancer, glioblastoma, melanoma and endometrial carcinoma (Kang *et al.*, 2005). *PTEN* is also frequently inactivated by other mechanisms, including gene deletion, targeting by micro-RNA, promoter methylation and phosphorylation (Keniry and Parsons, 2008; Salmena *et al.*, 2008). Several human tumour types including ovarian, pancreatic, breast and gastric cancers show amplification of *AKT1* or *AKT2*. A transforming mutation in the PH domain of *AKT1* (E17K) resulting in constitutive activation is observed in a small percentage of breast, colorectal, ovarian and bladder cancers (Carpten *et al.*, 2007; Askham *et al.*). However, this mutation was not found in gastric cancers from Korean and Japanese populations (Kim *et al.*, 2008; Li *et al.*, 2008). Elevated AKT phosphorylation in cancer has been

associated with activation of *PIK3CA* and inactivation of *PTEN* in some (Li *et al.*, 2005; Oki *et al.*, 2005) but not all studies (Vasudevan *et al.*, 2009).

1.4 PI3K inhibitors

The high frequency of PI3K pathway aberrations and the discovery of *PIK3CA* hotspot mutations have made PI3K an attractive target for anti-cancer drug development. A number of PI3K inhibitors have been developed and are now undergoing clinical trials (Table 1.1). Most of the protein kinase inhibitors that are now in clinical development are directed against the ATP-binding site of PI3K (Dancey and Sausville, 2003) and only a few allosteric protein kinase inhibitors exist (Walker *et al.*, 1999; Parang and Sun, 2004). Despite similarities in ATP-binding site amongst closely related protein kinases, the development of specific kinase inhibitors has been successful and these pharmacological inhibitors have also been instrumental in delineating signal transduction pathways.

Table 1.1. PI3K inhibitors in preclinical studies and in clinical trials.

Company	Target(s)	Status	Cancer Types	Drug
Pan-PI3K inhibitors				
Lilly	PI3K, other kinases	Preclinical	NA	LY294002
Wyeth/Pfizer	PI3K	Preclinical	NA	PWT-458
Zenyaku Kogyo Co. Ltd	PI3K	Phase I	Advanced solid tumours	ZSTK474
Oncothyreon Inc.	PI3K	Phase I	Advanced solid tumours, CRC, melanoma, Prostate, NSCLC, SCCHN, GBM	PX-866
Exelixis/Sanofi-Aventis	PI3K	Phase I	Advanced solid tumours, GBM, lymphoma, endometrial, ovarian, breast, NSCLC	XL-147/ SAR245408
GlaxoSmithKline	PI3K	Phase I	Terminated	GSK615/ GSK1059615
Chugai Pharma Europe Ltd	PI3K	Phase I	Advanced solid tumours	CH5132799
PIramedPharma/Roche/ Genentech	PI3K	Phase I	Advanced solid tumours, breast, NSCLC, non-Hodgkin's lymphoma	GDC-0941
Bayer	PI3K	Phase I, II	Neoplasm, NHLs	BAY 80-6946
Novartis	PI3K	Phase I, II	Advanced solid tumours, NSCLC, endometrial, prostate, breast, colorectal, pancreatic, RCC, GIST, melanoma, GBM, leukemia, SCCHN, TCC	NVP-BKM120
PI3K-mTOR inhibitors				
NA	PI3K, mTOR, DNA-PK, MAPK	Preclinical	NA	Wortmannin
PIramedPharma/Roche	PI3K, mTOR, DNA-PK	Preclinical	NA	PI-103
Semafore	PI3K, mTOR	Phase I	Advanced solid tumours	SF1126
Novartis	PI3K, mTOR	Phase I	Advanced solid tumours, breast	NVP-BGT226
Novartis	PI3K, mTOR	Phase I, II	Advanced solid tumours, breast, renal cell, endometrial, pNET, prostate, breast	NVP-BEZ235
Exelixis/Sanofi-Aventis	PI3K, mTOR	Phase I	Breast, GBM, astrocytoma, NSCLC	XL765/ SAR254409
Roche/Genentech	PI3K, mTOR	Phase I	Advanced solid tumours, NHLs, breast, prostate, endometrial, RCC	GDC-0980
GlaxoSmithKline	PI3K, mTOR, DNA-PK	Phase I	Terminated	GSK1059615
Pfizer	PI3K, mTOR	Phase I	Advanced solid tumours, endometrial	PKI-587/PF-05212384
Pfizer	PI3K, mTOR	Phase I	Advanced solid tumours, endometrial, breast	PF-04691502
Isoform-specific PI3K-I inhibitors				
Alexis/Enzo Life Sciences Inc.	p110β	Preclinical	NA	TGX-221
Novartis	p110α	Phase I	Advanced solid tumours, SCCHN, GIST, CRC, GC, esophageal, breast	BYL719*
Intellikine/MillenuimPharmaceuticas	p110α	Phase I	Advanced solid tumours	MLN1117
Genentech	p110α	Phase I	Advanced hormone receptor-positive breast cancer	GDC-0032
GlaxoSmithKline	p110β	Phase I	Advanced solid cancers	GSK2636771 **
Calistoga Pharmaceuticals	p110δ	I, II, and III	CLL, Hodgkin lymphoma, NHLs,MCL, AML, multiple myeloma	CAL-101

CRC: colorectal cancer; GC: gastric cancer; TCC: transitional cell carcinoma; NSCLC: non-small cell lung cancer; SCCHN: squamous cell carcinoma head and neck cancers; RCC: renal cell carcinoma; GBM: glioblastoma multiforme; NHLs: Non-Hodgkin lymphomas; CLL: chronic lymphocytic leukemia; MCL: mantle cell lymphoma; ALL: acute myeloid leukemia; pNET: pancreatic neuroendocrine tumours. *BYL719 has been administrated to patients whose tumours have an alteration of the *PIK3CA* mutation or amplification. **GSK2636771 has been be administrated to patients whose tumours have PTEN deficiency.

1.4.1 Wortmannin and LY294002

Wortmannin and LY294002 were the first generation of PI3K inhibitors (Marion *et al.*, 2006) and have served as probes for implicating PI3K in a wide range of physiological processes. The fungal metabolite wortmannin is an irreversible inhibitor that binds covalently to a conserved lysine residue in the ATP binding site of the p110 catalytic subunit. It inhibits PI3K at low nanomolar concentrations and is not specific to other lipid and protein kinases (Knight *et al.*, 2004). LY294002, a morpholino derivative of the broad-spectrum kinase inhibitor quercetin, is an ATP competitive inhibitor. LY294002 was also reported to inhibit casein kinase 2 with similar potency to PI3K (Davies *et al.*, 2000). It is important to emphasise that neither wortmannin nor LY294002 displays selectivity towards a specific isoform within the PI3K family (Finan and Thomas, 2004). These two compounds induce strong G1 arrest in a variety of tumour cell lines, but the induction of programmed cell death is only observed in combination with standard anticancer agents or radiation (Stauffer *et al.*, 2005). Due to the lack of selectivity of these compounds, the instability of wortmannin and the insolubility of LY294002, neither has shown therapeutic potential (Stokoe, 2005).

1.4.2 pan-PI3K inhibitors

Higher specificity pan-PI3K inhibitors have been developed, including GDC-0941, NVP-BKM120, PX866, ZSTK474 and GSK1059615 (Table 1.1). GDC-0941 is an ATP-competitive pan-class I PI3K inhibitors that inhibits phosphorylation of AKT and induces G1 arrest in cancer cell lines (Folkes *et al.*,

2008; Raynaud *et al.*, 2009). Currently, GDC-0941 is in Phase II clinical trials enrolling patients with advanced or metastatic breast cancer (NCT00960960). PX-866 is an irreversible pan-class I PI3K inhibitor whose structure is based on wortmannin (Ihle *et al.*, 2004). The primary metabolite of PX-866, 17-OH, is more potent than the parental compound in inhibiting p110α and p110β (Ihle *et al.*, 2009). PX-866 has significant anti-tumour effects both *in vitro* and *in vivo*, as well as a more prolonged inhibition of PI3K relative to wortmannin (Ihle *et al.*, 2009). A phase II trial is evaluating the efficacy and safety to daily PX-866 in patients with relapsed glioblastoma multiforme tumours at first relapse as assessed by objective response and early progression rates (NCT01259869).

Recently, two Class I PI3K inhibitors (BSP-A and BSP-B) were generated by Bayer HealthCare. BSP-A is more specific in inhibiting p110α/δ, whereas BSP-B is more specific in inhibiting p110α/β. As these drugs are currently in development, access to more detailed information regarding both drugs is currently limited.

1.4.3 PI3K-mTOR inhibitors

NVP-BEZ235 is a dual PI3K/mTOR inhibitor developed by Norvartis Pharma AG. It was the first dual inhibitor to enter Phase I clinical trials for dose escalation in patients with advanced solid tumours (Maira *et al.*, 2008; Schnell *et al.*, 2008). At low nanomolar IC_{50} values, NVP-BEZ235 inhibits phosphorylation of AKT and the mTOR signaling pathway, and inhibits the proliferation of human cancer

cell lines (Maira *et al.*, 2008; Serra *et al.*, 2008; Cao *et al.*, 2009; Liu *et al.*, 2009; Marone *et al.*, 2009). Moreover, NVP-BEZ235 acts synergistically with MEK inhibitors in lung cancers with *KRAS* mutation (Engelman *et al.*, 2008). Patients with advanced renal cell carcinoma are currently enrolled for Phase I/II clinical trials of NVP-BEZ235 (NCT01453595).

SF1126 is another dual PI3K/mTOR inhibitor that consists of an RGDS-conjugated LY294002 prodrug. It is designed to enhance efficacy through the binding of its conjugated peptide sequence to specific integrins on the surface of tumour cells (Garlich *et al.*, 2008). SF1126 has favourable pharmacokinetics and inhibits cell proliferation in neuroblastoma, breast, glioma and prostate cancer cells (Garlich *et al.*, 2008; Ozbay *et al.*). A phase I pharmacokinetic and pharmacodynamic dose escalation trial of SF1126 is tested in patients with advanced or metastatic tumours (NCT00907205).

1.4.4 Isoform-specific PI3K-I inhibitors

Many studies have focused on the roles of different PI3K isoforms in normal physiology. For example, transgenic knock-in studies were performed to investigate the role of p110α in insulin signalling while RNA interference was used to investigate the function of p110β (Kubo *et al.*, 2005; Foukas *et al.*, 2006). However, compensatory mechanisms arise because of the length of time the gene product is absent from the cell. The conclusions drawn from such experiments can therefore be somewhat ambiguous. This has led to the development of isoform-

specific PI3K inhibitors with the aim of elucidating the physiological role of different PI3K isoforms in human cancers. This should be of interest clinically in terms of deciding which isoforms to target in diseases with different genetic contexts. Moreover, it is thought that targeting isoform-specific PI3K inhibitors will help to reduce the side effects and toxicity of treatment. For instance, the ability to target p110α and p110β only, while sparing p110γ and p110δ might avoid side-effects associated with toxicity to immune cells.

Several p110α isoform-specific inhibitors are currently being evaluated in phase I clinical trials, such as BYL719, MLN1117 and GDC-0032 (Brana and Siu). The clinical trial of BYL719 is the first PI3K inhibitor study with molecular prescreening from the dose escalation part, in which only patients with *PIK3CA* mutation or amplification were enrolled to the trial (NCT01219699). TGX-221 is a cell permeable analogue of LY294002. It is a specific inhibitor of p110β with an IC_{50} of 5 nM and a 1000-fold higher selectivity over p110α. The main therapeutic utility of this compound seems to be as an anti-thrombotic agent (Jackson *et al.*, 2005). IC87114 is a p110δ-specific inhibitor which inhibits proliferation of acute myeloid leukemia (AML) cells but not normal haematopoietic progenitor cells, suggesting an application for the treatment of this disease (Sujobert *et al.*, 2005; Billottet *et al.*, 2006). IC87114 was a preclinical precursor of CAL-101, which is currently the only delta isoform-specific inhibitor in clinical trials for oncology applications (Herman *et al.*, 2010). CAL-101 is currently in phase II safety and efficacy study in relapsed or refractory Hodgkin lymphoma (NCT01393106).

1.5 Predictive biomarkers in cancer treatment

Personalized cancer medicine is based on the concept of providing the right treatment to the right individual. Over the past few years, strong associations were observed between the presence of kinase mutations and response to molecular targeted drug response. For instance, chronic myeloid leukemia (CML) patients with Bcr-Abl aberration show a high response rate to the Bcr-Abl kinase inhibitor imatinib (Gadzicki *et al.*, 2005). Other well-known examples include associations between *EGFR* mutations and response to EGFR inhibitors (gefitinib or erlotinib) in non-small cell lung cancer (NSCLC) (Paez *et al.*, 2004) and *HER2* amplification and response to HER2 inhibitors (trastuzumab or lapatinib) in breast cancer (Smith *et al.*, 2007). These findings strongly support the notion that predictive biomarkers are useful for the selection of patients who are most likely to respond to a given targeted therapy.

Studies with agents such as gefitinib have revealed that differences in the frequency of predictive markers between different ethnic groups can help to identify the most responsive patient subgroups (Paez *et al.*, 2004). Emerging approaches using mutually exclusive markers, such as *KRAS* and *BRAF* mutations to predict resistance to cetuximab (Di Nicolantonio *et al.*, 2008) have also demonstrated how an understanding of co-occurrence patterns of pathway aberration can also improve patient selection.

1.6 Predictive biomarkers for response to PI3K inhibitors

Among the drug determinants that have been identified for PI3K inhibitors, *PIK3CA* mutations were found to be a drug determinant consistently in a number of studies (Serra *et al.*, 2008; Brachmann *et al.*, 2009; Ihle *et al.*, 2009; O'Brien *et al.*, 2010; Sanchez *et al.*, 2011; Santiskulvong *et al.*, 2011). Indeed, the association between *PIK3CA* mutation and drug response has been validated in a larger panel of cancer cell lines comprising of breast, ovarian and endometrial cancer cells using CH5132799 (Tanaka *et al.*, 2011). The effect of *PIK3CA* mutation in conferring drug sensitivity has also been confirmed in a mouse model, in which treatment of BEZ235 to the p110α H1047R driven lung adenocarcinomas led to remarkable tumour regression (Engelman *et al.*, 2008).

HER2 amplification has also repeatedly been shown to be associated with sensitivity of PI3K inhibitors in breast cancer (Brachmann *et al.*, 2009; O'Brien *et al.*, 2010). It has been demonstrated that cells harbouring amplification of *HER2* are dependent on PI3K pathway activation and sensitive to its inhibition through targeting of PI3K (Brachmann *et al.*, 2009; O'Brien *et al.*, 2010; Tanaka *et al.*, 2011).

PTEN deficiency has been reported to predict PI3K pathway inhibitor response in ovarian cancer (Ihle *et al.*, 2009; Santiskulvong *et al.*, 2011). However, the association between PTEN loss and response is less clear in breast cancer (She *et al.*, 2008; Brachmann *et al.*, 2009; Lehmann *et al.*, 2011; Tanaka *et al.*, 2011; Weigelt and Downward). In one study, breast cancer cell lines with PTEN loss were found to be sensitive to BKM120 (Sanchez *et al.*, 2011). In

contrast, Brachmann et al. study showed PTEN null breast cancer cells to be preferentially resistant to treatment with BEZ235 (Brachmann *et al.*, 2009). This suggests that the correlation between PI3K aberrations and drug sensitivity could be tumour subtype specific.

Nonetheless, in the evaluation of the *in vitro* efficacy of 25 PI3K pathway inhibitors in a panel of 39 human cancer cell lines, *PIK3CA*, *HER2*, *PTEN* mutations were not associated with sensitivity to PI3K inhibitors (Dan *et al.*, 2010). Instead, cell lines with high p-AKT were found to be more responsive to PI3K pathway inhibitors than those with lower expression levels. Recently, a large scale systemic identification of genetic drug determinants was performed using 639 human cancer cell lines, including 17 GC and 34 CRC cell lines and tested with 130 drugs (Garnett *et al.*, 2012). These cancer cell lines were subjected to sequencing of full coding exons of 64 commonly mutated cancer genes, copy number variation profiling and gene expression profiling. Among the 130 drugs, 3 of them were PI3K inhibitors, AZD6428 (p110β specific inhibitor), BEZ235 (PI3K/mTOR inhibitor) and GDC-0941 (PI3K inhibitor). In this study, significant association was identified between *PIK3CA* mutations and the sensitivity of AZD6428, but not with BEZ235 and GDC-0941. Furthermore, mutations of *APC* and *KRAS* were also reported to be associated with higher IC_{50} value of PI3K inhibitors in this study. The lack of consistent associations between *PIK3CA* mutation, *HER2* amplification, PTEN deficiency and sensitivity to PI3K inhibitors has cast uncertainty over their reliability as predictive biomarkes.

1.7 Predictive biomarkers of PI3K inhibitors (clinical trials)

To date, the association between PI3K pathway aberrations and the clinical outcome of phase I clinical trials is still inconclusive due to small sample size or lack of assessment of PI3K aberrations in the tumours (Bendell *et al.*; Hong *et al.*).

A pooled analysis of patients treated with PI3K pathway inhibitors (mTOR or PI3K inhibitors) was performed by Janku et al. (Janku *et al.*, 2012). In this study, advanced breast, cervical, endometrial and ovarian cancers were sequenced for the presence of activating *PIK3CA* mutations. A partial response was observed in 30% of the 23 patients with tumours harbouring a *PIK3CA* mutation in contrast to 10% of 70 patients whose tumours were *PIK3CA* wildtype (Janku *et al.*). However, the majority of the patients received combination therapies with an mTOR inhibitor and not a PI3K inhibitor.

Some studies have begun to recruit patients with specific PI3K aberrations during the dose escalation part (Brana and Siu), except BYL719 (NCT01219699) and GSK2636771 (NCT01458067). The preliminary clinical results of BYL719 has been recently presented (Juric D, 2012). A total of 35 patients have been enrolled and three patients whom received doses ≥ 270 mg/day demonstrated partial response. These responders were a breast cancer patient with estrogen positive receptor, a cervical cancer patient and a colorectal cancer patient with *KRAS* mutation. The clinical response observed in the colorectal cancer patient with co-existing *KRAS* and *PIK3CA* mutations contrasts with the preclinical finding that co-occurrence of these mutations conferred resistance to BYL719

(Brana and Siu). GSK2636771 (p110β isoform specific inhibitor) is currently being tested in a clinical trial of PTEN deficient malignancies due to the recent finding in preclinical models suggested that PTEN deficient cancers may depend on p110β rather than p110α signaling (Jia *et al.*, 2008; Wee *et al.*, 2008; Ni *et al.*). However, results from this trial have not yet been reported.

1.8 Rationale for this study

Major elements of the PI3K pathway are known to be mutated or amplified in GC and CRC. For instance, *PIK3CA* mutations have been reported in GC and CRC at a frequency of approximately 11% and 14%, respectively (Velho *et al.*, 2005). In addition to mutation, GC also shows a high prevalence (~40%) of *PIK3CA* amplification (Byun *et al.*, 2003). A high frequency of PTEN loss of expression has also been reported in GC (Bai *et al.*, 2007) and CRC (18%) (Frattini *et al.*, 2007). The relatively high frequencies of these PI3K pathway aberrations suggest they may have clinical potential for the selection of GC and CRC patients to receive targeted PI3K pathway therapy.

Over the past decade, studies on molecular-targeted drugs have conveyed important lessons for the further development of this class of agent (Martini *et al.*, 2011). Knowledge of PI3K pathway aberrations in GC and CRC tumours is still quite limited, especially (1), the co-occurrence patterns of individual aberrations and (2), geographic or ethnic differences in the frequency of aberrations. Such knowledge is critical if biomarkers are to be introduced routinely to stratify

patient populations based on their molecular characteristics for treatment with PI3K inhibitors.

In addition, trials with imatinib and trastuzumab have shown that pre-selection of patients for treatment based on biologically relevant predictive markers can improve drug efficacy (Esteva *et al.*, 2002; Gianni *et al.*, 2011). One of the limitations of extrapolating data from the literature in this field to GC and CRC is that the majority of preclinical studies have been performed in breast cancer cell lines. Moreover, the large scale studies provide poor information at the tumour type level. Predictive biomarkers could well be different between different tumour types. For instance, *PTEN* deletion was associated with drug sensitivity in ovarian cancer (Santiskulvong *et al.*, 2011) but not in breast cancer (Brachmann *et al.*, 2009). Therefore, it is necessary to identify predictive biomarkers for PI3K inhibitors specifically according to the cancer type.

1.9 Aims of the study

The aims of this study were:

Aim 1: To consolidate knowledge on inter-ethnic frequencies, clinical associations and co-occurrence patterns of prominent PI3K pathway aberrations in GC and CRC using meta-analysis and single laboratory approaches.

These results are addressed in Chapter 3.

Aim 2: To screen and functionality evaluate predictive biomarkers that could determine sensitivity to PI3K inhibitors in GC and CRC cells

(A) using OncoCarta in GC and CRC cells

These results are addressed in Chapter 4.

(B) using RNA-sequencing in *PIK3CA* wildtype GC cells.

These results are addressed in Chapter 5.

2 Materials and Methods

2.1 Clinical samples

Formalin-fixed and paraffin embedded (FFPE) tissue blocks of tumour samples selected for maximal tumour cell content, together with corresponding normal tissues were obtained from the Department of Pathology, National University Hospital. In all, 140 GC and 150 CRC cases from patients who underwent surgery for their disease during 1997-2008 were investigated. The clinicopathological features for each of these cases are listed in Table 3.4 and Table 3.5. This study was approved by the National University of Singapore Institutional Review Board (NUS 654).

2.2 Cell lines

A total of 36 GC and 15 CRC cell lines (Table 2.1) were obtained from American Type Culture Collection (ATCC), Japanese Collection of Research Bioresources (JCRB), Cell lines Service GmbH (CLS) and Yonsei Cancer Centre (Yonsei CC) and grown in RMPI 1640 or DMEM supplemented with a final concentration of 10% fetal bovine serum (FBS; all from Gibco, Life Technologies, Carlsbad, CA).

Table 2.1. GC and CRC cell lines.

Cell Line	Tissue Type	Source	Catalog Number
AGS	Gastric	ATCC	CRL-1739
Az521	Gastric	JCRB	JCRB0061
CLS145	Gastric	CLS	NA
Fu97	Gastric	JCRB	JCRB1074
HGC27	Gastric	CLS	NA
Hs738	Gastric	ATCC	CRL-7869
Hs746T	Gastric	ATCC	HTB-135
IM95	Gastric	JCRB	JCRB1075.0
KATOIII	Gastric	ATCC	HTB-103
MKN1	Gastric	JCRB	JCRB0252
MKN28	Gastric	JCRB	JCRB0253
MKN45	Gastric	JCRB	JCRB0254
MKN7	Gastric	JCRB	JCRB1025
MKN74	Gastric	JCRB	JCRB0255
NCI-N87	Gastric	ATCC	CRL-5822
NUGC2	Gastric	JCRB	JCRB0821
NUGC3	Gastric	JCRB	JCRB0822
NUGC4	Gastric	JCRB	JCRB0834
OCUM1	Gastric	JCRB	JCRB0192
RERF-GC-1B	Gastric	JCRB	JCRB1009
SCH	Gastric	JCRB	JCRB0251
SNU1	Gastric	ATCC	CRL-5971
SNU16	Gastric	ATCC	CRL-5974
SNU5	Gastric	ATCC	CRL-5973
TMK1	Gastric	Japan	NA
YCC1	Gastric	Yonsei CC	NA
YCC3	Gastric	Yonsei CC	NA
YCC6	Gastric	Yonsei CC	NA
YCC7	Gastric	Yonsei CC	NA
YCC10	Gastric	Yonsei CC	NA
YCC11	Gastric	Yonsei CC	NA
YCC16	Gastric	Yonsei CC	NA
YCC17	Gastric	Yonsei CC	NA
YCC18	Gastric	Yonsei CC	NA
YCC19	Gastric	Yonsei CC	NA
YCC20	Gastric	Yonsei CC	NA
CCK81	Colorectal	JCRB	JCRB0208
COLO205	Colorectal	ATCC	CCL-222
COLO320	Colorectal	ATCC	CCL-220.1
DLD1	Colorectal	ATCC	CCL-221
HCC56	Colorectal	JCRB	JCRB1037
HCT116	Colorectal	ATCC	CCL-247
HT29	Colorectal	ATCC	HTB-38
LoVo	Colorectal	ATCC	CCL-229
LS513	Colorectal	ATCC	CRL-2134
RCM1	Colorectal	JCRB	JCRB0256
RKO	Colorectal	ATCC	CRL-2577
SW403	Colorectal	ATCC	CCL-230
SW480	Colorectal	ATCC	CCL-228
SW620	Colorectal	ATCC	CCL-227
WiDR	Colorectal	JCRB	JCRB0224

2.3 Compounds

PI3K inhibitors (BSP-A and BSP-B (BAY1082439)) and a MEK inhibitor (BSP-C) were obtained from Bayer HealthCare Pharmaceuticals (Bayer AG, Leverkusen, Germany). Commercially available PI3K inhibitors (NVP-BKM120, GDC-0941, XL-147 and BYL719) were purchased from Selleck Chemicals (Houston, TX).

2.4 DNA extraction

For FFPE, a single 15 µm section was cut from each block and processed according to methods described previously (Soong and Iacopetta, 1997). Cell line DNA extraction was performed using DNeasy kit (Qiagen) following the manufacturer's protocol.

2.5 RNA extraction

Total RNA was isolated using RNeasy Mini kit (Qiagen) following the manufacturer's protocol. Extracted RNA was treated with DNase I to remove possible genomic DNA contamination (Qiagen). The quality of RNA was assessed using Bioanalyzer (Agilent Technologies, Santa Clara, CA) with the RNA 6000 Nano kit. Only RNA with RNA integrity number value greater than 8 and with a 28S rRNA band at 4.9 kb that is twice that of the 18S rRNA band at 1.9 kb, was selected for analysis.

2.6 Sanger sequencing

Primers were designed to amplify *PIK3CA* exon 9 (forward: 5' GAA TCC AGA GGG GAA AAA TA 3'; reverse: 5' TTT AGC ACT TAC CTG TGA CTC CA 3') and exon 20 (forward: 5' TTC GAA AGA CCC TAG CCT TAG A 3'; reverse: 5' TGC TGT TTA ATT GTG TGG AAG ATC 3'), in which 196 bp and 129 bp amplicons were generated for the respective primers. The majority (>80%) of mutations in *PIK3CA* have been observed in these two exons (Samuels *et al.*, 2004). A total of 50 ng DNA was amplified in a 25 µL reaction mix containing 1x FastStart Reaction Buffer, 2 mM magnesium chloride, 10 µM deoxynucleotide mix and 1 unit FastStart Taq Polymerase (Roche Diagnostics, Mannheim, Germany). PCR cycling comprised initial denaturation at 95^{o}C for 4 min followed by 40 cycles of 30 sec at 95^{o}C, 30 sec at 65^{o}C (exon 9) or 60^{o}C (exon 20), and 1 min at 72^{o}C before completion with 1 min at 72^{o}C. PCR products were purified using ExoSAP-IT reagent (Affymetrix, Santa Clara, CA) before undergoing bi-directional sequencing using the BigDye Terminator v3.0 kit (Life Technologies) with forward and reverse PCR primers respectively. Sequencing products were electrophoresed and analyzed on the ABI PRISM 3100 Genetic Analyzer using the Sequencing Analysis 3.0 software (Life Technologies).

2.7 Pyrosequencing

KRAS was amplified using primers (forward: 5' AGG CCT GCT GAA AAT GAC TGA A 3'; reverse: 5' biotin-TTA GCT GTA TCG TCA AGG CAC TCT 3'). The PCR condition was 45 cycles of 95ºC for 30 sec, 60ºC for 30 sec and 72ºC for 1 min, followed by 72ºC for 5 min. Amplified PCR product with 82 bp size were subsequently analysed by Pyrosequencing using the PSQ96MA instrument (Qiagen, Hilden, Germany). The reaction mix comprised of Pyro Gold Reagent kit (Qiagen), 1x annealing buffer (Qiagen), binding buffer at pH7.6 (10 mM Tris-HCl, 2 M NaCl, 1mM EDTA, 1 mL/L Tween 20), 3 µL of streptavidin sepharose beads and 15 µM pyrosequencing primer (5' CTT GTG GTA GTT GGA GCT 3'). The nucleotide dispensation order was TAC GAC TCA GAT GCG TAG (Dufort *et al.*, 2009).

2.8 Mutation analysis by Mass Spectrometry

Mutation analysis of 304 nucleotide commonly mutated in cancer was performed by analyzing the OncoCarta panel (Table 2.2) using the Sequenom MassARRAY (Sequenom, San Diego, CA). Multiplexed PCR was performed in 5 µL volumes containing 0.8 µL of HPLC H_2O, 1 unit of SQNM PCR enzyme, 20 ng of genomic DNA, 2 mM of $MgCl_2$, 500 µM of dNTP and 2 µL of OncoCarta PCR primers. Thermocycling was performed at 94^{o}C for 2 min followed by 45 cycles of 94^{o}C for 30s, 56^{o}C for 30s and 72^{o}C for 1 min. A total of 2 µL of shrimp alkaline phosphatase (SAP) mixture was added to the PCR product to deactivate unincorporated deoxynucleotides and the mixture was incubated at 37^{o}C for 40

min followed by 85^{o}C for 5 min. Primer extension was carried out using 5.4 pmol of each primer extension probe, 50 μmoL of the appropriate dNTP/ddNTP combination and 1.3 units of Thermosequenase. The mixture was incubated at 94^{o}C for 30 sec, followed by 40 cycles of 94^{o}C for 5 sec, 52^{o}C for 5 sec and 80^{o}C for 5 sec. After the addition of a cation exchange resin to remove residual salt from the reactions, 7 μL of the purified primer extension reaction was loaded onto a matrix pad (3-hydoxypicoloinic acid) of a SpectroCHIP (Sequenom). SpectroCHIPs were analysed using a Bruker Biflex III matrix-assisted laser desorption/ionization-time of flight (MALDI-TOF) mass spectrometer (Sequenom).

Table 2.2. List of 29 genes screened for hotspot mutations OncoCarta panel.

Gene	Mutation	No of assay
ABL1	G250E, Q252H, Y253H, Y253F, E255K, E255V, D276G, F311L, T315I, F317L, M351T, E355G, F359V, H396R	14
AKT1	V461L, P388T, L357P, E319G, V167A, Q43X, E17del, E17K	8
AKT2	S302G, R371H	2
BRAF	R443T, R444W, R444Q, R462I, I463S, E586K, V600D, G615E, G464R, G464V/G464E, G466R, F468C, G469S/G469E/G469A, G469V/G469R, D594V/D594G, F595L, G596R, L597S/L597R, L597Q/L597V, T599I, V600E/V600K, V600R/V600L, K601N, K601E	24
CDK	R24C, R24H	2
CTNNB1	D32N/D32H/D32Y, S33P, S33Y/S33C/S33F, G34R, G34E/G34V, S37A, S37Y/S37C/S37F, T41A/T41S, T41I, S45P, S45Y/S45C/S45F	11
EGFR	R108K, T263P, A289V, G598V, E709K/E709H, E709A/E709G/E709V, G719S/G719C, G719A, M766_A767insAI, S768IV769_D770insASV, V769_D770insCV, D770_N771>AGG, D770_N771insG, N771_P772>SVDNR, P772_H773insV, H773>NPYH773_V774insNPH, H773_V774insPH, H773_V774insH, V774_C775insHV, T790M, L858R, L861Q, L747_T750del, P insE746_A750del,T751AT751AE746_T751del,I insS752_I759delL747_E749del,A750PE746_A750delL747_E749delL747_S752del, P753SE746_T751del,V insL747_S752del,Q insL747_S752del, E746_T751del, S752DL747_T750del, E746_T751delL747_T751del, E746_A750del, V ins, A750P, S752I/FT751, T751I, T751P, L747_Q ins, L755P, G776V, CA775_G776 insYVMA, P780_Y781 insGSP	47
ERBB2	L755P, G776S/G776LC, G776V, CA775_G776 insYVMA, P780_Y781 insGSP, S779_P780 insVGS	6
FBX4	S8R, S12L, L23Q, G30N, P76T	5
FBXW7	R465C, R465H, R479G, R479Q/R479L	4
FGFR1	S125L, P252T	2
FGFR2	S252W, Y376C	5
FGFR3	G370C, Y373C, A391E, K650Q/K650E, K650T/K650M, A281V	1
FLT3	I836del, D835H/D835Y	2
GNAQ	Q209P/Q209L	1
HRAS	G12V/G12D, G13C/G13R/G13S, Q61H/Q61H, Q61L/Q61R/Q61P, Q61K	5
JAK2	V617F	1
KIT	D52N, Y503_F504insAY, W557R/W557R/W557G, V559D/V559A/V559G, V559I, V560D/V560G, K550_K558del, K558_V560del, K558_E562del, V559del, V559_V560del, V560del, P551_V555del, Y553_Q556del, Y570_L576del, E561K, L576P, P585P, D579del, K642E, D816V, D816H/D816Y, V825A, E839K, M552L, Y568D, F584S	65
KRAS	G12A/G12C/G12D, G12F/G12R, G12S/G12V, G13V/G13D, A59T, Q61E/Q61K, G13A/G13V/G13D, T58I, A59V, G60D	10
MAP2K1	F53S, K57N, D67N, Y134C, E203K/E203Q	5
MAP2K2	F57I, F57C, F57L, K61E, R388Q	5
MET	R970C, T992I, Y1230C, Y1235D, M1250T	5
NRAS	G12V/G12A/G12D, G12C/G12R/G12S, G13V/G13A/G13D, A18T, Q61H, G48S	6
PDGFRA	V561D, T674I, F808L, D846Y, N870S, D1071N, D842_H845del, I843_D846del, S566_E571>K, I843_S847>T, D842V, N659K, D842Y, D842F, Y849C	15
PIK3CA	R88Q, N345K, C420R, P539R, E542K, E545K, Q546K, H701P, H1047R/H1047L, H1047Y, R38H, C901F, M1043I/M1043I, E418K, E542Q, E542V, E545Q, E545A/E545G, Q546E, Q546P/Q546R, Q546H, M1004I, G1007R, Y1021H, Y1021C, R1023Q, T1025A, T1025S/T1025I, A1035T, A1035V, Y1038C, M1043V, N1044K, I1058F, H1065L	35
PTPN11	T507K	1
RET	C634R, C634W, C634Y, E632_L633del, M918T, A664D	6
SOS1	R248H, R688Q, H888Q	3
TP53	V143A, R175H/R175L, G245S/G245R/G245C, R248G/R248W, R273C, R273H/R273L, D281H/D281Y, D281G	8

2.9 Copy number analysis

DNA copy numbers were quantified by real-time PCR (qPCR) in 20 µL reaction mixes that consisted of 10 µL of 2x Taqman Genotyping Master Mix, 1 µL of 20x Taqman Copy Number Assay, 1 µL of 20x Taqman Copy Number reference assay (Life Technologies) and 20 ng of DNA. The pre-designed TaqMan Copy Number Assays used were PIK3CA_Hs02708380_cn (amplicon size: 110 bps), PTEN_Hs02724235_cn (amplicon size: 95 bps) and Ribonuclease P. Thermal cycling consisted of 10 min at 95°C followed by 40 cycles of 15 sec at 95°C and 1min at 60°C in the ABI 7900 HT Sequence Detection System (Life Technologies). Each sample was analyzed in triplicate and the mean copy number was calculated using Copy Caller software (Life Technologies). Thresholds for defining gene amplification and loss were determined by analysis of normal tissue from 21 randomly selected cases of GC and CRC. Tumour samples were considered to show amplification (or loss) when their copy number was greater (or less) than two standard deviations of the median copy number observed in normal tissue. The median ± standard deviations of copy numbers in normal tissue for *PIK3CA* were 1.09±0.44 for GC and 1.25±0.48 for CRC, and for *PTEN* they were1.78±0.43 for GC and 2.28±0.54 for CRC.

2.10 RNA-sequencing

Ribo-Zero^{TM} Magnetic Kit (Epicentre Biotechnologies, Madison, WI) was used to remove the ribosomal RNA from the total RNA of the cell lines. A total of 5 µg RNA sample was combined with 4 µL of Ribo-Zero reaction buffer, 10 µL of

Ribo-Zero rRNA removal solution, and topped up with RNase-free water to 40 µL. The mixture was incubated at 68°C for 10 min, followed by incubation at room temperature for 5 min. The mixture was transferred to 1.5 mL eppendorf tube containing 225 µL of magnetic beads and was immediately mixed by pipetting at least 10 times. The tube was vortexed at medium setting for 10 sec and place at room temperature. After 5 min incubation, the mixture was vortexed and transferred to a 50°C heating block for 5 min, followed by transferring to a magnetic stand and leaving it to stand for at least 1 min until the solution appeared clear. The clear supernatant was removed and transferred to a new 1.5 mL eppendorf tube. The rRNA-depleted RNA was further purified by Qiagen RNeasy TM MinElute Cleanup Kit (Qiagen). The amount of rRNA-depleted RNA was quantified by NanoDrop ® UV-Vis Spectrophotometer (Thermo Scientific, Wilmington, DE).

RNA libraries were constructed according to the protocol of ScriptSeq^{TM} v2 mRNA-Seq Library Preparation Kit (Epicentre Biotechnologies). RNA fragmentation was achieved by incubating 12 µL solution containing 50 ng of rRNA-depleted RNA, 1 µL RNA fragmentation solution, 2 µL cDNA synthesis at 85°C for 5 min. The fragmentation reaction was stopped by placing the tube on ice. cDNA synthesis was achieved by adding 4 µL of the cDNA synthesis master mix containing 3 µL cDNA synthesis premix, 0.5 µL 100mM DTT and 0.5 µL StarScript reverse transcriptase to the fragmented RNA mixture. The reactions were incubated at 25°C for 5 min, 42°C for 20 min and were cooled to 37°C. Tubes were taken out from the PCR machine and 1 µL of finishing solution was

added, followed by 10 min incubation at 37°C and 3 min incubation at 95°C. The reactions were cooled to 25°C and terminal tagging master mix containing 7.5 µL terminal tagging premix and 0.5 µL DNA polymerase was added to each reaction. After this, the mixture was incubated at 25°C for 15 min, 95°C for 3 min and kept at 4°C. The generated cDNA was purified by Agencourt AMPure XP system (BeckmanCoulter, Brea, CA) according to the manufacturer's protocol.

Purified cDNA was amplified in a 50 µL reaction containing 25 µL of FailSafe PCR Premix E, 1 µL of forward PCR primer, 1 µL of barcode reverse PCR primer and 0.5 µL (1.25 U) of FailSafe PCR enzyme. PCR cycling comprising 1 min at 95°C, followed by 10 cycles of 30 sec at 95°C, 30 sec at 55 °C and 3 min at 68 °C. After the last PCR cycle, the mixture was incubated at 68 °C for 7 min in a Master Cycler. Post-PCR purification was performed by using the Agencourt AMPure XP system (BeckmanCoulter), as according to the manufacturer's protocol. The quality of cDNA library was confirmed by Bioanalyzer (Agilent Technologies) using High sensitivity DNA chips.

Paired-end sequencing and read length of 76 nucleotides were performed on an Illumina HiSeq^{TM}2000 sequencing machine (San Diego, CA). Two barcoded samples were pooled together in a single lane of a flow cell (Illumina). Sequencing on the Illumina Hiseq^{TM}2000 was performed with TruSeq PE Cluster Kit v3-cBot-Hs and Truseq SBS Reagent v3 sequencing kits (Illumina) according to manufacturer's instructions.

The images generated by the sequencers were converted into nucleotide sequences by a base-calling pipeline. The raw reads were saved in the fastq format, and I removed reads with sequence adaptors and reads with more than 2% "N" bases. All subsequent analysis was based on clean reads. The reference sequences used were genome and transcriptome sequences downloaded from the UCSC website (version hg19). Clean reads were respectively aligned to the reference genome and transcriptome using BWA (Li and Durbin, 2010). No more than 3 mismatches were allowed in the alignment for each read. The gene expression level was measured by the number of uniquely mapped reads per kilobase of exon region per million mapped reads (RPKM). The Log_2 transformed RPKM values were used to identify the differentially expressed genes between sensitive and resistant cell lines based on the following criteria: -4>fold change>4.

2.11 Quantitative reverse transcription -PCR (qRT-PCR)

RNA from cell lines was collected using RNeasy Mini kit (Qiagen) and converted to cDNA using High Capacity cDNA Reverse Transcription Kit (Life Technologies). A 20 µL reverse transcription reaction contained 2 µL of 10x RT buffer, 0.8 µL of 25x dNTP Mix, 2 µL of 10x RT Random Primers, 1 µL MultiScribe Reverse Transcriptase and 2 µg of total RNA. Thermal cycling of reverse transcription consisted of 10 min at 25°C, 120 min at 37°C and 5 min at 85°C. Primers were designed to amplify *ACTB* (forward: 5' GTC GTC GAC AAC GGC TCC GG 3'; reverse: 5' CCA CCA TCA CGC CCT GGT GC 3') and

IGFBP3 (forward: 5' TTC GAA AGA CCC TAG CCT TAG A 3'; reverse: 5' TGC TGT TTA ATT GTG TGG AAG ATC 3'). qRT-PCR comprising 12.5 µL of Maxima SYBR Green/ROX qPCR Master Mix (Thermo Scientific), 0.3 µM of forward primer, 0.3 µM of reverse primer and 100 ng of cDNA. Thermal cycling consisted of 10 min at 95°C followed by 40 cycles of 15 sec at 95°C and 1min at 60°C in the ABI 7900 HT Sequence Detection System (Life Technologies).

2.12 Immunohistochemistry

Three 4 µm sections were obtained from tissue microarray blocks of GC and CRC described previously (Das *et al.*, 2008) and which contained the same cases from which DNA was extracted. The sections were stained by immunohistochemistry using the BOND-MAX autostainer (Leica Microsystems, Buffalo Grove, IL) according to the manufacturer's recommended protocols and reagents. The following proteins (antibody concentration, clone, source) were selected for analysis based on their published validation for functional sensitivity and specificity: p110α (1:300; 611398; BD Transduction Laboratories, San Jose, CA) (Lee *et al.*), PTEN (1:400; 6H2.1, Cascade Bioscience, Winchester, MA) (Goel *et al.*, 2004; Nassif *et al.*, 2004) and pAKT (Ser473) (1:200; 587F11, Cell-Signaling Technology, Beverly, MA) (Loupakis *et al.*, 2009). The intensity of staining in tumour cytoplasm was scored independently on a scale of 0 to 3 by two pathologists who were blinded to the results for other aberrations. In cases of discordance, a consensus score was reached after discussion. For PI3K p110α and pAKT, tumours with an intensity score of 3 were considered to have high

expression, as reported previously (Oki *et al.*, 2005). For PTEN, tumours without any staining (score 0) were considered to show PTEN loss, as described previously (Zhu *et al.*, 2012). Endothelial cells in the neovascular capillaries and vessels were used as internal positive controls for PTEN.

2.13 Drug proliferation assays

Cells (3000 cells/well) were seeded in 96 well plates containing 90 µL media with 10% FBS. After 24 h, 10 µL of drug diluted in DMSO was added to the plated cells with a final concentration ranging from 1-5000 nM. Cell viability was assessed after 72 h using CellTiter 96® AQueous One Solution Cell Proliferation Assay (Promega, Madison, WI). The drug concentration that inhibited cell proliferation by 50% compared with vehicle controls (DMSO) was calculated and indicated as IC_{50} (Bhattacharya *et al.*, 2012).

2.14 Short interfering RNA experiments and cell viability assays

ON-TARGET*plus* si-*KRAS* and si-*IGFBP3* containing pools of 4 siRNAs per genes were purchased from Thermo Scientific. A total of 80 µL of cells (5000 cells) and 1.6 mL of cells ($3x10^5$ cells) were seeded in 96 and 6 well plate respectively, and transfected with siRNA using Lipofectamine 2000 (Life Technologies) at a final concentration of 25 nM. Assays were performed together with ON-TARGET*plus* non-targeting siRNA (Thermo Scientific) as a negative control. After 24 h incubation, media was removed from the wells and replaced

with new media. Cell viability was assessed by CellTiter 96® AQueous One Solution Cell Proliferation Assay (Promega).

To determine the combined effects of siRNA knockdown of target genes on sensitivity to PI3K inhibitors, different drug concentrations were added to the well after 24 h transfection as described above. Assays were performed in triplicate and the fractions of cell viability were normalized with control (non-targeting siRNA). Cell viability was measured at 72 h after drug treatment using CellTiter 96® AQueous One Solution Cell Proliferation Assay (Promega).

2.15 Establishment of YCC1 isogenic cell lines

Control plasmid, pBOBI-GFP was kindly provided by Dr Dominic Voon. The coding region of human IGFBP3 was cloned into a pBOBI vector (a kind gift of Vinay Tergoankar, IMCB, A*STAR) using 5' XbaI and 3' Xho1 sites. The sequence of IGFBP3 was confirmed by Sanger sequencing (Life Technologies). Lentiviruses were produced in HEK293T cells using ViraPower packaging vectors (Invitrogen) and FuGENE HD (Promega). Supernatants containing viral particles were harvested at 48 hours after transfection. For transduction with lentiviruses, YCC1 cells were incubated with virus-containing supernatants in the presence of 8 µg/mL polybrene (Sigma-Aldrich) for 24 hours before replenishment with normal culture medium.

2.16 SDS-PAGE and western blot analysis

Assessment of protein expression in cell culture extracts were performed by western blotting. Cell protein lysates were separated through 10% SDS-PAGE and transferred to nitrocellulose membrane. The membrane was blocked in 5% milk and then immunoblotted with the anti-phospho-AKT (Ser473), total AKT, phospho-ERK1/ERK2 (Thr202/Tyr204)), total ERK1/ERK2, p110α, GAPDH antibodies from Cell Signaling Technology. Anti-KRAS was purchased from Santa Cruz Biotechnology (Dallas, Texas). Anti-IGFBP3 was purchased from Sigma-Aldrich (St.Louis, MO). Primary antibodies were diluted in 5% bovine serum albumin (BSA) (Sigma-Aldrich) and were used at dilutions recommended by the manufacturers. Secondary anti-rabbit and anti-mouse were purchased from Cell Signaling Technology. Detection of antibody binding was performed by using the Amersham^{TM} ECL^{TM}prime Western blotting detection reagent (GE Healthcare Biosciences, Pittsburgh, PA) according to the manufacturer's instructions.

2.17 Statistical analysis

For meta-analysis, studies were combined using a random effects model, with weighting by the inverse of variance. Homogeneity amongst studies was assessed using the Cochran Q statistic and the I^2 statistic. The Likelihood ratio or Fisher's exact test was used to test for differences in the frequency of aberrations between Asians and Caucasians, as well as associations with clinicopathological features. Fisher's exact test was used to test for differences in PI3K aberrations between

GC and CRC. Binary logistic regression was used to test the significance of the association between different PI3K activation events. For survival analysis, univariate Cox proportional hazards regression analysis was performed to estimate hazard ratios. Multivariate Cox regression analysis (Method: Enter) of factors significant in univariate analysis was performed to identify independent prognostic factors. Correlations between drug sensitivity and mutation status, gene expression and protein expression were estimated by Spearman's rank correlation method, and differences between groups were calculated with Student's t test. Analyses were performed using Comprehensive Meta Analysis version 2.2 (Biostat, Englewood, NJ) and SPSS statistical software package for Microsoft Windows version 19.0 (SPSS, Chicago, IL). All tests of significance were two-sided, and p values<0.05 were considered significant. Quantile normalization of IC_{50} values was performed using R software. Clustering of GC cell lines was performed with MeV 4.4.01 software, using unsupervised hierarchical clustering analysis on the basis of Pearson's dissimilarity as distance measure.

2.18 Pathway analysis

Differential expressed genes were uploaded to the Database for Annotation, Visualization and Integrated Discovery (DAVID) software to analyze the genes that were involved in biological pathways. Parameters in a "Functional Annotation Tool" were set to retrieve pathway information from Kyoto Encyclopedia of Genes and Genomes (KEGG). Analysis of the gene biological

functions and pathways were performed using GO ANOVA analysis in the Partek Genomic Suite 6.6.

3 Results: Phosphatidylinositol-3-kinase Pathway Aberrations in Gastric and Colorectal Cancer: Meta-analysis, Co-occurrence and Ethnic Variation

3.1.1 Literature review

Relevant publications were identified through a PubMed search in January 2013 using the terms "PI3K and gastric cancer", "PTEN and gastric cancer", "AKT and gastric cancer", "PI3K and colorectal cancer", "PTEN and colorectal cancer", and "AKT and colorectal cancer". A restriction to human studies was applied. Other publications were identified from references cited in the retrieved articles. Information on the first author, year of publication, country of origin of the study population, frequencies of aberrations and total cases was recorded (Table 3.1). The country of origin of the study population was used to determine ethnicity, with East Asian populations defined as those from China, Hong Kong, Japan, Korea, Singapore and Malaysia, and Caucasian populations as those from Europe, Australia and North American countries. Studies on populations outside these two regions were annotated (Table 3.1), but not considered in the meta-analysis according to ethnicity.

Table 3.1. Frequencies of PI3K pathway aberrations in GC and CRC from previous publications and the current study. (continued next page)

First Author	Year	PMID	Cancer Type	Study Population	Ethnicity	Aberration	Method	Aberrant Cases	Total Cases	Frequency
Current Study	**2013**		**Gastric**		**Asian**	***PIK3CA* Mutation**	**Sanger (exon 9, 20)**	**3**	**79**	**4%**
Li VS	2005	15784156	Gastric	Hong Kong	Asian	*PIK3CA* Mutation	Sanger (exon 9, 18, 20)	4	94	4%
Lee J	2012	22723903	Gastric	Korea	Asian	*PIK3CA* Mutation	Sequenom (OncoMap v4)	12	237	5%
Lee JW	2005	16397024	Gastric	Korea	Asian	*PIK3CA* Mutation	SSCP (exon 9, 20)	12	185	6%
Shi J	2012	22292935	Gastric	China	Asian	*PIK3CA* Mutation	Sanger (exon 9, 20)	8	113	7%
Velho S	2005	15994075	Gastric	Portugal	Caucasian	*PIK3CA* Mutation	Sanger (exon 9, 20)	5	47	11%
Corso G	2011	20937558	Gastric	Portugal	Caucasian	*PIK3CA* Mutation	Sanger (exon 9, 20)	9	63	14%
Wang K	2011	22037554	Gastric	Hong Kong	Asian	*PIK3CA* Mutation	Exome Sequencing	3	22	14%
Barbi S	2010	20398348	Gastric	Italy	Caucasian	*PIK3CA* Mutation	Sanger (exon 9, 20)	42	264	16%
Zang ZJ	2012	22484628	Gastric	Singapore	Asian	*PIK3CA* Mutation	Exome Sequencing	3	15	20%
Samuels Y	2004	15016963	Gastric	USA	Caucasian	*PIK3CA* Mutation	Sanger (all exons)	3	12	25%
Yasutaka	2012	23236232	Gastric	Japan	Asian	*PIK3CA* Mutation	Pyrosequencing (exon 1, 9, 20)	20	231	9%
Kiyose S	2012	22691185	Gastric	Japan	Asian	*PIK3CA* Amplification	FISH	10	353	3%
Byun DS	2003	12569555	Gastric	Korea	Asian	*PIK3CA* Amplification	PCR (semi-quantitative)	17	55	31%
Current Study	**2013**		**Gastric**		**Asian**	***PIK3CA* Amplification**	**QPCR**	**36**	**79**	**46%**
Shi J	2012	22292935	Gastric	China	Asian	*PIK3CA* Amplification	QPCR	88	131	67%
Current Study	**2013**		**Gastric**		**Asian**	***PTEN* Deletion**	**QPCR**	**1**	**79**	**1%**
Mina S	2012	22639407	Gastric	Germany	Caucasian	*PTEN* Deletion	FISH	8	180	4%
Oki E	2005	16051030	Gastric	Japan	Asian	*PTEN* Deletion	Capillary Electrophoresis	13	76	17%
Oki E	2006	16704528	Gastric	Japan	Asian	*PTEN* Deletion	Capillary Electrophoresis	13	76	17%
Byun DS	2003	12569555	Gastric	Korea	Asian	*PTEN* Deletion	PCR (semi-quantitative)	14	55	25%
Li YL	2005	15633233	Gastric	China	Asian	*PTEN* Deletion	Capillary Electrophoresis	9	30	30%
Current Study	**2013**		**Gastric**	**Singapore**	**Asian**	**p110α High**	**BD Biosciences Pharmingen, 1:300**	**4**	**79**	**5%**
Bai Z	2007	18184409	Gastric	China	Asian	PTEN Loss	Zymed 1:50	27	91	30%
Yang L	2003	12508347	Gastric	China	Asian	PTEN Loss	Maixim Biotech	96	184	52%
Current Study	**2013**		**Gastric**		**Asian**	**PTEN Loss**	**Cascade Bioscience 6H2.1, 1:400**	**43**	**79**	**54%**
Yang Z	2013	22521126	Gastric	China	Asian	PTEN Loss	Abcam ab76431, 1:150	30	50	60%
Bamias A	2010	20130877	Gastric	Greece	Caucasian	PTEN Loss	Dako 6H2.1, NA	51	66	77%
Fei G	2002	11953696	Gastric	Germany	Caucasian	PTEN Loss	Chemicon	21	26	81%
Current Study	**2013**		**Gastric**	**Singapore**	**Asian**	**pAKT High**	**Cell Signaling, 587F11, 1:200**	**14**	**79**	**18%**
Oki E	2005	15900596	Gastric	Japan	Asian	pAKT High	Cell Signaling, 1:10	22	76	29%
Yasutaka Sukawa	2012	23236232	Gastric	Japan	Asian	pAKT High	Cell Signaling, 1:100	119	231	52%
Murakami D	2007	17334718	Gastric	Japan	Asian	pAKT High	Cell Signaling, 1:100	81	140	58%
Cinti C	2008	18841391	Gastric	Italy	Caucasian	pAKT High	NEB	34	50	68%
Nam SY	2003	14678019	Gastric	Korea	Asian	pAKT High	NEB	237	301	79%
Murayama T	2009	19223902	Gastric	Japan	Asian	pAKT High	Cell Signaling, 1:50	94	109	86%
Ching-Shian Leong V	2008	19027487	Colorectal	Malaysia	Asian	*PIK3CA* Mutation	Sanger (exon 9, 20)	0	24	0%
Balschun K	2011	21704278	Colorectal	Germany	Caucasian	*PIK3CA* Mutation	Sanger (exon 20)	0	20	0%
Patel H	2007	17721920	Colorectal	UK	Caucasian	*PIK3CA* Mutation	Sanger (exon 9, 20)	5	127	4%
Soeda H	2012	22638623	Colorectal	Japan	Asian	*PIK3CA* Mutation	Sanger (exon 9, 20)	2	43	5%
Ohta M	2008	18619647	Colorectal	Japan	Asian	*PIK3CA* Mutation	Sanger (exon 9, 20)	4	52	8%
He Y	2009	19903786	Colorectal	the Netherlands	Caucasian	*PIK3CA* Mutation	Sanger (exon 9, 20)	19	240	8%
Ollikainen M	2007	17471559	Colorectal	Finland	Caucasian	*PIK3CA* Mutation	SSCP(exon 1, 9, 20)	6	70	9%
Tol J	2010	20413299	Colorectal	the Netherlands	Caucasian	*PIK3CA* Mutation	Sanger (exon 9, 20)	43	436	10%
Current Study	**2013**		**Colorectal**	**Singapore**	**Asian**	***PIK3CA* Mutation**	**Sanger (exon 9, 20)**	**12**	**116**	**10%**
Kato S	2007	17590872	Colorectal	Japan	Asian	*PIK3CA* Mutation	Sanger (exon 9, 20)	18	158	11%
Prenen H	2009	19366826	Colorectal	Belgium	Caucasian	*PIK3CA* Mutation	Sequenom (exon 9, 20)	23	200	12%
Tian Sun	2012	22798500	Colorectal	Netherlands	Caucasian	*PIK3CA* Mutation	Sanger (exon 9, 20)	44	381	12%
Lurkin I	2010	20098682	Colorectal	Netherlands	Caucasian	*PIK3CA* Mutation	Sanger (exon 9, 20)	34	294	12%
Sartore-Bianchi A	2009a	19806185	Colorectal	Italy	Caucasian	*PIK3CA* Mutation	Sanger (exon 9, 20)	17	132	13%
Perrone F	2009	18669866	Colorectal	Italy	Caucasian	*PIK3CA* Mutation	Sanger (exon 9, 20)	4	31	13%

Velho S	2005	15994075	Colorectal	Portugal	Caucasian	*PIK3CA* Mutation	SSCP (exon 9, 20)	14	103	14%
Velho S	2008	18782444	Colorectal	Portugal	Caucasian	*PIK3CA* Mutation	Sanger (exon 9. 20)	14	103	14%
Sartore-Bianchi A	2009b	19223544	Colorectal	Italy	Caucasian	*PIK3CA* Mutation	Sanger (exon 9, 20)	15	110	14%
Ekstrand AI	2010	19731079	Colorectal	Sweden	Caucasian	*PIK3CA* Mutation	Sanger (exon 9, 20)	5	36	14%
PERKins G	2010	20049837	Colorectal	France	Caucasian	*PIK3CA* Mutation	Sanger (NA)	6	42	14%
Nosho K	2008	18516290	Colorectal	USA	Caucasian	*PIK3CA* Mutation	Pyrosequencing (exon 9, 20)	91	590	15%
Souglakos J	2009	19603024	Colorectal	Greece	Caucasian	*PIK3CA* Mutation	Sequenom (exon 9, 20)	26	168	15%
Benvenuti S	2008	18022911	Colorectal	Italy	Caucasian	*PIK3CA* Mutation	Sanger (exon 9, 20)	28	175	16%
Barault L	2008	18224685	Colorectal	France	Caucasian	*PIK3CA* Mutation	Sanger (exon 1, 2, 9, 20)	98	586	17%
Ogino S	2009	19704056	Colorectal	USA	Caucasian	*PIK3CA* Mutation	Pyrosequencing (exon 9, 20)	75	439	17%
Simi L	2008	18628094	Colorectal	Italy	Caucasian	*PIK3CA* Mutation	HRMA (exon 9, 20)	20	116	17%
Ogino S	2009	19237633	Colorectal	USA	Caucasian	*PIK3CA* Mutation	Pyrosequencing (exon 9, 20)	82	450	18%
Campbell IG	2004	15520168	Colorectal	Australia	Caucasian	*PIK3CA* Mutation	SSCP, DHPLC (all exons)	6	32	19%
Frattini M	2005	16322273	Colorectal	Italy	Caucasian	*PIK3CA* Mutation	Same as Samuels	12	60	20%
Miyaki M	2007	17546593	Colorectal	Japan	Asian	*PIK3CA* Mutation	SSCP (exon 1, 7, 9, 20)	7	34	21%
Samuels Y	2004	15016963	Colorectal	USA	Caucasian	*PIK3CA* Mutation	Sanger (all exons)	74	234	32%
TCGA	2012	22810696	Colorectal	USA	Caucasian	*PIK3CA* Mutation	Exome Sequencing	34	276	12%
Current Study	**2013**		**Colorectal**	**Singapore**	**Asian**	***PIK3CA* Amplification**	**QPCR**	**5**	**116**	**4%**
Ollikainen M	2007	17471559	Colorectal	Finland	Caucasian	*PIK3CA* Amplification	QPCR	5	67	7%
Patel H	2007	17721920	Colorectal	UK	Caucasian	*PIK3CA* Amplification	QPCR	33	70	47%
Current Study	**2013**		**Colorectal**	**Singapore**	**Asian**	***PTEN* Deletion**	**QPCR**	**9**	**116**	**8%**
Nassif NT	2004	14724591	Colorectal	Australia	Caucasian	*PTEN* Deletion	Capillary Electrophoresis	7	41	17%
Goel A	2004	15126336	Colorectal	USA	Caucasian	*PTEN* Deletion	Capillary Electrophoresis	6	26	23%
Current Study	**2013**		**Colorectal**	**Singapore**	**Asian**	**p110α High**	**BD Biosciences Pharmingen, 1:300**	**1**	**116**	**1%**
Ekstrand AI	2010	19731079	Colorectal	Sweden	Caucasian	p110α High	Cell Signaling 4254, 1:50	24	49	49%
Tamer Colakoglu	2008	18440486	Colorectal	Turkey	Caucasian	PTEN Loss	Neomarkers Ab4	4	76	5%
Negri FV	2010	19953097	Colorectal	Italy	Caucasian	PTEN Loss	Millipore	5	43	12%
Razis E	2008	18700047	Colorectal	Greece	Caucasian	PTEN Loss	Novocastra, 28H6	10	72	14%
Frattini M	2005	16322273	Colorectal	Italy	Caucasian	PTEN Loss	Neomarkers , 1:50	7	40	18%
Laurent-Puig P	2009	19884556	Colorectal	France	Caucasian	PTEN Loss	R&D Systems AF847	31	162	19%
Molinari F	2009	19293803	Colorectal	Switzerlandd	Caucasian	PTEN Loss	Neomarkers, 1:50	8	38	21%
Ekstrand AI	2010	19731079	Colorectal	Sweden	Caucasian	PTEN Loss	Cell Signaling 9559, 1:100	11	49	22%
Nassif NT	2004	14724591	Colorectal	Australia	Caucasian	PTEN Loss	Cascase bioscience 6H2.1	10	41	24%
Goel A	2004	15126336	Colorectal	USA	Caucasian	PTEN Loss	Cascase bioscience 6H2.1	3	10	30%
Sartore-Bianchi A	2009a	19806185	Colorectal	Italy	Caucasian	PTEN Loss	Thermo Fisher Scientific, 1:200;	41	114	36%
Ollikainen M	2007	17471559	Colorectal	Finland	Caucasian	PTEN Loss	Cascase bioscience 6H2.1	24	62	39%
Sartore-Bianchi A	2009b	19223544	Colorectal	Italy	Caucasian	PTEN Loss	Thermo Fisher Scientific, 1:200;	32	81	40%
Frattini M	2007	17940504	Colorectal	Italy	Caucasian	PTEN Loss	Neomarkers, 1:50	11	27	41%
Tol J	2010	20413299	Colorectal	the Netherlands	Caucasian	PTEN Loss	Dako, 1:100	207	493	42%
Loupakis F	2009	19398573	Colorectal	Italy	Caucasian	PTEN Loss	Neomarkers 17.A, 1:20	36	85	42%
Mao C	2012	22586484	Colorectal	China	Asian	PTEN Loss	Unknown, 1:50	33	69	48%
Jang KS	2010	20102402	Colorectal	Korea	Asian	PTEN Loss	Novocastra Laboratories, 1:200	241	482	50%
Sawai H	2008	19036165	Colorectal	Japan	Asian	PTEN Loss	Santa Cruz, 28H6, 1:300	52	69	75%
Current Study	**2013**		**Colorectal**	**Singapore**	**Asian**	**PTEN Loss**	**Cascade Bioscience 6H2.1, 1:400**	**91**	**116**	**78%**
Schmitz KJ	2007	17149612	Colorectal	Germany	Caucasian	pAKT High	Cell Signaling, 1:20	28	133	21%
Current Study	**2013**		**Colorectal**	**Singapore**	**Asian**	**pAKT High**	**Cell Signaling, 587F11, 1:200**	**25**	**116**	**22%**

3.1.2 Frequency of PI3K pathway aberrations according to meta-analysis

Figure 3.1 and Table 3.2 summarize the frequencies of PI3K pathway aberrations obtained from the meta-analyses of all relevant publications and according to ethnicity. Details of the frequencies from individual studies and the methods used are provided in Table 3.1. The results from meta-analysis indicated that PTEN loss and high pAKT expression are the most frequent type of PI3K pathway aberration, with each found in approximately half of GC cases. PTEN loss was present in one-third of CRC cases and high p110α and pAKT expression was in half of CRC cases. The frequencies of *PIK3CA* mutations and amplifications were in the range of 12-23% for both GC and CRC, with *PIK3CA* amplification being about twice as common as mutation in both cancer types (Table 3.2).

GC from East Asian patients showed significantly fewer *PIK3CA* mutations than Caucasian patients (7% vs. 15% respectively) but more frequent *PTEN* deletion (23% vs. 4%; Figure 3.1). The increased incidence of *PTEN* deletion in East Asian GC patients was not reflected in PTEN loss however, which was significantly lower compared to Caucasians (47% vs 78%). In contrast to GC, PTEN loss in CRC was more frequent in Caucasians compared to East Asians (58% vs 26%). It should be noted however that with the exception of *PIK3CA* mutation, a high level of study heterogeneity (I^2>80) was observed for the all PI3K pathway aberrations (Table 3.2).

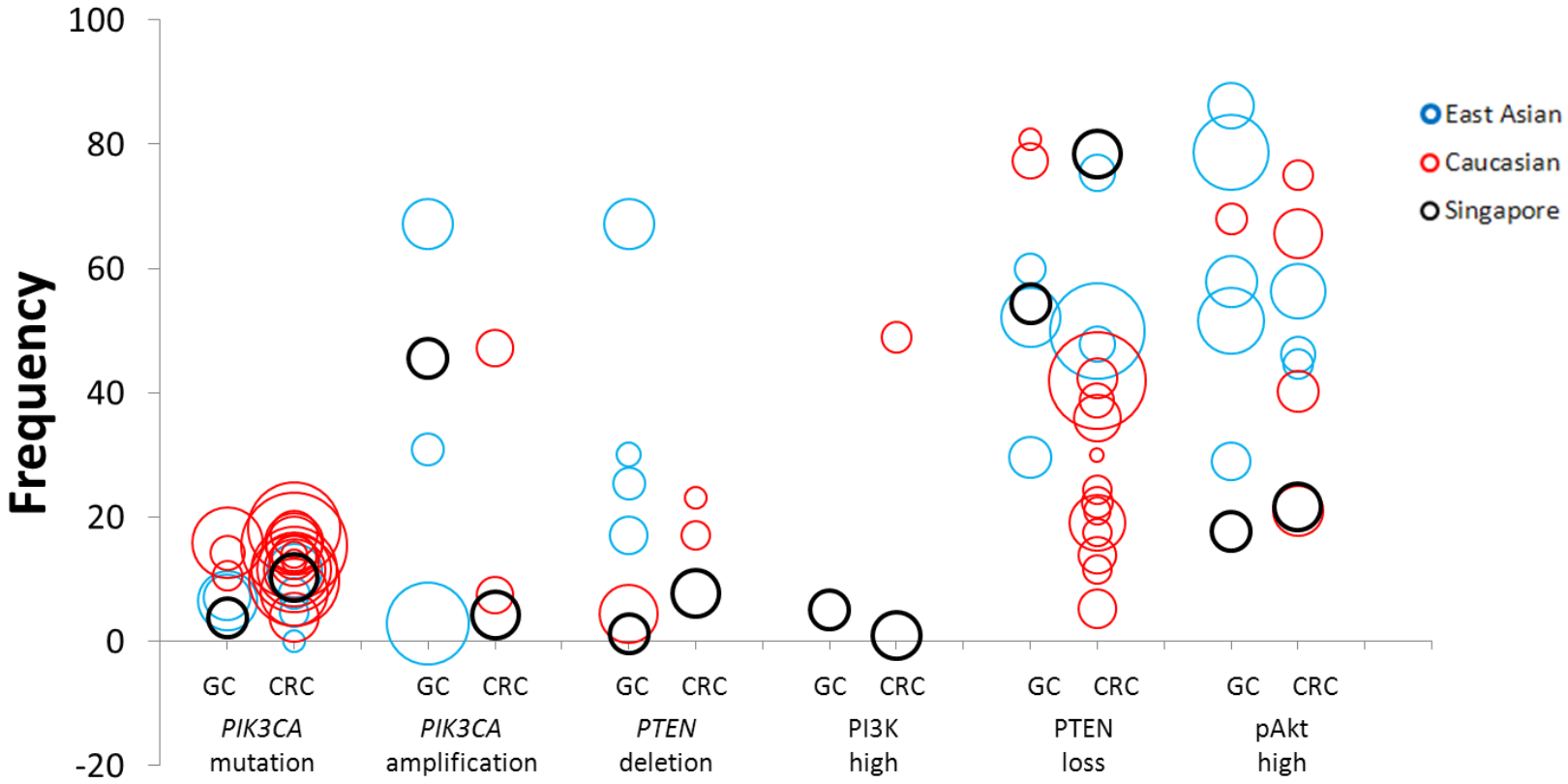

Figure 3.1. Frequencies of PI3K pathway aberrations in GC and CRC from published studies and laboratory analysis in the current study. The centre of each circle represents the frequencies reported in respective studies. The size of each circle is proportional to the sample size of the study. Studies on Caucasian populations are indicated by red circles, East Asian populations by blue circles, and the current study by black circles.

Table 3.2. Summarized frequencies of PI3K pathway aberrations from meta-analysis of published studies of GC and CRC, and laboratory analysis in the current study.

	Meta-analysis (All Studies)			Meta-analysis (Caucasian Studies)			Meta-analysis (East Asian Studies)			
Aberration	**Frequency [95%CI]**	**Studies (n)[1]**	**I^2 (%)**	**Frequency [95%CI]**	**Studies (n)[1]**	**I^2 (%)**	**Frequency [95%CI]**	**Studies (n)[1]**	**I^2 (%)**	**Current Study**
Gastric Cancer										
PIK3CA Mutation[2]	12.1% [9.8-14.9]	5 (672)	66.2	15.1% [11.8-19.1]	3 (374)	NA	6.7% [4.4-10.2]*	2 (298)	NA	3.8% (3/79)
PIK3CA Amplification	23.2% [2.6-77.3]	3 (539)	98.5	NA	NA	NA	23.2% [2.6-77.3]	3 (539)	98.5	45.6% (36/79)
PTEN Deletion	15.6% [11.4-20.9]	4 (341)	86.9	4.4% [2.2-8.6]	1 (180)	NA	23.0% [16.4-31.2]*	3 (161)	19.3	1.3% (1/79)
PI3K High	NA	NA	NA	NA	NA	NA	NA	NA	NA	5.1% (4/79)
PTEN Loss	68.9% [59.8-76.9]	5 (417)	90.1	78.2% [68.6-85.5]	2 (92)	NA	46.7% [30.6-63.6]*	3 (325)	87.3	54.4% (43/79)
pAKT High	66.1% [54.9-75.8]	6 (907)	95	68.0% [54.0-79.4]	1 (50)	NA	62.8% [43.7-78.6]	5 (857)	96	17.7% (14/79)
Colorectal Cancer										
PIK3CA Mutation[2]	12.4% [10.7-14.2]	19 (3756)	57.5	12.8% [10.7-14.2]	15 (3479)	61	9.1% [5.8-14.0]	4 (277)	8.7	10.3% (12/116)
PIK3CA Amplification	21.7% [2.6-74.5]	2 (137)	95.3	21.7% [2.6-74.5]	2 (137)	95.3	NA	NA	NA	4.3% (5/116)†
PTEN Deletion	19.6% [11.7-30.9]	2 (67)	NA	19.6% [11.7-30.9]†	2 (67)	NA	NA	NA	NA	7.8% (9/116)
PI3K High	49.0% [35.4-62.7]	1 (49)	NA	49.0% [35.4-62.7]	1 (49)	NA	NA	NA	NA	0.9% (1/116)
PTEN Loss	32.1% [25.5-39.6]†	16 (1905)	90.4	24.0% [17.7-31.7]†	13 (1285)	85.5	57.6% [42.2-71.7]*	3 (620)	86.7	78.4% (91/116)†
pAKT High	50.7% [43.2-58.1]†	7 (663)	91.2	49.8% [26.2-73.6]†	4 (393)	95.3	50.7% [42.9-58.6]†	3 (270)	34.8	21.6% (25/116)

[1]Number of studies (number of cases); [2] only studies which sequenced exon 9 and exon 20 of *PIK3CA* were included

* *p* value <0.05, Asian *vs* Caucasian; † indicates *p* value <0.05 between GC and CRC; NA= not available

3.1.3 Frequency of PI3K pathway aberrations according to single laboratory analysis

The 6 aberrations were evaluated in a single cohort of 140 GC and 150 CRC cases from a Singaporean population. These were analyzed using Sanger sequencing to detect *PIK3CA* mutations in exons 9 and 20, qPCR quantification of DNA copy numbers for *PIK3CA* and *PTEN*, and IHC for the expression of PI3K (p110α), PTEN and pAKT. Representative examples of these analyses are shown in Figure 3.2. Complete data for all 6 aberrations was obtained from 79 GC and 116 CRC cases and hence the subsequent analyses were restricted to these cases.

Figure 3.1 shows the frequency of aberrations observed in the present study (black circles) compared to results from the meta-analysis of East Asian patients. For both GC and CRC, the frequency of *PIK3CA* mutations was not significantly different to results from other East Asian studies (GC: 4% vs 7%; CRC: 10% vs 9%). However, in keeping with the high level of study heterogeneity noted earlier in the meta-analysis, a poor concordance was observed for the remaining aberrations.

The use of consistent analytical methods for PI3K pathway aberration allowed GC and CRC to be compared directly. Significant differences in the frequencies of *PIK3CA* amplification (46% vs. 4%, respectively) and PTEN loss (54% vs. 78%) were observed (Figure 3.1).

Fig.3.2 (Legend over page)

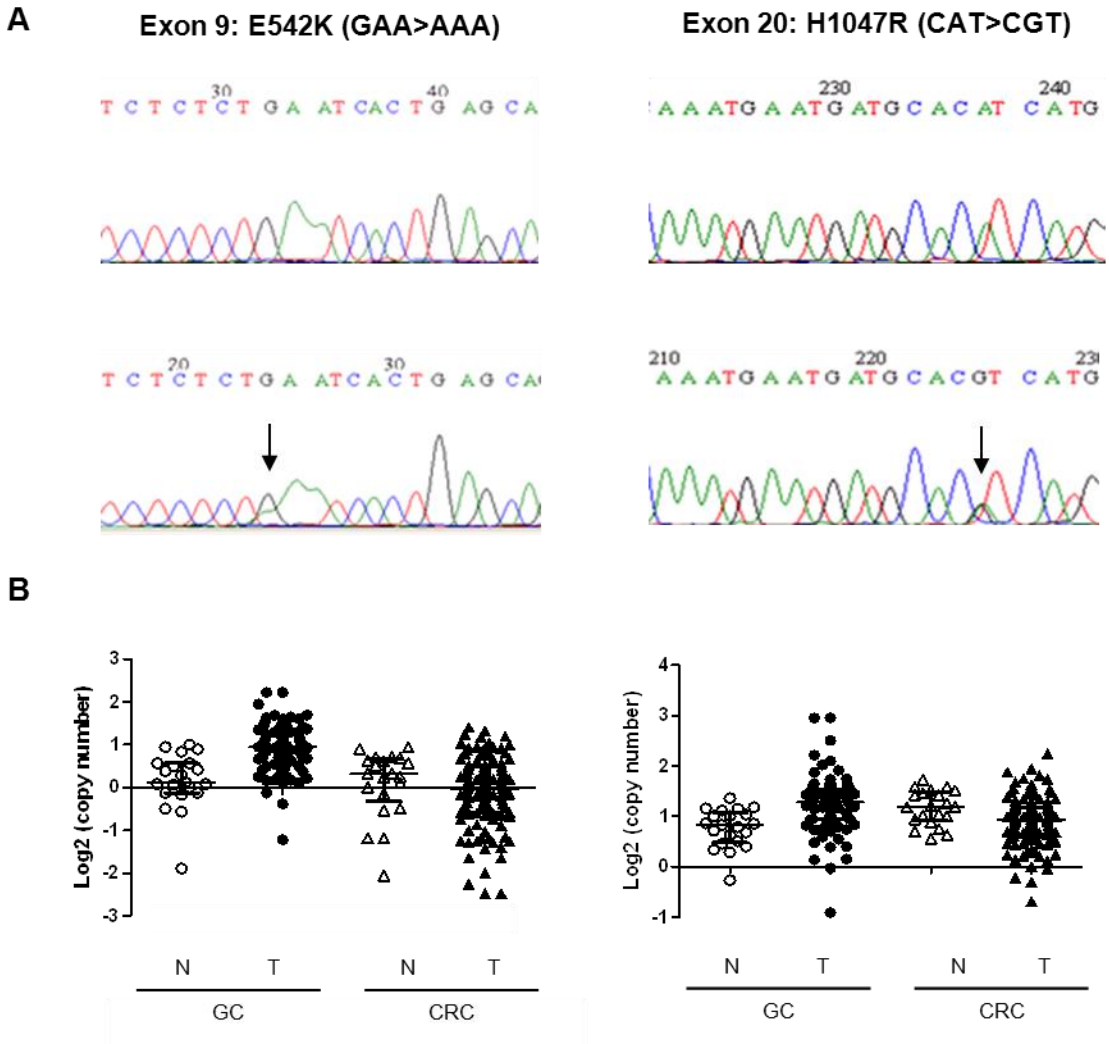

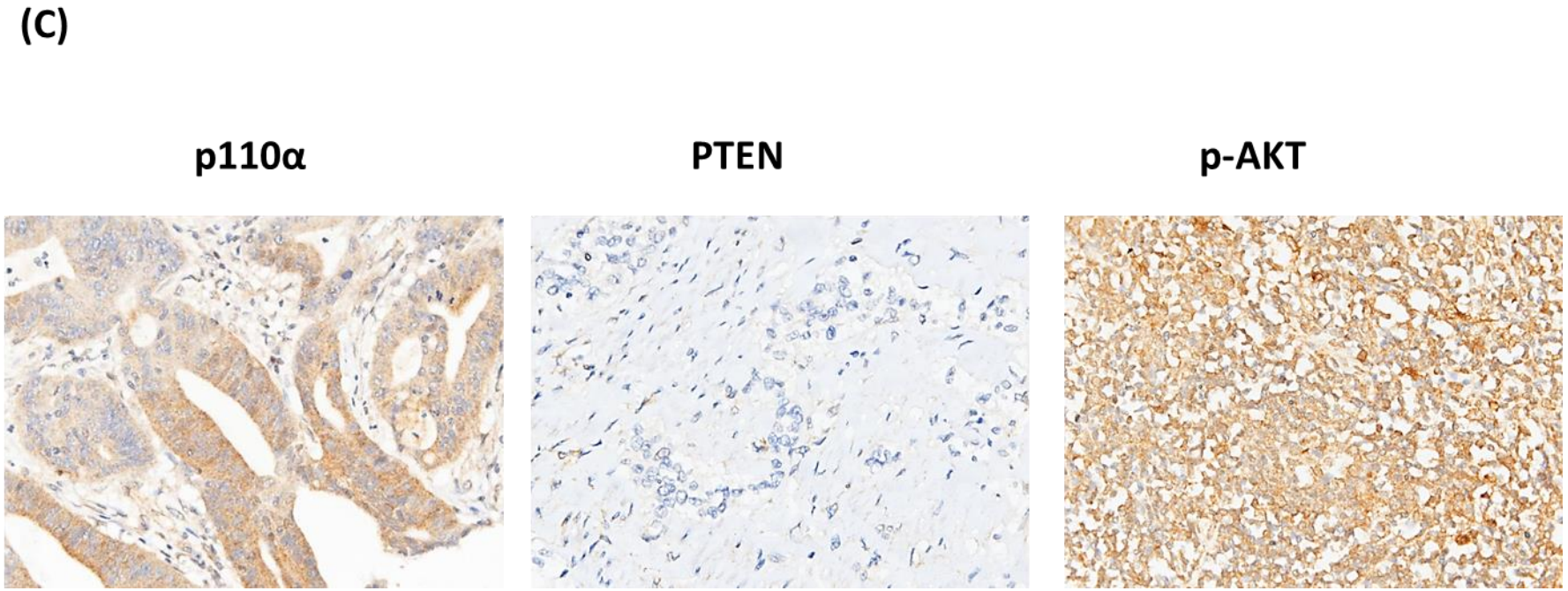

Figure 3.2. Representative data from Sanger sequencing, qPCR and IHC. (A) Representative chromatograms from Sanger sequencing of *PIK3CA* mutations of E542K (left panels) and H1047R (right panels) in normal tissue (upper panels) and tumour (lower panels). (B) Distribution of copy numbers for *PIK3CA* (left panel) and *PTEN* (right panel) in tumour (T) and normal tissue (N) from gastric cancer (GC) and colorectal cancer (CRC). The values of the mean ± 2 standard deviations are indicated for each group of values. (C) Representative images of immunohistochemistry for p110α (left panel) PTEN (middle panels) and p-AKT (right panels) expression in GC and CRC (40x magnification).

3.1.4 Co-occurrence of PI3K pathway aberrations

Figure 3.3 displays the co-occurrence of PI3K pathway alterations in individual GC and CRC samples from the current laboratory analysis. At least one PI3K pathway aberration was found in 86% of GC and 90% of CRC samples. The majority of aberrations were mutually exclusive, with 52% of GC and 60% of CRC having just one aberration. The genetic aberrations in particular showed rare co-occurrence, with only 3/65 (5%) cases showing two aberrations (*PIK3CA* mutation and amplification in GC, *PIK3CA* amplification and *PTEN* deletion in GC, *PIK3CA* mutation and *PTEN* deletion in CRC). The analysis of co-occurrence also revealed the two most common aberrations in GC were PTEN loss alone (27%) and *PIK3CA* amplification/PTEN loss (20%), while in CRC they were PTEN loss alone (52%) and PTEN loss/high pAKT (13%).

(A)

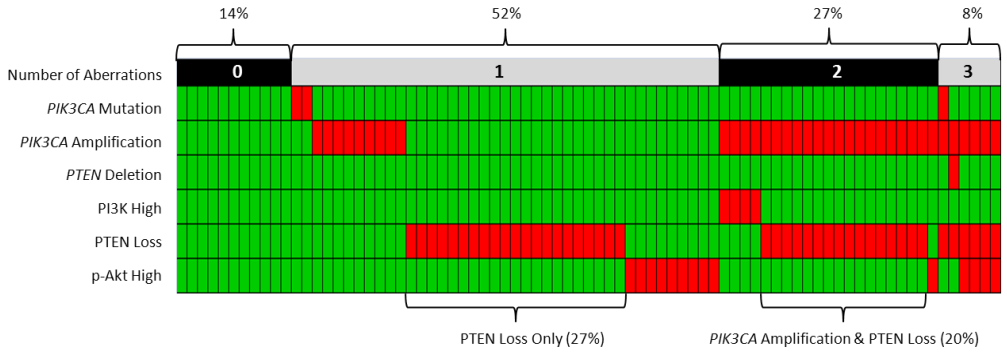

(B)

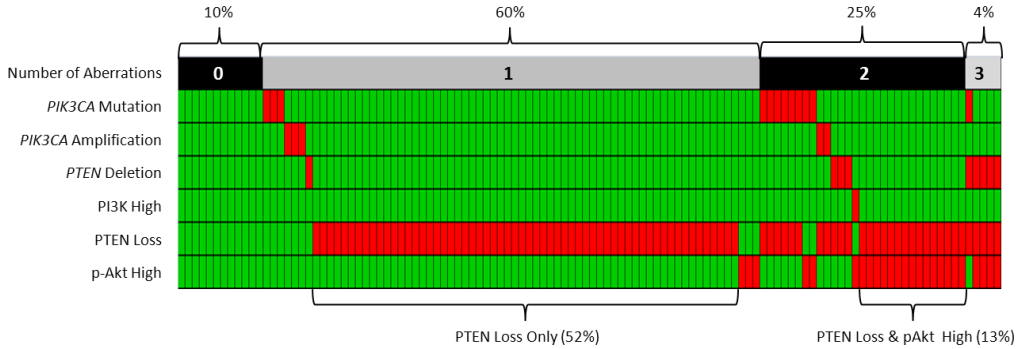

Figure 3.3. Co-occurence patterns for PI3K pathway aberrations in (A) GC and (B) CRC. Each column represents a tumour sample and each row corresponds to a PI3K aberration.Tumours are grouped according to the number of observed aberrations in each tumour (0, 1, 2 or 3). Green and red bars represent absence and presence respectively of the PI3K aberration.

3.1.5 Association between PI3K pathway aberrations

Pair-wise association analysis was performed between different PI3K pathway aberrations to assess the relationship of aberrations to each other (Table 3.3).The only significant association observed was between PTEN loss and high pAKT expression in GC (p=0.04). Other expected associations, such as between high pAKT expression and *PIK3CA* mutation, *PIK3CA* amplification, *PTEN* deletion or PTEN loss, did not reach significance.

3.1.6 Associations with clinicopathological features

The frequencies of PI3K pathway aberrations according to clinicopathological features in GC and CRC are shown in Table 3.4 and Table 3.5, respectively. The frequencies of the two most common patterns of aberration from analysis of co-occurrence described above were also examined. In GC, *PIK3CA* amplification was more frequent in older patients (p=0.04). In CRC, PTEN loss alone was more common in female patients (p=0.02) and PTEN loss/high pAKT was more frequent in male patients (p=0.01)

Table 3.3. Association between PI3K pathway aberrations in GC and CRC. Odds ratio (95% CI).

	***PIK3CA* Amplification**	***PTEN* Deletion**	**PI3K High**	**PTEN Loss**	**p-AKT High**
Gastric Cancer					
PIK3CA Mutation	0.59 (0.05-6.74)	NA	NA	0.41 (0.04-4.65)	NA
PIK3CA Amplification		NA	NA	1.65 (0.67-4.04)	0.6 (0.18-2.02)
PTEN Deletion			NA	NA	NA
PI3K High				NA	NA
PTEN Loss					0.27* (0.08-0.94)
Colorectal Cancer					
PIK3CA Mutation	NA	1.10 (0.13-9.56)	1.53 (0.30-7.85)	0.33 (0.10-1.16)	0.70 (0.14-3.44)
PIK3CA Amplification		NA	NA	0.17 (0.03-1.05)	NA
PTEN Deletion			NA	2.31 (0.28-19.43)	3.28 (0.81-13.27)
PI3K High				NA	NA
PTEN Loss					0.84 (0.29-2.38)

* p value < 0.05; NA= not applicable (mutually exclusive

Table 3.4. Associations between different PI3K pathway aberrations and clinicopathological parameters in GC.

Parameter	*PIK3CA* Mutation	*PIK3CA* Amplification	*PTEN* Deletion	PI3K High	PTEN Loss	pAKT High	PTEN Loss Only	Amplification & PTEN Loss
Ethnicity								
Chinese (68)	3 (4%)	30 (44%)	1 (1%)	3 (4%)	37 (54%)	12 (18%)	19 (28%)	13 (19%)
Non-Chinese (11)	0 (0%)	6 (55%)	0 (0%)	1 (9%)	6 (55%)	2 (18%)	2 (18%)	3 (27%)
Gender								
Male (64)	3 (5%)	29 (45%)	1 (2%)	4 (6%)	33 (52%)	12 (19%)	15 (23%)	13 (20%)
Female (15)	0 (0%)	7 (47%)	0 (0%)	0 (0%)	10 (67%)	2 (13%)	6 (40%)	3 (20%)
Age								
<69 (37)	3 (8%)	12 (32%)*	1 (3%)	0 (0%)	21 (57%)	7 (19%)	12 (32%)	6 (16%)
≥69 (42)	0 (0%)	24 (57%)*	0 (0%)	4 (10%)	22 (52%)	7 (17%)	9 (21%)	10 (24%)
Stage								
I & II (30)	2 (7%)	10 (33%)	0 (0%)	1 (3%)	15 (50%)	7 (23%)	8 (27%)	6 (20%)
III & IV (49)	1 (2%)	26 (53%)	1 (2%)	3 (6%)	28 (57%)	7 (14%)	13 (27%)	10 (20%)
Differentiation								
Well/Moderate (23)	0 (0%)	8 (35%)	0 (0%)	1 (4%)	10 (43%)	6 (26%)	5 (22%)	5 (22%)
Poor/NOS (56)	3 (5%)	28 (50%)	1 (2%)	3 (5%)	33 (59%)	8 (14%)	16 (29%)	11 (20%)
Tumour Size								
<4cm (32)	1 (3%)	16 (50%)	0 (0%)	3 (9%)	14 (44%)	6 (19%)	5 (16%)	8 (25%)
≥4cm (47)	2 (4%)	20 (43%)	1 (2%)	1 (2%)	29 (62%)	8 (17%)	16 (34%)	8 (17%)
Perforation								
Absent (75)	3 (4%)	35 (47%)	1 (1%)	4 (5%)	41 (55%)	14 (19%)	19 (25%)	16 (21%)
Present (4)	0 (0%)	1 (25%)	0 (0%)	0 (0%)	2 (50%)	0 (0%)	2 (50%)	0 (0%)
Lauren classification								
Intestinal (48)	1 (2%)	23 (48%)	1 (2%)	4 (8%)	26 (54%)	9 (19%)	11 (23%)	12 (25%)
Non-intestinal (31)	2 (6%)	13 (42%)	0 (0%)	0 (0%)	17 (55%)	5 (16%)	10 (32%)	4 (13%)
Lymphatic invasion								
Absent (36)	2 (6%)	14 (39%)	0 (0%)	1 (3%)	19 (53%)	5 (14%)	7 (19%)	7 (19%)
Present (43)	1 (2%)	22 (51%)	1 (2%)	3 (7%)	24 (56%)	9 (21%)	10 (23%)	9 (21%)
Perineural invasion								
Absent (36)	2 (6%)	13 (36%)	0 (0%)	2 (6%)	18 (50%)	6 (17%)	6 (17%)	6 (17%)
Present (43)	1 (2%)	23 (53%)	1 (2%)	2 (5%)	25 (58%)	8 (19%)	11 (26%)	9 (21%)
H.pylori								
Absent (69)	3 (4%)	32 (46%)	1 (1%)	4 (6%)	37 (54%)	11 (16%)	18 (26%)	14 (20%)
Present (10)	0 (0%)	4 (40%)	0 (0%)	0 (0%)	6 (60%)	3 (30%)	3 (30%)	2 (20%)

* represent p value <0.05

Table 3.5. Associations between different PI3K pathway aberrations and clinicopathological parameters in CRC.

Parameter	*PIK3CA* Mutation	*PIK3CA* Amplification	*PTEN* Deletion	PI3K High	PTEN Loss	pAKT High	PTEN Loss Only	PTEN Loss & pAKT_High
Ethnicity								
Chinese (100)	11 (11%)	5 (5%)	7 (7%)	0 (0%)	79 (79%)	20 (20%)	54 (54%)	12 (12%)
Non-Chinese (16)	1 (6%)	0 (0%)	2 (13%)	1 (6%)	12 (75%)	5 (31%)	6 (38%)	3 (19%)
Gender								
Male (54)	7 (13%)	3 (6%)	3 (6%)	1 (2%)	41 (76%)	18 (33%)	21 (39%)*	12 (22%)*
Female (62)	5 (8%)	2 (3%)	6 (10%)	0 (0%)	50 (81%)	7 (11%)	39 (63%)*	3 (5%)*
Age								
<65 (57)	7 (12%)	3 (5%)	3 (5%)	1 (2%)	43 (75%)	12 (21%)	29 (51%)	6 (11%)
≥65 (59)	5 (8%)	2 (3%)	6 (10%)	0 (0%)	48 (81%)	13 (22%)	31 (53%)	9 (15%)
Site								
Proximal colon (26)	2 (8%)	1 (4%)	3 (12%)	0 (0%)	17 (65%)	7 (27%)	11 (42%)	4 (15%)
Distal colon/rectal (90)	10 (11%)	4 (4%)	6 (7%)	1 (1%)	74 (82%)	18 (20%)	49 (54%)	11 (12%)
Stage								
I & II (54)	8 (15%)	1 (2%)	5 (9%)	1 (2%)	40 (74%)	14 (26%)	24 (44%)	7 (13%)
III & IV (62)	4 (6%)	4 (6%)	4 (6%)	0 (0%)	51 (82%)	11 (18%)	36 (58%)	8 (13%)
Grade								
Well/Moderate (102)	12 (12%)	5 (5%)	7 (7%)	1 (1%)	80 (78%)	22 (22%)	52 (51%)	14 (14%)
Poor (14)	0 (0%)	0 (0%)	2 (14%)	0 (0%)	11 (79%)	3 (21%)	8 (57%)	1 (7%)
Tumour Size								
<4cm (51)	5 (10%)	0 (0%)	4 (8%)	0 (0%)	43 (84%)	9 (18%)	30 (59%)	6 (12%)
≥4cm (65)	7 (11%)	5 (8%)	5 (8%)	1 (2%)	48 (74%)	16 (25%)	30 (46%)	9 (14%)
Perforation								
Absent (111)	12 (11%)	5 (5%)	9 (8%)	1 (1%)	87 (78%)	25 (23%)	56 (50%)	15 (14%)
Present (5)	0 (0%)	0 (0%)	0 (0%)	0 (0%)	4 (80%)	0 (0%)	4 (80%)	0 (0%)
Vascular invasion								
Absent (99)	11 (11%)	3 (3%)	8 (8%)	1 (1%)	80 (81%)	23 (23%)	51 (52%)	14 (14%)
Present (17)	1 (6%)	2 (12%)	1 (6%)	0 (0%)	11 (65%)	2 (12%)	9 (53%)	1 (6%)
Lymphatic invasion								
Absent (102)	11 (11%)	4 (4%)	8 (8%)	1 (1%)	80 (78%)	24 (24%)	51 (50%)	15 (15%)
Present (14)	1 (7%)	1 (7%)	1 (7%)	0 (0%)	11 (79%)	1 (7%)	9 (64%)	0 (0%)
Perineural invasion								
Absent (111)	12 (11%)	5 (5%)	9 (8%)	1 (1%)	88 (79%)	25 (23%)	57 (51%)	15 (14%)
Present (5)	0 (0%)	0 (0%)	0 (0%)	0 (0%)	3 (60%)	0 (0%)	3 (60%)	0 (0%)

* represent *p* value <0.05.

3.1.7 Associations with survival

Survival analysis was performed in 59 GC and 86 CRC patients that did not receive chemotherapy. These were selected to allow the prognostic value of PI3K pathway aberrations to be assessed without the confounding influence of chemotherapy. The median survival time of these patients was 15 months (range 1-131) for GC and 23 (range 0-141) months for CRC. The prognostic impact of clinicopathological features and PI3K pathway aberrations are shown for GC and CRC in Table 3.6 and Table 3.7, respectively. In GC, the features of tumour stage, intestinal subtype, perforation, lymphatic and perineural invasion were associated with worse survival, but none of the PI3K pathway aberrations showed prognostic significance. In CRC, tumour stage and the presence of vascular, lymphatic and perineural tumour invasion were associated with worse survival. *PIK3CA* amplification was also associated with worse survival in univariate analysis (HR=3.20, 95%CI=1.12-9.14, p=0.03) but failed to reach significance in multivariate analysis (HR=2.75, 95%CI= 0.90-8.41, p=0.08).

Table 3.6. Prognostic significance of PI3K pathway aberrations and clinicopathological variables in GC patients treated with surgery alone (n=59).

Parameter	HR	95%CI	*P value*
Univariate survival analysis			
Clinicopathological Features			
Ethnicity (non-Chinese vs Chinese)	0.68	0.16-2.88	0.60
Gender (female vs male)	1.07	0.40-2.85	0.89
Age (≥69 vs <69)	1.67	0.74-3.76	0.21
Stage (III & IV vs I & II)	4.77	1.80-12.61	<0.01
Tubular differentiation (poor/NOS vs well/moderate)	2.43	0.92-6.37	0.07
Lauren classification (Intestinal vs non-intestinal)	3.14	1.49-6.63	<0.01
Tumour Size (≥4 vs <4)	2.26	1.00-5.08	0.05
Perforation (yes vs no)	16.72	3.87-72.16	<0.01
Lymphatic invasion (yes vs no)	2.65	1.20-5.84	0.02
Perineural invasion (yes vs no)	4.21	1.79-9.91	<0.01
H.pylori (yes vs no)	0.57	0.17-1.90	0.36
PI3K pathway aberrations			
PIK3CA mutation (mutation vs wildtype)	0.05	0.00-1728.00	0.57
PIK3CA amplification (amplification vs wildtype)	1.35	0.66-2.76	0.42
PTEN deletion (deletion vs wildtype)	1.52	0.21-11.29	0.68
PI3K overexpression (presence vs absence)	0.05	0.00-78.20	0.42
PTEN (loss vs normal)	1.56	0.74-3.27	0.24
pAKT overexpression (presence vs absence)	0.77	0.29-2.01	0.59
Major PI3K pathway aberrations (combined analysis)			
PTEN only (presence vs absence)	1.24	0.56-2.73	0.60
PIK3CA amplification & PTEN loss (presence vs absence)	1.00	0.38-2.64	>0.99
Multivariate survival analysis			
Stage (III & IV vs I & II)	1.78	0.57-5.61	0.32
Lauren classification (Intestinal vs non-intestinal)	2.63	1.13-6.10	0.03
Perforation (yes vs no)	13.74	2.84-66.44	<0.01
Lymphatic invasion (yes vs no)	1.16	0.42-3.20	0.77
Perineural invasion (yes vs no)	2.24	0.70-7.19	0.18

CI: confidence intervals; HR: hazard risk ratio.

Table 3.7. Prognostic significance of PI3K pathway aberrations and clinicopathological variables in CRC patients treated with surgery alone (n=86).

Parameter	HR	95%CI	*P value*
Univariate survival analysis			
Clinicopathological Features			
Ethnicity (non-Chinese vs Chinese)	0.61	0.22-1.73	0.35
Gender (female vs male)	1.28	0.66-2.50	0.46
Age (≥65 vs <65)	1.42	0.71-2.82	0.32
Site (distal & rectal vs proximal)	1.36	0.60-3.11	0.46
Stage (III & IV vs I & II)	5.07	2.54-10.13	<0.01
Grade (poor vs well/moderate)	1.29	0.46-3.66	0.63
Tumour Size (≥4 vs <4)	0.71	0.37-1.35	0.30
Perforation (yes vs no)	1.76	0.54-5.75	0.35
Vascular invasion (yes vs no)	2.58	1.06-6.28	0.04
Lymphatic invasion (yes vs no)	4.06	1.64-10.06	<0.01
Perineural invasion (yes vs no)	5.74	1.63-20.27	<0.01
PI3K pathway aberrations			
PIK3CA mutation (mutation vs wildtype)	0.17	0.02-1.27	0.08
PIK3CA amplification (amplification vs wildtype)	3.20	1.12-9.14	0.03
PTEN deletion (deletion vs wildtype)	0.22	0.03-1.57	0.13
PI3K High (presence vs absence)	0.05	0.00-2529	0.59
PTEN (loss vs normal)	1.78	0.70-4.58	0.23
pAKT High (presence vs absence)	0.74	0.29-1.90	0.53
Major PI3K pathway aberrations (combined analysis)			
PTEN loss only (presence vs absence)	2.00	1.02-3.93	0.05
PTEN loss & High pAKT (presence vs absence)	1.18	0.46-3.03	0.76
Multivariate survival analysis			
Stage (III & IV vs I & II)	4.47	2.09-9.53	<0.01
Vascular invasion (yes vs no)	0.79	0.28-2.22	0.66
Lymphatic invasion (yes vs no)	1.47	0.56-3.88	0.43
Perineural invasion (yes vs no)	3.43	0.82-14.4	0.09
PIK3CA amplification (amplification vs wildtype)	2.75	0.90-8.41	0.08

CI: confidence intervals; HR: hazard risk ratio.

3.2 Discussion

The entry of PI3K pathway inhibitors into clinical trials has generated a keen interest in identifying predictive biomarkers that can be used to select patients who are most likely to benefit. Numerous authors have suggested that *PIK3CA* mutation could be a useful biomarker, with several independent studies reporting an association with *in-vitro* drug sensitivity or clinical response (Table 3.8).

The relatively low frequency of *PIK3CA* mutations, together with observed activity of PI3K inhibitors in *PIK3CA* wildtype tumour cells, has led to consideration of other factors as possible biomarkers. *PTEN* loss, *PTEN* mutation, *KRAS* mutation, *HER2* amplification, *BRAF* mutation and elevated expression of phosphorylated AKT have all been associated with sensitivity and response to PI3K inhibitors (Table 3.8). However, the lack of reproducibility of these associations have also cast doubt about their potential utility as biomarkers. Nonetheless, several of these molecular features have been incorporated into clinical trials. For example, the recruitment of patients to trials BYL719 (NCT01219699) and GSK2636771 (NCT01458067) is based on their tumours containing *PIK3CA* mutation or amplification, or PTEN deficiency, respectively.

Table 3.8 Reported associations between candidate biomarkers of PI3K pathway inhibitors and sensitivity or response to PI3K pathway inhibitors. Red cells indicate a positive association, green cells indicate an inverse association and black cells indicate a observed lack of significant association.

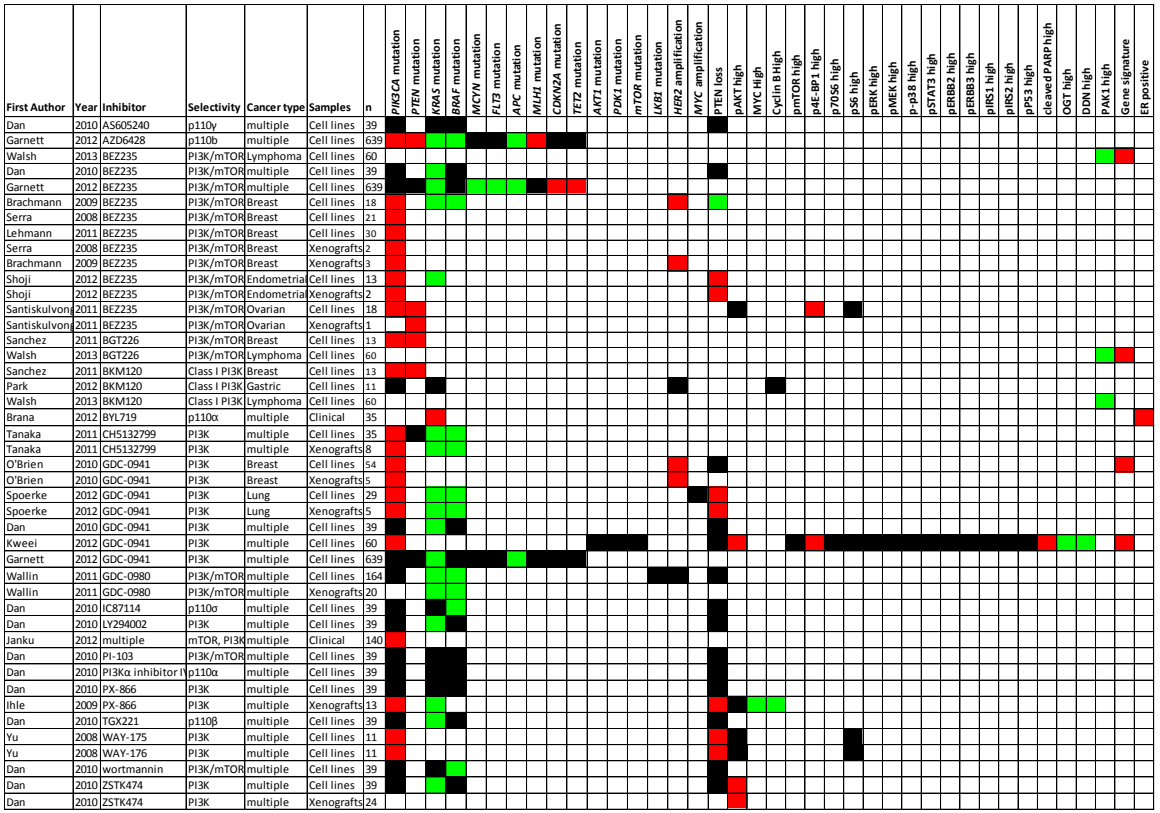

First Author	Year	Inhibitor	Selectivity	Cancer type	Samples	n	*PIK3CA* mutation	*PTEN* mutation	*KRAS* mutation	*BRAF* mutation	*MCYN* mutation	*FLT3* mutation	*APC* mutation	*MLH1* mutation	*CDKN2A* mutation	*TET2* mutation	*AKT1* mutation	*PDK1* mutation	*mTOR* mutation	*LKB1* mutation	*HER2* amplification	*MYC* amplification	PTEN loss	pAKT high	MYC High	Cyclin B High	pmTOR high	p4E-BP1 high	p70S6 high	p56 high	pERK high	pMEK high	p-p38 high	pSTAT3 high	pERBB2 high	pERBB3 high	pIRS1 high	pIRS2 high	pPS3 high	cleaved PARP high	OGT high	DDN high	PAK1 high	Gene signature	ER positive
Dan	2010	AS605240	p110γ	multiple	Cell lines	39																																							
Garnett	2012	AZD6428	p110b	multiple	Cell lines	639																																								
Walsh	2013	BEZ235	PI3K/mTOR	Lymphoma	Cell lines	60																																								
Dan	2010	BEZ235	PI3K/mTOR	multiple	Cell lines	39																																							
Garnett	2012	BEZ235	PI3K/mTOR	multiple	Cell lines	639																																							
Brachmann	2009	BEZ235	PI3K/mTOR	Breast	Cell lines	18																																							
Serra	2008	BEZ235	PI3K/mTOR	Breast	Cell lines	21																																							
Lehmann	2011	BEZ235	PI3K/mTOR	Breast	Cell lines	30																																							
Serra	2008	BEZ235	PI3K/mTOR	Breast	Xenografts	2																																							
Brachmann	2009	BEZ235	PI3K/mTOR	Breast	Xenografts	3																																							
Shoji	2012	BEZ235	PI3K/mTOR	Endometrial	Cell lines	13																																							
Shoji	2012	BEZ235	PI3K/mTOR	Endometrial	Xenografts	2																																							
Santiskulvong	2011	BEZ235	PI3K/mTOR	Ovarian	Cell lines	18																																							
Santiskulvong	2011	BEZ235	PI3K/mTOR	Ovarian	Xenografts	1																																							
Sanchez	2011	BGT226	PI3K/mTOR	Breast	Cell lines	13																																							
Walsh	2013	BGT226	PI3K/mTOR	Lymphoma	Cell lines	60																																							
Sanchez	2011	BKM120	Class I PI3K	Breast	Cell lines	13																																							
Park	2012	BKM120	Class I PI3K	Gastric	Cell lines	11																																							
Walsh	2013	BKM120	Class I PI3K	Lymphoma	Cell lines	60																																							
Brana	2012	BYL719	p110α	multiple	Clinical	35																																							
Tanaka	2011	CH5132799	PI3K	multiple	Cell lines	35																																							
Tanaka	2011	CH5132799	PI3K	multiple	Xenografts	8																																							
O'Brien	2010	GDC-0941	PI3K	Breast	Cell lines	54																																							
O'Brien	2010	GDC-0941	PI3K	Breast	Xenografts	5																																							
Spoerke	2012	GDC-0941	PI3K	Lung	Cell lines	29																																							
Spoerke	2012	GDC-0941	PI3K	Lung	Xenografts	5																																							
Dan	2010	GDC-0941	PI3K	multiple	Cell lines	39																																							
Kweei	2012	GDC-0941	PI3K	multiple	Cell lines	60																																							
Garnett	2012	GDC-0941	PI3K	multiple	Cell lines	639																																							
Wallin	2011	GDC-0980	PI3K/mTOR	multiple	Cell lines	164																																							
Wallin	2011	GDC-0980	PI3K/mTOR	multiple	Xenografts	20																																							
Dan	2010	IC87114	p110α	multiple	Cell lines	39																																							
Dan	2010	LY294002	PI3K	multiple	Cell lines	39																																							
Janku	2012	multiple	mTOR, PI3K	multiple	Clinical	140																																							
Dan	2010	PI-103	PI3K/mTOR	multiple	Cell lines	39																																							
Dan	2010	PI3Kα inhibitor IV	p110α	multiple	Cell lines	39																																							
Dan	2010	PX-866	PI3K	multiple	Cell lines	39																																							
Ihle	2009	PX-866	PI3K	multiple	Xenografts	13																																							
Dan	2010	TGX221	p110β	multiple	Cell lines	39																																							
Yu	2008	WAY-175	PI3K	multiple	Cell lines	11																																							
Yu	2008	WAY-176	PI3K	multiple	Cell lines	11																																							
Dan	2010	wortmannin	PI3K/mTOR	multiple	Cell lines	39																																							
Dan	2010	ZSTK474	PI3K	multiple	Cell lines	39																																							
Dan	2010	ZSTK474	PI3K	multiple	Xenografts	24																																							

Since the frequencies of PI3K pathway aberrations represent an increasingly important consideration in the development of PI3K inhibitors, this study was undertaken to consolidate the available information on 6 prominent PI3K pathway aberrations in GC and CRC. Through meta-analysis of published results, I have been able to summarize the overall frequency of aberrations and to investigate differences according to ethnicity and cancer type (Figure 3.1). These results should provide useful benchmarks and insights for further assessment, similar to previous meta-analyses of other genetic alterations such as *TP53* mutation (Soussi *et al.*, 2006), *KRAS* mutation (Ren *et al.*, 2012), *EGFR* mutations (Bria *et al.*, 2011), *HER2* amplification (Chan *et al.*, 2012) and microsatellite instability (Des Guetz *et al.*, 2009). In addition, the collation of individual study data containing information about the assays used, threshold values and study populations (Table 3.1) should facilitate further detailed investigation of individual PI3K pathway aberrations as potential biomarkers.

In the study of frequencies of PI3K pathway according to ethnicity, GC from East Asian patients notably showed lower frequencies of *PIK3CA* mutations and PTEN loss, but a higher frequency of *PTEN* deletion, compared to GC from Caucasian patients. PTEN loss was also more frequent in CRC from East Asian compared to Caucasian patients. Further confirmation of these findings could be important for understanding differences in the aetiology and biology of GC and CRC between Asian and Caucasian populations, as well as for the planning of clinical trials.

I caution however that with the exception of *PIK3CA* mutation, a high degree of study heterogeneity was observed in the current meta-analysis. Different methodologies are likely to explain much of the variation, as suggested by individual study data for *PTEN* deletion in GC (Table 3.1). The four East Asian studies were performed by semi-quantitative PCR or by capillary electrophoresis. These methods are likely to result in higher frequencies of aberration compared to the more conservative fluorescent in-situ hybridization method used in the single publication on Caucasian GC. The large variability in antibodies and staining conditions used to investigate PTEN loss probably also contributed to the wide range of reported frequencies for this aberration. The low study heterogeneity observed for *PIK3CA* mutation frequency indicates the differences between East Asians and Caucasians are real and could impact upon the results of clinical trials for PI3K inhibitors.

Single laboratory analysis of the 6 PI3K pathway aberrations performed in this study allowed direct comparison between GC and CRC and revealed several new insights. At least one PI3K pathway aberration was observed in 86% of GC and in 90% of CRC, indicating a significant involvement of this pathway in the development of gastrointestinal cancers (Figure 3.3). A high degree of mutual exclusion of the aberrations was also observed, with a larger proportion of tumours having single rather than multiple aberrations (52% vs 35% for GC; 60% vs 29% for CRC). This was especially apparent for genetic aberrations, with only 5% of cases showing concurrent changes. These results support the concept that single aberrations within the PI3K pathway are sufficient for hyperactivity, in a

manner akin to the sufficiency of either *KRAS* or *BRAF* mutations for MEK pathway activation.

Using common analytical methods I observed significant differences between GC and CRC for the frequencies of *PIK3CA* amplification (46% vs 4%, respectively), *PTEN* deletion (1% vs 8%) and PTEN loss (54% vs 78%). This could reflect varying dependence of gastric and colorectal tissue on different components of the PI3K pathway. In both GC and CRC, the much lower frequency of *PTEN* deletion compared to loss of PTEN expression suggests that alternate mechanisms such as *PTEN* methylation and possibly also mutation contribute to the reduced expression.

In conclusion, this meta-analysis and single laboratory study found evidence for ethnic and cancer type differences in the frequencies of some PI3K aberrations in GC and CRC. Analysis of co-occurrence uncovered that aberrations in the PI3K pathway occur in a large majority of GC and CRC tumours in a primarily mutually exclusive pattern. A degree of irreproducibility in reported frequencies and associations, as well as a high degree of heterogeneity in analytical methods, were also apparent. This heterogeneity could be clearly viewed as confounding the identification of reliable markers of response to PI3K pathway inhibitors. Caution should also be taken in interpreting ethnic differences observed in this study, as ethnicity was inferred from the country of origin of study populations. In a prior meta-analysis of sufficient study numbers, I found exclusion of US and multinational trials did not affect observations of ethnic differences in patient outcomes (Loh *et al.*, 2012). Nonetheless, the ethnic

heterogeneity of modern populations should be acknowledged and considered in interpreting observations of ethnic differences. Clarity in the field awaits further standardized and combined assessment of candidate PI3K response predictors in large, independent sample series and clinical trials.

4 Results: Identification of Potential Biomarkers using OncoCarta Analysis

4.1.1 Correlation of mutation profiles with IC_{50} values of BSP-A

For this study, BSP-A was used as a PI3K inhibitor to identify biomarkers of sensitivity as part of collaboration with Bayer Healthcare. I first screened a panel of GC and CRC cell lines for their sensitivity to BSP-A. BSP-A inhibited the proliferation of GC and CRC cell lines at concentration ranging from 18 nM to greater than 5000 nM (Figure 4.1). Among 34 GC and 14 CRC cell lines, 50% (24/48) had IC_{50} less than 1000 nM, 30% (14/48) had IC_{50} between 1000-5000 nM and 20% (10/48) had IC_{50} more than 5000 nM. The median IC_{50} values of BSP-A for all cell lines were 987 nM.

OncoCarta analysis was performed to identify 304 common hot-spot cancer mutations in 29 genes. Mutations of nine different genes (*PIK3CA, KRAS, BRAF, CTNBB1, FBX4, FBXW7, TP53, KIT and MAP2K1*) were identified in the GC and CRC cell lines (Table 4.1). Overall, cell lines with *PIK3CA* mutations were more sensitive to BSP-A than cell lines without *PIK3CA* mutations (p=0.001; Figure 4.1). There was no significant association between *KRAS* mutation and drug sensitivity in the cell lines. However, when the CRC cell lines were further divided into different types of *KRAS* mutation, *KRAS* (G12V) was significantly associated with higher IC_{50} values (p=0.004) compared to cell lines without *KRAS* (G12V) mutation. Taken together, this provides evidence that

PIK3CA mutation could be used as biomarker for response to BSP-A in GC and CRC, while *KRAS* (G12V) mutation could be used as biomarkers for response to BSP-A in CRC only.

Table 4.1. Mutation status of 36 GC and 14 CRC cell lines determined by OncoCarta analysis.

Cell Lines	Cancer Type	Mutations
AGS	GC	*KRAS*(G12D), *CTNNB1*(G34E), *PIK3CA*(E545A)
AZ521	GC	*CTNNB1*(S37F)
CLS145	GC	WT
FU97	GC	WT
HGC27	GC	*PIK3CA*(E542K)
HS746T	GC	WT
IM95	GC	*PIK3CA*(E542K)
IST1	GC	WT
KATOIII	GC	WT
MKN1	GC	*FBX4* (S8R)
MKN28	GC	WT
MKN45	GC	WT
MKN7	GC	WT
MKN74	GC	*KRAS*(G12V)
NCI-N87	GC	WT
NUGC2	GC	*KRAS*(T58I), *TP53*(G245S)
NUGC3	GC	WT
NUGC4	GC	WT
OCUM1	GC	*CTNNB1*(S45C)
RERF	GC	WT
SCH	GC	WT
SNU1	GC	*KRAS*(G12D)
SNU16	GC	WT
SNU5	GC	WT
TMK1	GC	*FBX4*(S8R)
YCC1	GC	*TP53*(R175H)
YCC10	GC	*PIK3CA*(H1047R)
YCC11	GC	WT
YCC16	GC	*KRAS*(Q61H), *PIK3CA*(E545K), *MAP2K1*(Y134C)
YCC17	GC	*BRAF*(G596R), *PIK3CA*(E545K), *TP53*(R273H)
YCC18	GC	*TP53*(R273C)
YCC19	GC	*KIT*(D52N)
YCC20	GC	WT
YCC3	GC	*FBX4*(S8R), *TP53*(R175H)
YCC6	GC	WT
YCC7	GC	*FBX4*(S8R), *TP53*(R175H)
CCK81	CRC	*PIK3CA*(C420R), *CTNNB1*(T41A), *FBXW7*(R465C)
COLO205	CRC	*BRAF*(V600E)
COLO320	CRC	*TP53*(R248W)
DLD1	CRC	*KRAS*(G13D), *PIK3CA*(E545K)
HCC56	CRC	*KRAS*(G12V)
HCT116	CRC	*KRAS*(G13D), *PIK3CA*(H1047R), *CTNNB1*(S45P)
HT29	CRC	*BRAF*(V600E), *TP53*(R273H)
LS513	CRC	*KRAS*(G12D)
RCM1	CRC	*KRAS*(G12V)
RKO	CRC	*BRAF*(V600E), *PIK3CA*(H1047R)
SW403	CRC	*KRAS*(G12V)
SW480	CRC	*KRAS*(G12V), *TP53*(R273H)
SW620	CRC	*KRAS*(G12V), *TP53*(R273H)
WIDR	CRC	*BRAF*(V600E), *TP53*(R273H)

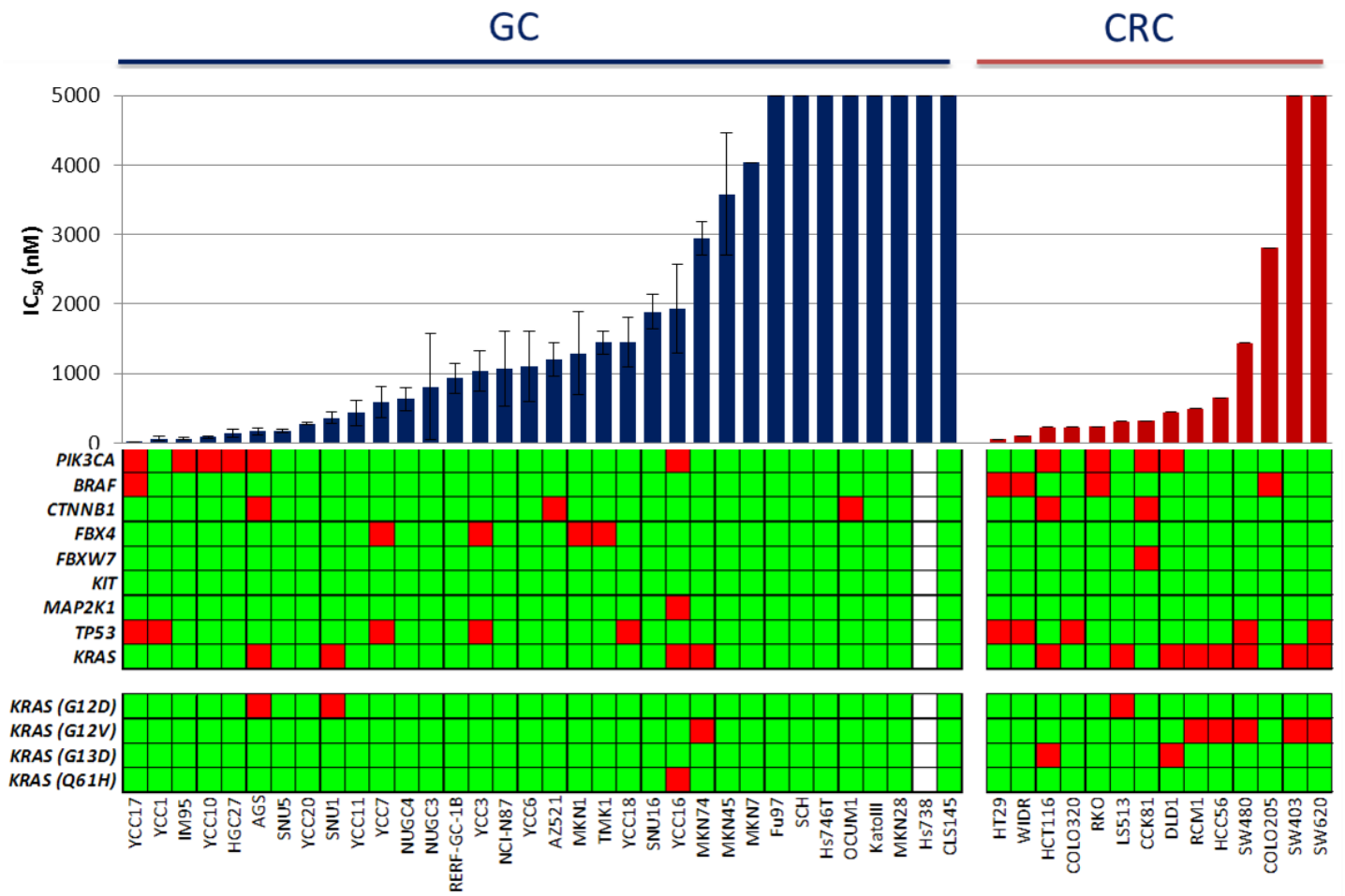

Figure 4.1. IC_{50} values for BSP-A in 34 GC and 14 CRC cell lines. The IC_{50} values of PI3K inhibitors in the GC cell lines were obtained from the average value of three independent experiments. The IC_{50} values of PI3K inhibitors in the CRC cell lines were obtained from single experiment. Each experiment was performed in three technical replicates. Heatmap (top panel) represents the mutation status of selected genes in the cell lines. Green indicates absence of mutation and red indicates presence of mutation. The heatmap (bottom panel) represents subtypes of *KRAS* mutations in the cell lines.

4.1.2 Signal transduction of KRAS/PI3K/ERK pathway

CRC cell lines with *KRAS* (G12V) mutations were resistant to BSP-A, suggesting that cells with this mutation are not addicted to the PI3K pathway and may depend on other pathways for survival. One such alternate pathway could be the ERK pathway, as it has been reported that mutant *KRAS* (G12V) interacts with Raf-1 and transduces signals mainly through the ERK pathway in NIH3T3 cells (Cespedes *et al.*, 2006). Therefore, I sought to confirm whether CRC cell lines with *KRAS* (G12V) are resistant to PI3K inhibition due to their dependency on the ERK pathway. Colo320, LS513, SW403 and LOVO cell lines with different mutant *KRAS* genotypes were selected to further evaluate the impact of different oncogenic *KRAS* mutations in regulating the AKT and ERK pathway. These cell lines harboured wildtype *EGFR, BRAF* and *PIK3CA* status according to the Cosmic mutation database (http://cancer.sanger.ac.uk/cancergenome/projects/cell_lines/). Their *KRAS* mutation status was confirmed by pyrosequencing, as shown in Figure 4.2.

si-*KRAS* was used to study the effect of KRAS in regulating cell proliferation and downstream effectors. The CRC cell lines with mutant *KRAS* showed significant reduction in cell proliferation compared to the *KRAS* wildtype cell line Colo320 (Figure 4.3), suggesting they were dependent on KRAS for growth. In addition, knockdown of KRAS in SW403 (KRAS G12V) showed dramatically decreased pERK and slightly decreased in pAKT levels compared to Colo320, LS513 or LOVO cells (Figure 4.4). This result indicated that *KRAS* (G12V) transduces signals mainly through the ERK pathway, whereas wildtype

KRAS and other mutant form of *KRAS* (G12D or G13D) had minimal effect on the activities of ERK and AKT pathways in this series of CRC cell lines.

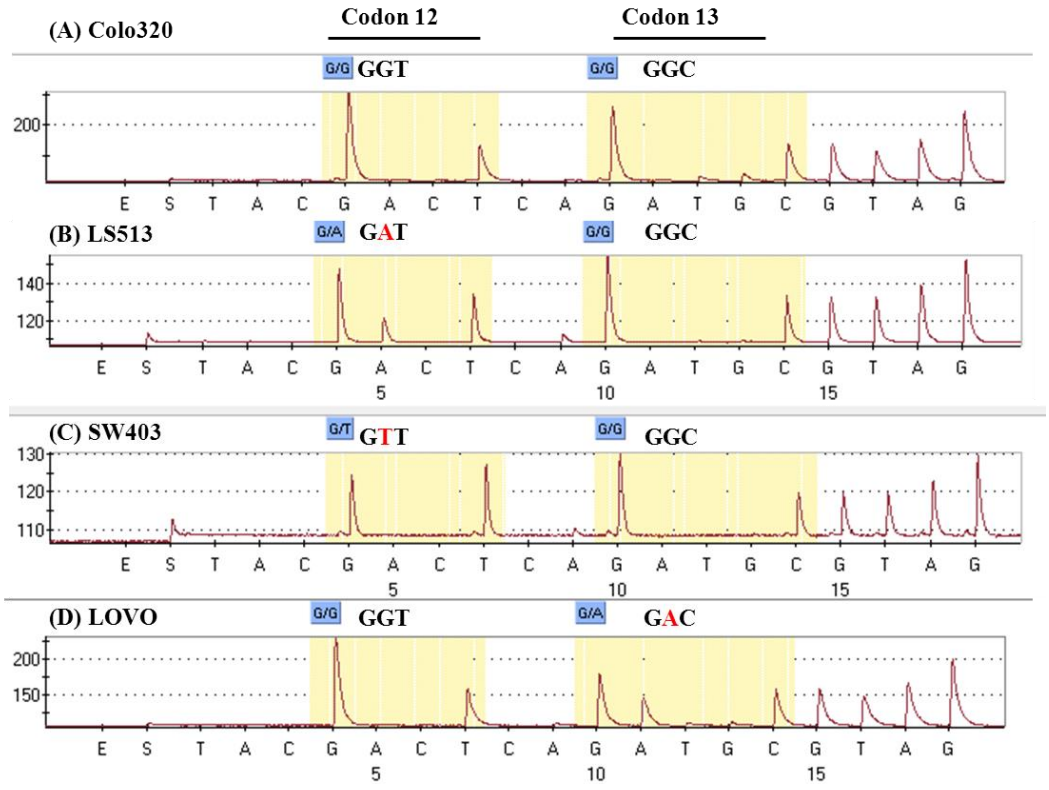

Figure 4.2. Pyrosequencing analysis of *KRAS* mutations in Colo320 (WT), LS513 (G12D), SW403 (G12V) and LOVO (G13D) cell lines. Pyrograms generated using the allele quantification (AQ) output for different cell lines as labeled. AQ was performed for the nucleotides within the yellow-shaded region. *KRAS* wildtype and three different *KRAS* mutations have been identified. (A) WT: codon 12: GGT; codon 13: GGC (B) G12D: codon 12: GAT; codon 13: GGC (C) G12V: codon 12: GTT; codon 13: GGC (D) G13D: codon 12: GGC; codon 13: GAC.

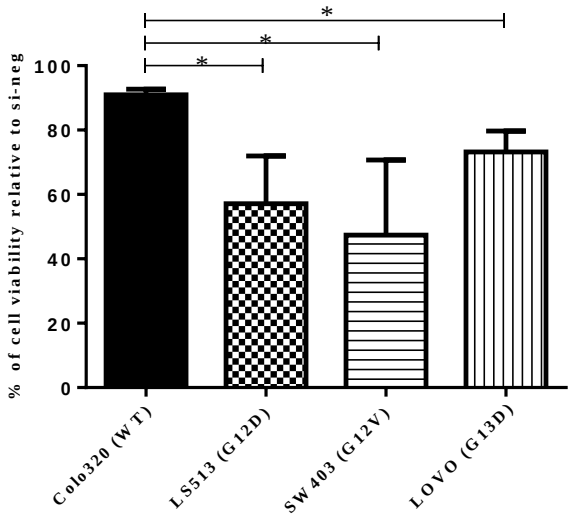

Figure 4.3. Effect of KRAS knockdown on cell proliferation in CRC cell lines. Cell lines were silenced with 25nM of siRNA and MTS assay was performed at 72 hour. * indicates $p<0.05$. Data from two independent experiments performed in triplicate is shown.

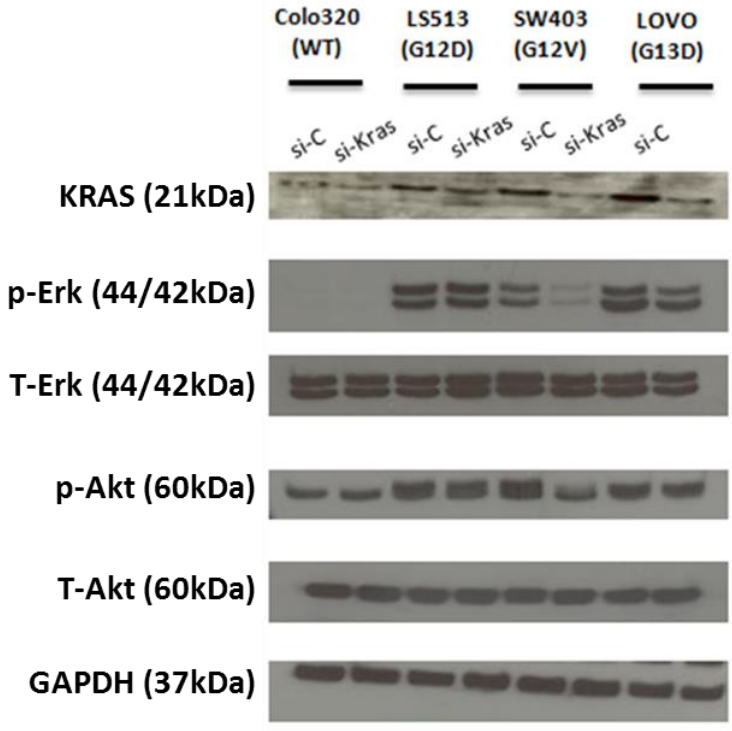

Figure 4.4. Protein expression levels of p-ERK (Thr202/Tyr204) and p-AKT (Ser473) after KRAS knockdown. Protein lysates were collected 48hr after siRNA treatment. Representative data from three independent experiments is shown.

4.1.3 Response of CRC cell lines with different KRAS mutations to MEK and PI3K inhibitors

As *KRAS* (G12V) appeared to transduce signals mainly through the ERK pathway, I therefore hypothesized this mutation could be more responsive to MEK inhibition compared to PI3K inhibition. Four of the CRC cell lines were further treated with the MEK and PI3K inhibitors BSP-C (Iverson *et al.*, 2009) and BSP-A, respectively. As hypothesized, SW403 was sensitive to the MEK inhibitor but resistant to the PI3K inhibitor (Figure 4.5). This further confirmed the finding that SW403 is more dependent on the ERK signaling pathway than on the PI3K signaling pathway in the control of cell proliferation.

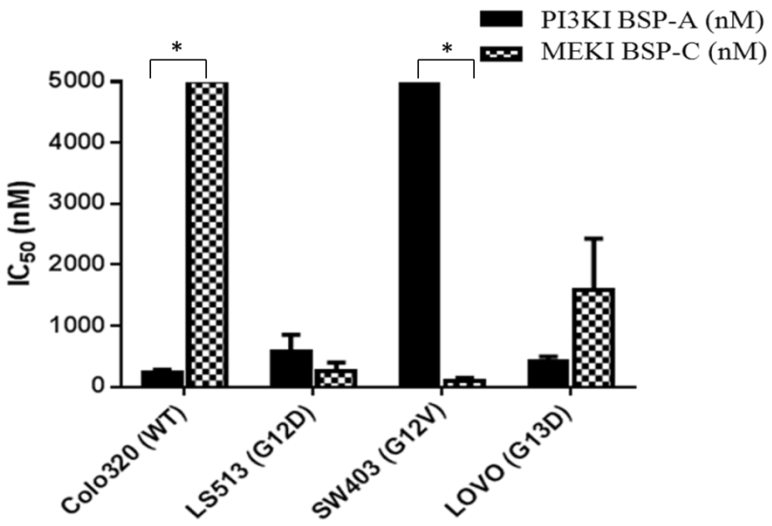

Figure 4.5. IC_{50} values for BSP-A and BSP-C in CRC cell lines with different *KRAS* mutations. Results are derived from MTS assay performed at 72 h. * indicates $p<0.05$. Data from three independent analyses is shown.

4.2 Discussion

This work is the first to report on the drug sensitivity of PI3K inhibitors in a large panel of GC and CRC cell lines. The *in vitro* data showed that GC cell lines with *PIK3CA* mutations were particularly sensitive to BSP-A (Figure 4.1), indicating this genetic alteration is a predictive biomarker for PI3K inhibitors. Several studies have reported that *PIK3CA* with gain of function mutations promotes cell proliferation *in vitro* and *in vivo* (Samuels and Velculescu, 2004; Engelman *et al.*, 2008). In addition, MCF10A cells transfected with oncogenic *PIK3CA* mutants were sensitive to the classical PI3K inhibitor LY294002 compared with wildtype *PIK3CA*, suggesting that *PIK3CA* mutation could mediate PI3K addiction (Zhang *et al.*, 2008).

To date, it is still unclear whether *KRAS* mutations confer resistance to single agent PI3K inhibitors as there are conflicting results in the literature (Dan *et al.*, 2010; Tanaka *et al.*, 2011; Park *et al.*, 2012). In this study, no significant association was found between *KRAS* mutation and sensitivity to BSP-A. However, new evidence has begun to highlight that a simple classification of *KRAS* mutant status may not be appropriate. De Roock and colleagues reported that primary CRC and CRC cell lines with different *KRAS* mutations exhibit different sensitivity to the anti-EGFR drug cetuximab (De Roock *et al.*, 2010). Garassino et al. also found that different *KRAS* mutations were associated with different sensitivity to a number of chemotherapeutic agents in NSCLC (Garassino *et al.*, 2011). Therefore, in the present study *KRAS* mutations were stratified into different types and investigated for associations with drug

sensitivity. Interestingly, *KRAS* (G12V) was associated with resistance to PI3K inhibitors in CRC cell lines (Figure 4.1). It was reported previously that *KRAS* (G12V) transduces signals mainly through the ERK rather than PI3K pathway in mouse fibroblasts (Cespedes *et al.*, 2006). To confirm this finding in CRC, KRAS was knocked down in cell lines having different *KRAS* mutations. Cells with KRAS (G12V) showed a large decrease in pERK, but not cell lines with wildtype or other *KRAS* mutation types (G12D/G13D) (Figure 4.4). The dependency of *KRAS* (G12V) mutant cell lines on the ERK pathway may explain their reduced dependence on the PI3K pathway. Moreover, this study showed the SW403 cell line harbouring KRAS (G12V) was sensitive to MEK inhibition (Figure 4.5). This suggests that different *KRAS* mutations could have non-synonymous functional activities, thus leading to different outcomes in patients treated with PI3K inhibitors.

It was shown here that *KRAS* (G12V) cells were more dependent on ERK signaling than on PI3K signaling (Figure 4.4). This may explain why CRC cell lines with *KRAS* (G12V) mutation were observed to be more resistant to PI3K inhibitor than other *KRAS* mutant cell lines. It also suggests that inhibition of PI3K signaling may be useful in patients with *KRAS* (G12D) or *KRAS* (G13D) mutant tumours. However, the observation was made in a small number of CRC cell lines (n=14) and only one cell line with *KRAS* (G12V) mutation was used to dissect the downstream signalling of mutant *KRAS*. Hence, greater numbers of cell lines are needed to confirm the findings and also to further investigate whether other cancer types with the *KRAS* (G12V) mutation show similar

behavior. Moreover, isogenic cell line models which haboured different *KRAS* mutations may help to confirm this finding. The results obtained could have important implications for the treatment of *KRAS* mutant tumours.

5 Results: Identification of Potential Biomarkers in *PIK3CA* Wildtype GC Cell Lines using RNA-sequencing

5.1.1 Sensitivity of PI3K inhibitors in 8 GC cell lines with PIK3CA wildtype background

My results presented in Chapter 4 showed that the cell lines with *PIK3CA* mutation were more sensitive to PI3K inhibitors than cell lines without *PIK3CA* mutations. However, some *PIK3CA* wildtype cells also were sensitive to these inhibitors. To identify biomarkers in GC cell lines with wildtype *PIK3CA*, I decided to make use of RNA-sequencing technology. I selected 8 *PIK3CA* wildtype cells (Kato3, MKN28, NUGC3, NUGC4, SNU5, YCC1, YCC11 and HS746T) to identify other factors that can determine sensitivity to PI3K inhibitors. The RNA-sequencing analysis was performed in 8 cell lines only and there were no technical replicates performed due to cost constraints. These GC cell lines were wildtype in all the 29 genes tested by OncoCarta, except YCC1 which haboured a p53 (R175H) mutation (Table 4.1). In addition to BSP-A, other PI3K inhibitors (BSP-B, BKM120, GDC-0941, BYL719 and XL147) were included for IC_{50} screening of all GC cell lines to ensure the observations were more specific to PI3K inhibitors than BSP-A (Table 5.1).

Table 5.1. IC_{50} values (nM) ± standard deviation for PI3K inhibitors in 8 GC cell lines. The IC_{50} values of PI3K inhibitors in the GC cell lines were obtained from the average value of three independent experiments. Each experiment was performed in three technical replicates.

Cell lines	BSP-A	BSP-B	GDC-0941	BKM120	BYL719	XL147
HS746T	1155±200	>5000	>10000	3576±178	>10000	>10000
Kato3	1125±746	>5000	>10000	5612±959	>10000	9644±504
MKN28	2090±1365	>5000	>10000	3615±872	>10000	>10000
NUGC3	230±163	3301±1110	2661±2041	3068±1339	>10000	>10000
NUGC4	336±88	>5000	2121±1915	1583±976	>10000	>10000
SNU5	522±446	>5000	5402±4219	909±581	>10000	>10000
YCC1	193±181	945±119	1133±703	2288±1266	3014±885	>10000
YCC11	376±103	>5000	2755±1610	1950±381	8713±1383	>10000

To further classify the cell lines into sensitive and resistant groups, unsupervised clustering was performed using quantile normalized IC_{50} values. As shown in Figure 5.1, two major clusters were observed where NUGC3, NUGC4, SNU5, YCC1 and YCC11 were classified as sensitive group, whereas Kato3, MKN28 and HS746T were classified as resistant group.

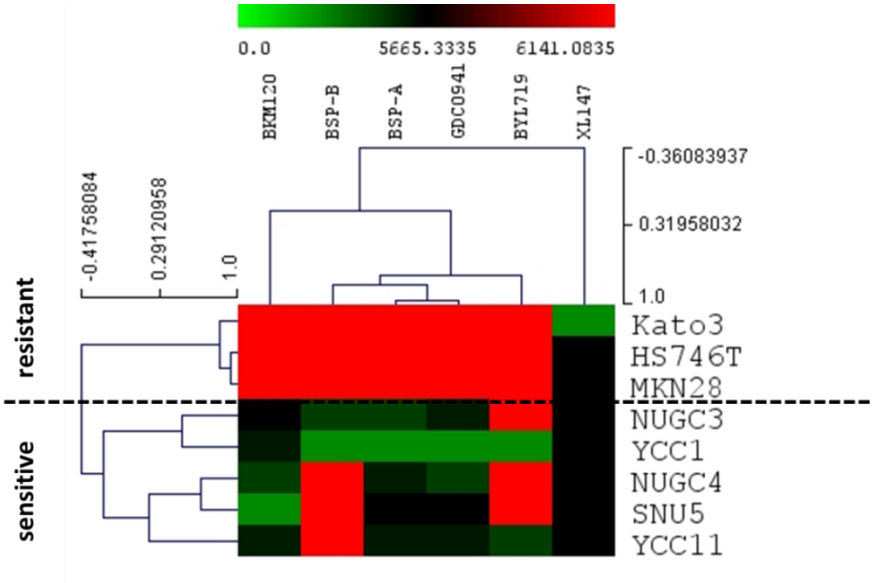

Figure 5.1. Unsupervised clustering of 8 GC cell lines based on quantile normalized IC_{50} values of PI3K inhibitors.

5.1.2 Correlation between IC_{50} values of PI3K inhibitors and the gene expression profile of 8 GC cell lines

The assessment of RNA integrity is a critical first step in obtaining meaningful gene expression data. All samples had a RIN>8, and their cDNA libraries for RNA-sequencing were prepared thereafter. Quality analysis of the libraries was performed using the Agilent Bioanalyzer and results are displayed in Appendix Figure 1. The majority of cDNA was fragmented in the range of 200-500 bp, which is the optimal size for the subsequent sequencing step. RNA sequencing was completed successfully for all samples (Appendix Table 1), with an average of 66 million reads per sample obtained. Median quality scores for all reads across all samples were more than 28, as shown in the per base sequence quality plot (Appendix Figure 2), suggesting good quality reads. To better understand the cellular pathways involved with resistance to PI3K inhibition, differential expressed gene transcripts between sensitive and resistant cell lines was analysed by ANOVA using Partek software. Volcano plot as shown in Figure 5.2 displayed the distribution of *p-value* and fold-change of individual transcript. ANOVA analysis revealed 617 transcripts were differentially expressed at least by 1.5 fold with $p<0.05$ (Table 5.2). These comprised of 258 transcripts that were up-regulated and 359 that were down-regulated in the sensitive cell lines. IGFBP3, one of the major upstream activators of the PI3K pathway, exhibited the highest fold change (67-fold) between the sensitive and resistant groups.

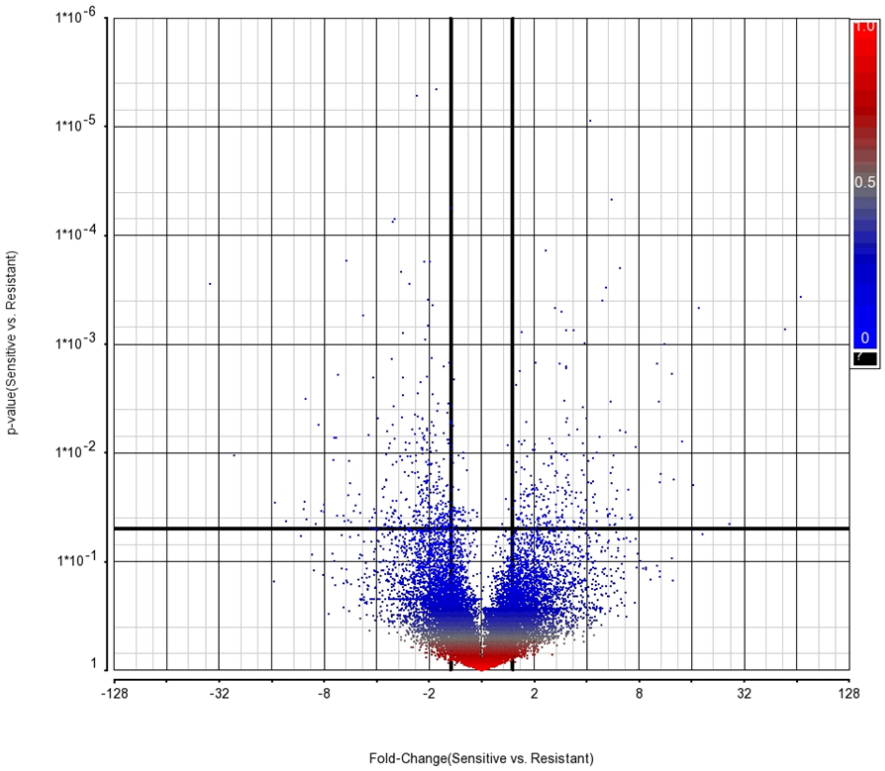

Figure 5.2. Fold change and *p-value* of different transcripts between sensitive and resistant cell lines.

Table 5.2. Genes differentially expressed between cell lines sensitive and resistant to PI3K inhibitors according to RNA Sequencing Analysis. The candidates are filtered for fold change greater than 1.5 with $p<0.05$, and sorted according to fold change.

Gene Symbol	Transcript	*p-value*	Fold-Change
IGFBP3	NM_001013398	0.000	67.429
IGFBP3	NM_000598	0.001	54.785
PDK4	NM_002612	0.045	26.210
DNAJC15	NM_013238	0.000	17.650
RPL36	NM_033643	0.020	16.398
ID1	NM_181353	0.008	14.085
PECR	NM_018441	0.018	12.644
HOXA10	NR_037939	0.002	12.348
NUP210	NM_024923	0.001	11.201
IAH1	NM_001039613	0.016	10.625
CYP51A1	NM_000786	0.018	10.436
ZNF32	NM_006973	0.003	10.386
HHEX	NM_002729	0.002	10.124
KBTBD7	NM_032138	0.009	7.605
NETO2	NM_001201477	0.039	7.247
FOXC1	NM_001453	0.040	7.151
HNMT	NM_006895	0.037	7.070
ALDH3B1	NM_001030010	0.022	6.909
HOXA13	NM_000522	0.006	6.667
FAM213A	NM_032333	0.040	6.379
SLC25A4	NM_001151	0.000	6.189
FAM127B	NM_001134321	0.006	6.174
LONRF2	NM_198461	0.022	5.944
PRKAG1	NM_002733	0.027	5.903
NETO2	NM_018092	0.045	5.839
ZIC5	NM_033132	0.037	5.831
DHRS3	NM_004753	0.046	5.735
SNORA45A	NR_002580	0.011	5.669
TRAPPC3	NR_073098	0.033	5.635
HOMER2	NM_199330	0.014	5.629
RNASE4	NM_194431	0.019	5.555
TP53TG1	NR_015381	0.000	5.545
LINC00997	NR_036501	0.015	5.493
SNORD76	NR_003942	0.003	5.455
MGST2	NM_001204368	0.046	5.447
FAM213A	NM_001243781	0.036	5.435

C9orf16	NM_024112	0.037	5.319
FAM213A	NM_001243778	0.038	5.256
SNORA18	NR_002959	0.033	5.208
SNORA14B	NR_002956	0.000	5.133
GPR137B	NM_003272	0.000	4.922
LAMTOR2	NM_014017	0.007	4.710
SNORA43	NR_002975	0.035	4.591
POLD2	NM_006230	0.043	4.561
SNORD89	NR_003070	0.010	4.551
ZNF606	NM_025027	0.050	4.479
RPLP0	NM_001002	0.024	4.448
FAM213A	NM_001243782	0.029	4.423
ZIC2	NM_007129	0.018	4.372
NUP62CL	NM_017681	0.025	4.361
SNORD8	NR_002916	0.011	4.355
OS9	NM_006812	0.019	4.232
SLC2A6	NM_001145099	0.000	4.184
RNPS1	NM_001286627	0.012	4.093
PAX8-AS1	NR_047570	0.019	4.089
SNORD94	NR_004378	0.046	4.009
ZNF480	NM_001297624	0.050	3.992
CARHSP1	NM_001042476	0.005	3.978
ASPHD1	NM_181718	0.034	3.966
PARVB	NM_001243386	0.027	3.955
ANKRD16	NM_019046	0.001	3.914
SNORA62	NR_002324	0.010	3.850
RNU4ATAC	NR_023343	0.045	3.845
OPN3	NM_014322	0.036	3.834
RPL17	NM_001199341	0.016	3.827
TP53	NM_001126115	0.004	3.795
TP53	NM_001276697	0.004	3.795
HCFC1R1	NM_001288666	0.008	3.794
SPIN3	NM_001010862	0.034	3.772
POLD4	NR_046411	0.040	3.767
HIST1H2BD	NM_138720	0.014	3.754
LOC100652758	NM_001278082	0.039	3.703
ACADM	NM_001286042	0.023	3.699
HSPA4L	NM_014278	0.035	3.699
ZFP3	NM_153018	0.044	3.653
SNORD9	NR_003029	0.048	3.634
ANXA2R	NM_001014279	0.031	3.589
SNORA52	NR_002585	0.006	3.532

CDNF	NM_001029954	0.023	3.471
MPC2	NR_026550	0.026	3.446
SLC22A3	NM_021977	0.043	3.408
SESTD1	NM_178123	0.043	3.365
NEO1	NM_001172624	0.001	3.350
SCARNA11	NR_003012	0.029	3.279
COX5B	NM_001862	0.022	3.272
IRAK1BP1	NM_001010844	0.049	3.240
RNU6ATAC	NR_023344	0.024	3.188
RPL31P11	NR_002595	0.007	3.154
TRIQK	NM_001191036	0.020	3.144
MTERF1	NM_001301134	0.016	3.114
MTERF1	NM_006980	0.016	3.111
RPL18	NM_001270490	0.018	3.110
CRAT	NM_000755	0.012	3.096
SNORA10	NR_002327	0.048	3.079
SNORA38B	NR_003706	0.005	3.078
FAM117B	NM_173511	0.049	3.071
TMEM17	NM_198276	0.031	3.060
TSPAN31	NM_005981	0.023	3.060
ENKD1	NM_032140	0.010	3.054
ZNF32	NM_001005368	0.027	3.044
PIK3R3	NM_003629	0.002	3.044
NTPCR	NM_032324	0.017	3.043
SEZ6L2	NM_001243333	0.001	3.042
LOC100132352	NR_034006	0.002	3.039
RNASEL	NM_021133	0.005	3.034
PCED1A	NM_022760	0.024	3.012
CACYBP	NM_001007214	0.022	2.994
STAT3	NM_213662	0.003	2.983
ST6GALNAC4	NM_175040	0.042	2.965
CCNG1	NM_199246	0.011	2.965
SNORA34	NR_002968	0.043	2.957
SNORA9	NR_002952	0.029	2.919
LSS	NM_001145437	0.040	2.918
UBE2D4	NM_015983	0.033	2.916
FAHD2A	NM_016044	0.021	2.902
SEMA3B	NM_001290061	0.037	2.895
PDCD6	NM_013232	0.048	2.873
KIAA0895	NM_015314	0.039	2.871
TM2D2	NM_078473	0.010	2.871
NEO1	NM_002499	0.000	2.868

GGA1	NM_001172688	0.002	2.807
ARAP1	NM_015242	0.042	2.794
SNORA20	NR_002960	0.039	2.756
VMAC	NM_001017921	0.020	2.737
RBM26	NM_001286632	0.043	2.728
SNORA21	NR_002576	0.022	2.720
MMAA	NM_172250	0.015	2.713
BBS1	NM_024649	0.039	2.686
PAIP2	NM_001033112	0.048	2.685
TTC14	NM_001288582	0.015	2.679
TTC14	NM_001042601	0.035	2.671
SNORD97	NR_004403	0.030	2.669
PON2	NM_001018161	0.010	2.648
RRNAD1	NM_015997	0.016	2.646
TMLHE	NM_001184797	0.000	2.638
KRT8	NR_045962	0.023	2.586
PHKB	NM_000293	0.046	2.548
SNORA8	NR_002920	0.013	2.547
SNORA24	NR_002963	0.008	2.546
SCYL3	NM_020423	0.011	2.508
TSEN34	NM_024075	0.011	2.494
UFC1	NM_016406	0.042	2.489
SNORA31	NR_002967	0.049	2.480
LINC00263	NR_026762	0.023	2.477
L3HYPDH	NM_144581	0.034	2.450
TMEM161B-AS1	NR_105019	0.007	2.437
TAPT1-AS1	NR_027696	0.044	2.431
PDCD6	NM_001267558	0.026	2.413
ATP6V0E2	NM_001100592	0.013	2.411
ZNF717	NM_001290210	0.036	2.406
SCARNA13	NR_003002	0.043	2.396
SEZ6L2	NM_201575	0.031	2.393
TIMP1	NM_003254	0.020	2.383
HMBOX1	NM_001135726	0.045	2.364
IFT140	NM_014714	0.032	2.364
GMPR2	NM_001002002	0.048	2.364
ARV1	NM_022786	0.047	2.359
GALK2	NM_002044	0.038	2.334
LRRC37A6P	NR_003525	0.021	2.332
NRIP1	NM_003489	0.038	2.325
ZNF669	NM_024804	0.000	2.322
ANKRD9	NM_152326	0.037	2.307

FUT10	NM_032664	0.044	2.290
SELO	NM_031454	0.027	2.282
GRAMD1B	NM_020716	0.044	2.275
IFITM3	NM_021034	0.025	2.265
TRMT1L	NM_001202423	0.013	2.261
SNORA48	NR_002918	0.038	2.252
UBAP2L	NM_001287815	0.027	2.241
SNORA70	NR_000011	0.039	2.231
FAM213A	NM_001243780	0.033	2.202
TPT1	NM_003295	0.024	2.199
MOSPD3	NM_023948	0.033	2.191
FASTKD1	NR_104020	0.019	2.179
CEBPZOS	NR_037879	0.046	2.157
TPCN1	NM_017901	0.017	2.154
GRAMD1B	NM_001286563	0.040	2.136
FBXL19-AS1	NR_024348	0.025	2.132
C1RL	NM_001297642	0.039	2.119
POLR1B	NM_001282776	0.042	2.117
MTX2	NR_027850	0.045	2.106
RAB12	NM_001025300	0.022	2.097
PPIA	NM_021130	0.041	2.095
DUSP19	NM_001142314	0.047	2.090
FRAT1	NM_005479	0.028	2.069
ABCA2	NM_001606	0.021	2.061
TBCE	NM_001287802	0.025	2.047
SNORA71C	NR_003017	0.001	2.042
FAM89B	NM_001098784	0.049	2.035
ZNF213-AS1	NR_110900	0.031	2.033
MTIF3	NM_001166261	0.009	2.016
REL	NM_002908	0.022	2.013
CCDC22	NM_014008	0.020	2.008
SIRT5	NM_001242827	0.008	2.001
RPL7A	NM_000972	0.044	1.998
MPHOSPH9	NR_103517	0.024	1.972
MTR	NM_001291939	0.009	1.966
REL	NM_001291746	0.021	1.963
PRKAA1	NM_006251	0.020	1.945
PRKAA1	NM_206907	0.020	1.944
ATP6V0A1	NM_005177	0.037	1.944
ATP6V0A1	NM_001130021	0.037	1.944
CNIH4	NR_102347	0.049	1.940
TLCD1	NM_001160407	0.022	1.932

NFU1	NM_001002756	0.016	1.922
USP15	NM_001252079	0.044	1.910
CDK13	NM_031267	0.040	1.895
ABCA2	NM_212533	0.024	1.884
SLC10A7	NM_001029998	0.024	1.877
EXOC8	NM_175876	0.031	1.857
RPS15A	NM_001030009	0.025	1.851
UBL5	NM_024292	0.030	1.841
PSME1	NM_176783	0.011	1.833
HSPA1L	NM_005527.2	0.040	1.823
SURF4	NM_001280792	0.025	1.822
SPG7	NM_003119	0.024	1.821
TNIP1	NM_001258456	0.049	1.810
RPL17-C18orf32	NM_001199355	0.047	1.810
SNORD10	NR_002604	0.038	1.809
STAT3	NM_139276	0.021	1.798
RPS24	NM_033022	0.005	1.794
RPS24	NM_001142284	0.005	1.793
RPS24	NM_001142283	0.005	1.793
ZNHIT1	NM_006349	0.032	1.761
ZFC3H1	NM_144982	0.028	1.760
ALKBH7	NM_032306	0.008	1.756
BTBD2	NM_017797	0.014	1.753
HFE	NM_001300749	0.023	1.749
MAN1B1	NR_045721	0.024	1.744
PCSK6	NM_001291309	0.046	1.728
SPIN3	NR_027139	0.032	1.727
RALGDS	NM_006266	0.043	1.708
OGDH	NM_001003941	0.042	1.708
DNASE1L1	NM_001009932	0.036	1.703
RPS15	NM_001018	0.014	1.700
HGSNAT	NM_152419	0.001	1.689
RPS24	NM_001026	0.008	1.684
RPRD2	NM_001297674	0.037	1.680
RPRD2	NM_015203	0.036	1.680
R3HDM2	NM_014925	0.026	1.678
APBA3	NM_004886	0.031	1.678
TOR1AIP1	NM_015602	0.024	1.669
TOR1AIP1	NM_001267578	0.024	1.669
TOMM20	NM_014765	0.019	1.664
H2AFY	NM_138609	0.002	1.649
CUX1	NM_001202544	0.041	1.647

CUX1	NM_001913	0.041	1.646
USP20	NM_006676	0.008	1.640
PRMT2	NM_001242866	0.040	1.627
TUBB4B	NM_006088	0.048	1.621
GDE1	NM_016641	0.041	1.615
CCDC112	NM_152549	0.040	1.597
DCAF11	NR_028099	0.012	1.596
RPL13	NM_033251	0.037	1.573
SNRNP200	NM_014014	0.015	1.568
RPL13AP20	NR_003932	0.002	1.568
PSME2	NM_002818	0.028	1.553
UQCRHL	NM_001089591	0.032	1.522
ALKBH1	NM_006020	0.009	-1.506
FAM35DP	NR_027634	0.035	-1.512
WBP11P1	NR_003558	0.005	-1.515
SDCBP2-AS1	NR_040049	0.043	-1.519
RORA	NM_134261	0.045	-1.522
SSR3	NM_007107	0.045	-1.524
SATB2	NM_015265	0.034	-1.537
IGDCC4	NM_020962	0.035	-1.540
ZBTB2	NM_020861	0.001	-1.541
PRKAR1B	NM_001164760	0.038	-1.546
ATN1	NM_001940	0.045	-1.547
ATN1	NM_001007026	0.045	-1.547
ATF2	NR_045769	0.004	-1.550
MRPL1	NM_020236	0.046	-1.553
WDR53	NM_182627	0.008	-1.553
RAET1G	NM_001001788	0.048	-1.554
PSMD12	NM_002816	0.007	-1.556
NR1D2	NR_110524	0.028	-1.561
NR1D2	NM_005126	0.028	-1.561
PPARD	NM_001171819	0.038	-1.566
NR1D2	NM_001145425	0.042	-1.570
CRELD2	NM_024324	0.020	-1.572
TM2D2	NM_031940	0.048	-1.574
FAM198B	NM_001031700	0.036	-1.574
TTC19	NM_001271420	0.004	-1.576
UBXN2A	NM_181713	0.008	-1.582
INPP5A	NM_005539	0.031	-1.589
CFAP70	NM_145170	0.043	-1.591
NFYB	NM_006166	0.048	-1.592
ATP6V1C1	NM_001695	0.020	-1.594

KANSL1	NM_015443.1	0.036	-1.595
PTBP2	NR_125357	0.029	-1.605
TMED8	NM_213601	0.036	-1.605
FAM133A	NM_173698	0.036	-1.609
AKAP17A	NR_027383.1	0.031	-1.611
AKAP17A	NM_005088	0.031	-1.612
ATP13A3	NM_024524	0.046	-1.613
CEP44	NM_001145314	0.044	-1.618
NFATC2	NM_001258297	0.050	-1.622
ZNF212	NM_012256	0.044	-1.627
DGKZ	NM_001199266	0.038	-1.630
TCEB1	NM_001204861	0.048	-1.633
USP1	NM_001017415	0.040	-1.638
RALGAPB	NM_001282917	0.025	-1.654
RALGAPB	NM_001282918	0.038	-1.655
DAAM1	NM_014992	0.011	-1.656
ZNF609	NM_015042	0.002	-1.657
UBE2J2	NM_194457	0.022	-1.657
CASP7	NM_033340	0.007	-1.660
NOLC1	NM_001284388	0.025	-1.662
EPS15	NM_001981	0.029	-1.670
ADAM15	NM_207195	0.040	-1.671
FOXK2	NM_004514	0.047	-1.673
EFR3A	NM_015137	0.025	-1.674
ZNF98	NM_001098626	0.045	-1.674
VEPH1	NM_001167917	0.047	-1.675
MEF2A	NM_005587	0.036	-1.676
BTF3L4	NM_001243767	0.042	-1.678
TWISTNB	NM_001002926	0.036	-1.679
NHLRC2	NM_198514	0.033	-1.681
DNAJC9	NM_015190	0.017	-1.700
ZXDC	NM_001040653	0.039	-1.707
DNMT3B	NM_001207055	0.037	-1.707
BAIAP2	NM_001144888	0.047	-1.708
MED6	NM_005466	0.030	-1.712
DCAF13P3	NR_027642	0.028	-1.718
PIGA	NR_033836	0.044	-1.721
GGA1	NM_013365	0.036	-1.744
DHX33	NM_001199699	0.023	-1.744
HEMK1	NM_016173	0.038	-1.747
USP1	NM_001017416	0.015	-1.749
MAP4K5	NM_198794	0.044	-1.750

PABPC4	NM_003819	0.013	-1.753
MINA	NM_153182	0.017	-1.753
LDB1	NM_003893	0.044	-1.757
FAM193A	NR_046335	0.040	-1.758
HNRNPR	NM_001297622	0.016	-1.758
ZDHHC6	NM_022494	0.044	-1.761
RABEP1	NM_004703	0.040	-1.769
TBC1D23	NM_001199198	0.029	-1.770
TBC1D23	NM_018309	0.029	-1.770
TMEM51	NM_001136218	0.003	-1.773
CTC1	NM_025099	0.041	-1.785
HNRNPR	NM_001297621	0.043	-1.788
MINA	NM_001261829	0.020	-1.789
FLCN	NM_144997	0.004	-1.793
NUF2	NM_031423	0.034	-1.796
POFUT1	NM_015352	0.048	-1.796
DNMT1	NM_001130823	0.042	-1.798
CLASP2	NM_015097	0.021	-1.802
RFC1	NM_001204747	0.046	-1.804
SLC25A32	NM_030780	0.024	-1.804
RABEP1	NM_001083585	0.032	-1.805
PVR	NM_001135768	0.047	-1.805
PVR	NM_001135769	0.047	-1.805
ATXN3	NR_028458	0.032	-1.807
TTC29	NM_031956	0.000	-1.817
C2CD2L	NM_001290474	0.041	-1.818
RFC1	NM_002913	0.019	-1.824
MKRN2	NM_001271707	0.012	-1.825
SLC25A32	NR_102337	0.010	-1.827
SLC35B3	NR_109914	0.031	-1.828
CYB561D1	NM_001134404	0.049	-1.829
MEF2A	NM_001171894	0.048	-1.830
PTER	NM_001261838	0.037	-1.839
VPS16	NM_022575	0.032	-1.845
MRTO4	NM_016183	0.022	-1.850
CBWD1	NM_001145355	0.007	-1.850
TMEM181	NM_020823	0.042	-1.858
SAAL1	NM_138421	0.047	-1.860
C11orf45	NM_001256088	0.043	-1.865
SMNDC1	NM_005871	0.045	-1.875
ANKRD11	NM_013275	0.020	-1.880
ANKRD11	NM_001256182	0.020	-1.881

STX18	NM_016930	0.006	-1.893
RREB1	NM_001003699	0.023	-1.897
NCOA1	NM_003743	0.044	-1.898
MAPK7	NM_002749	0.000	-1.902
CENPO	NM_024322	0.008	-1.904
LOXL1-AS1	NR_040068	0.050	-1.920
KIAA1598	NM_018330	0.003	-1.922
ZSCAN9	NM_001199480	0.001	-1.928
LINC01426	NR_038886	0.035	-1.934
MEF2A	NM_001130928	0.031	-1.941
ZNF821	NM_001201556	0.045	-1.941
SPECC1L	NM_001254732	0.005	-1.942
TTPAL	NM_001261839	0.013	-1.946
CCDC186	NM_018017	0.031	-1.953
ZBTB38	NM_001080412	0.010	-1.959
SEC14L1	NM_003003	0.023	-1.961
UAP1L1	NM_207309	0.040	-1.964
MTFR2	NM_001099286	0.016	-1.968
MICAL3	NM_001136004	0.013	-1.969
POLE3	NR_027261	0.043	-1.970
NR2F2	NM_001145157	0.043	-1.970
FOXO3	NM_201559	0.007	-1.975
LMLN	NR_026786	0.000	-1.975
SHOC2	NM_007373	0.009	-1.980
ATL2	NR_024191	0.032	-1.984
ATPAF1	NM_022745	0.013	-1.993
YAP1	NM_001130145	0.022	-1.994
YAP1	NM_001195044	0.022	-1.995
RNF38	NM_022781	0.044	-2.002
RBL1	NM_002895	0.030	-2.006
MTMR14	NM_022485	0.025	-2.006
BAHD1	NM_014952	0.018	-2.013
SPECC1L	NM_001145468	0.012	-2.019
YAP1	NM_001282097	0.013	-2.022
C11orf45	NR_045767	0.000	-2.023
YAP1	NM_006106	0.013	-2.023
SCO2	NM_005138	0.040	-2.024
SNORA58	NR_002985	0.001	-2.030
EPN2	NM_014964	0.029	-2.030
CTBP2	NM_001290214	0.048	-2.033
PRIMPOL	NM_152683	0.031	-2.034
THAP7	NM_001008695	0.047	-2.043

ATG5	NM_001286106	0.022	-2.047
RAPGEF2	NM_014247	0.025	-2.047
GABPB1	NM_005254	0.019	-2.048
GAR1	NM_032993	0.046	-2.050
MFI2-AS1	NR_038285	0.006	-2.053
ANKRD11	NM_001256183	0.009	-2.053
ANAPC13	NM_001242374	0.035	-2.055
CDK5RAP1	NM_016082	0.021	-2.059
FOXJ2	NM_018416	0.006	-2.061
ZCCHC17	NM_001282571	0.018	-2.064
YAP1	NM_001282101	0.008	-2.065
WHSC1	NM_133335	0.016	-2.065
YAP1	NM_001282100	0.008	-2.066
RYBP	NM_012234	0.002	-2.072
SORBS1	NM_006434	0.019	-2.081
LINC00857	NR_038464	0.046	-2.082
BOP1	NM_015201	0.026	-2.084
SNAP29	NM_004782	0.017	-2.085
ZNF367	NM_153695	0.018	-2.091
NAGK	NM_017567	0.012	-2.096
PXK	NM_001289096	0.001	-2.100
PRIMPOL	NM_001300768	0.046	-2.108
EPG5	NM_020964	0.050	-2.112
ASCC1	NM_001198799	0.027	-2.114
SEPT8	NM_001098812	0.018	-2.124
GBF1	NM_004193	0.007	-2.125
YAP1	NM_001282099	0.007	-2.126
YAP1	NM_001282098	0.007	-2.126
RFC5	NM_181578	0.000	-2.141
PUS1	NM_025215	0.008	-2.147
TOP3A	NM_004618	0.024	-2.155
CAMTA2	NM_001171166	0.007	-2.157
SLC23A2	NM_203327	0.038	-2.160
CDC7	NM_001134419	0.032	-2.167
DGCR11	NR_024157	0.009	-2.177
CNBP	NM_001127192	0.007	-2.182
PPP1R8	NM_138558	0.009	-2.182
MED8	NM_201542	0.022	-2.184
PANX1	NM_015368	0.046	-2.186
RTN4	NM_020532	0.026	-2.193
ANAPC15	NM_001278494	0.005	-2.195
KLC1	NM_001130107	0.005	-2.195

NRBF2	NM_001282405	0.022	-2.196
IPPK	NM_022755	0.028	-2.199
PPRC1	NM_015062	0.028	-2.202
LINC00152	NR_024204	0.010	-2.203
MOV10	NM_001286072	0.020	-2.204
CENPP	NM_001286971	0.022	-2.204
PDRG1	NM_030815	0.043	-2.207
ARHGAP39	NM_025251	0.009	-2.212
S1PR2	NM_004230	0.029	-2.213
CSK	NM_004383	0.020	-2.229
NCOA1	NM_147233	0.002	-2.232
SGPL1	NM_003901	0.030	-2.238
RAB27A	NM_183236	0.025	-2.250
LYAR	NM_001145725	0.006	-2.261
PGS1	NR_110602	0.037	-2.262
AIFM2	NM_001198696	0.023	-2.264
SMC3	NM_005445	0.042	-2.273
TMEM64	NM_001008495	0.035	-2.277
TTC4	NM_004623	0.023	-2.282
TRMT2A	NM_001257994	0.034	-2.300
DCLRE1B	NM_022836	0.017	-2.300
RAB27A	NM_183235	0.024	-2.303
USP1	NM_003368	0.021	-2.315
TRIM6	NM_001003818	0.038	-2.316
IPMK	NM_152230	0.003	-2.323
ZNF710	NM_198526	0.005	-2.324
BCL2L13	NR_073068	0.015	-2.330
CCNJ	NM_001134376	0.045	-2.344
PTGES2	NM_001256335	0.008	-2.345
CTBP2	NM_001329	0.035	-2.364
PSMB6	NM_002798	0.000	-2.371
RUNX1-IT1	NR_026812	0.035	-2.376
TTPAL	NM_024331	0.010	-2.380
TTPAL	NM_001039199	0.010	-2.380
LOC103344931	NR_120684	0.030	-2.381
IFNLR1	NM_173065	0.041	-2.390
PIGG	NM_001289053	0.012	-2.399
C10orf12	NM_015652	0.007	-2.403
PTBP2	NM_001300990	0.015	-2.413
SLC25A14	NM_001282195	0.004	-2.417
MFSD2A	NR_109896	0.034	-2.439
ZFYVE9	NM_007324	0.043	-2.441

ZNF707	NR_110192	0.038	-2.455
SGK3	NM_170709	0.038	-2.463
VTI1A	NM_145206	0.039	-2.481
SCAPER	NM_020843	0.015	-2.508
SIRT2	NR_034146	0.012	-2.513
RREB1	NM_001003700	0.006	-2.520
CALU	NM_001199672	0.011	-2.571
SPECC1L	NM_015330	0.000	-2.598
FOXO3	NM_001455	0.008	-2.606
RAD54B	NM_001205262	0.032	-2.606
SNX25	NM_031953	0.049	-2.632
LRRC8E	NM_025061	0.016	-2.633
CTNS	NM_004937	0.045	-2.636
TRPV3	NM_145068	0.048	-2.647
EPHA4	NM_004438	0.011	-2.649
CPEB3	NM_001178137	0.026	-2.696
PRDM16	NM_022114	0.009	-2.715
WTAP	NM_152858	0.027	-2.729
KLHL7-AS1	NR_046220	0.008	-2.742
TYRO3	NM_006293	0.047	-2.750
CALU	NM_001199671	0.015	-2.759
DCLRE1A	NM_001271816	0.001	-2.817
OPHN1	NM_002547	0.002	-2.833
MSANTD2	NM_001301087	0.003	-2.843
SNX8	NM_013321	0.005	-2.872
HK1	NM_000188	0.012	-2.874
FAM133A	NM_001171111	0.038	-2.896
FAM69A	NM_001006605	0.000	-2.906
EIF6	NR_052023	0.023	-2.907
SLC16A1-AS1	NR_103743	0.042	-2.911
GFOD1	NM_018988	0.044	-2.915
NFKBIL1	NM_001144962.3	0.044	-2.937
ARL13B	NM_001174150	0.048	-2.954
DSN1	NM_001145318	0.011	-2.955
NIF3L1	NM_001142355	0.040	-2.964
ALKBH8	NM_001301010	0.039	-3.016
ZNF492	NM_020855	0.049	-3.066
MYO1B	NM_001130158	0.028	-3.085
NDST1	NM_001543	0.012	-3.100
LOC101927482	NR_110226	0.034	-3.123
ELF5	NM_001243080	0.034	-3.144
FRMD5	NM_001286491	0.000	-3.151

MYBL1	NM_001294282	0.007	-3.154
CCBL2	NM_001008661	0.043	-3.164
FZD6	NM_001164616	0.035	-3.178
CACHD1	NM_020925	0.043	-3.195
PHACTR2	NM_014721	0.036	-3.210
EHD4	NM_139265	0.004	-3.213
AGO3	NM_024852	0.006	-3.221
FRMD5	NR_104455	0.000	-3.222
ARG2	NM_001172	0.036	-3.225
DPH5	NM_015958	0.028	-3.228
DSN1	NM_001145316	0.013	-3.250
STK25	NM_001271977	0.001	-3.260
DMKN	NM_001035516	0.048	-3.277
FAIM	NM_018147	0.048	-3.283
ZNF175	NM_007147	0.039	-3.297
ZYX	NM_001010972	0.032	-3.339
SEMA7A	NM_001146030	0.008	-3.341
CCDC84	NR_104051	0.009	-3.395
NDRG1	NM_001258432	0.042	-3.403
FBXO32	NM_001242463	0.048	-3.419
SAMD4A	NM_001161577	0.048	-3.447
MANBAL	NM_022077	0.036	-3.472
LOC399815	NR_027282	0.006	-3.486
DLC1	NM_006094	0.040	-3.519
DCTN3	NM_001281426	0.010	-3.530
CDC7	NM_001134420	0.018	-3.530
APBB2	NM_001166050	0.018	-3.551
ZFPM2-AS1	NR_125796	0.045	-3.562
RTN4	NM_207521	0.046	-3.573
APBB2	NM_173075	0.020	-3.607
PPP1R15A	NM_014330	0.046	-3.616
AUTS2	NM_001127231	0.049	-3.652
PRKCQ-AS1	NR_036503	0.025	-3.677
NDRG1	NM_006096	0.021	-3.704
MROH1	NM_001099281	0.035	-3.735
MYBL1	NM_001144755	0.005	-3.959
CSTA	NM_005213	0.036	-4.035
C1S	NM_201442	0.050	-4.050
SNHG18	NR_045196	0.035	-4.107
APBB2	NM_004307	0.033	-4.153
KLK6	NM_001012964	0.050	-4.189
SYNE3	NM_152592	0.002	-4.210

NTN1	NM_004822	0.040	-4.257
DUXAP8	NR_122113	0.049	-4.379
TRPV3	NM_001258205	0.042	-4.408
FRMD5	NM_032892	0.007	-4.455
C3orf52	NM_001171747	0.001	-4.801
ELF5	NM_001422	0.036	-4.951
TMEM51	NM_018022	0.024	-5.005
LYAR	NM_017816	0.030	-5.307
MCOLN3	NM_018298	0.034	-5.443
HMOX1	NM_002133	0.043	-5.620
SPTLC3	NM_018327	0.019	-5.703
LINC00341	NR_026779	0.012	-5.760
ZNF697	NM_001080470	0.025	-5.808
TIAM1	NM_003253	0.041	-5.840
C3orf52	NM_024616	0.000	-5.984
ZNF532	NM_018181	0.043	-6.143
ABLIM3	NM_001301027	0.038	-6.236
ZNF503	NM_032772	0.002	-6.641
HAS2	NM_005328	0.038	-6.729
PTPRE	NM_130435	0.007	-6.864
SMIM3	NM_032947	0.007	-7.006
KLHL29	NM_052920	0.012	-7.095
DLC1	NM_001164271	0.035	-7.992
RND3	NM_005168	0.030	-8.005
PTGS2	NM_000963	0.034	-8.353
CRABP2	NM_001878	0.005	-8.647
PHLDB2	NM_001134439	0.045	-8.958
ZNF22	NM_006963	0.041	-10.130
INHBE	NM_031479	0.003	-10.215
NUPR1	NM_012385	0.028	-10.367
SNTB1	NM_021021	0.033	-10.501
SERPINE1	NM_000602	0.042	-13.327
BAMBI	NM_012342	0.029	-15.399
SLC2A3	NM_006931	0.011	-26.240
NUPR1	NM_001042483	0.000	-36.309

Pathway analysis was performed to better understand the cellular pathways associated with PI3K-inhibitor sensitivity. The list of differential expressed genes (n=617) was used to perform pathway enrichment analysis using

the online biological classification tool DAVID (Table 5.3). Five relevant pathways, ribosome, DNA replication, mismatch repair, nucleotide excision repair and homologous recombination were enriched. In addition to differential expressed genes, GO ANOVA analysis was also performed to identify the "gene sets" that are up- or down-regulated in the sensitive cell lines compared to the resistant cell lines. The top 10 "gene sets" (each representing a GO-category) with the highest fold change were shown in Table 5.4. The "protein tyrosine phosphatase activator activity" was up-regulated in the sensitive cell lines with 61 fold change. IGFBP3 was one the genes that is involved in the "protein tyrosine phosphatase activator activity".

Table 5.3. Pathway prediction of the differential expressed genes (KEGG pathway).

No	Term	Count	p-value	Genes
1	Ribosome	9	0.002	*RPL18, RPL17, RPL13, RPLP0, RPS15, RPL36, RPS15A, RPL7A, RPS24*
2	DNA replication	5	0.013	*RFC5, POLD4, RFC1, POLE3, POLD2*
3	Mismatch repair	4	0.020	*RFC5, POLD4, RFC1, POLD2*
4	Nucleotide excision repair	5	0.026	*RFC5, POLD4, RFC1, POLE3, POLD2*
5	Homologous recombination	4	0.034	*POLD4, POLD2, TOP3A, RAD54B*

Table 5.4. GO-ANOVA analysis of cell lines that is sensitive or resistant to PI3K inhibitor.

No	GO Description	p-value	Fold-Change	Description
1	protein tyrosine phosphatase activator activity	0.001	61	Sensitive up vs Resistant
2	insulin-like growth factor binding protein complex	0.004	24	Sensitive up vs Resistant
3	growth factor complex	0.004	24	Sensitive up vs Resistant
4	protein phosphatase activator activity	0.001	16	Sensitive up vs Resistant
5	phosphatase activator activity	0.001	16	Sensitive up vs Resistant
6	positive regulation of myoblast differentiation	0.001	15	Sensitive up vs Resistant
7	sterol 14-demethylase activity	0.034	9	Sensitive up vs Resistant
8	cholesterol biosynthetic process via 24,25-dihydrolanosterol	0.034	9	Sensitive up vs Resistant
9	negative regulation of transcription by transcription factor localization	0.005	9	Sensitive up vs Resistant
10	regulation of female gonad development	0.003	-9	Sensitive down vs Resistant

5.1.3 Validation of IGFBP3 expression in GC cell lines

Among the shortlisted genes from the discovery set, IGFBP3 of high interest due to its high fold change and its involvement in insulin/insulin-like growth factor (IGF) signalling. IGF signalling represents one of the major upstream activators of the PI3K pathway (Cortes-Sempere *et al.*, 2013). Moreover, low expression of IGFBP3 has been shown to be associated with resistance to Herceptin and cisplatin (Jerome *et al.*, 2006; Cortes-Sempere *et al.*, 2013).

qRT-PCR was used to confirm the expression level of *IGFBP3* in the GC cell lines. Figure 5.3 demonstrated a strong positive correlation (pearson correlation =0.85, *p-value* = 0.008) between qRT-PCR and RNA-sequencing.

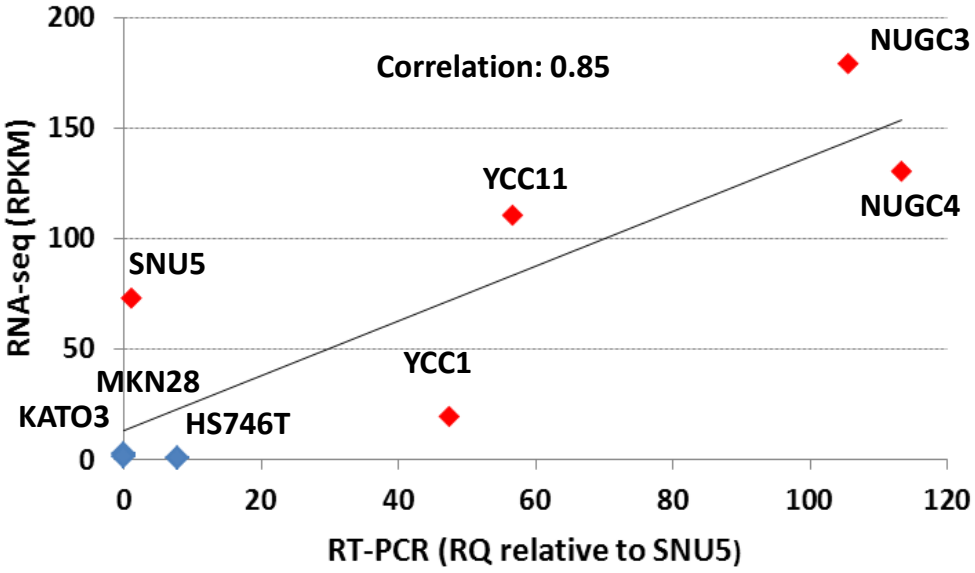

Figure 5.3. Correlation of *IGFBP3* expression between RNA-seq and qRT-PCR in the 8 GC cell lines. Relative quantification (RQ) values were obtained as an average from three technical replicates as relative to SNU5. Blue dots represent resistant cell lines, whereas red dots represent sensitive cell lines.

5.1.4 Functional validation of IGFBP3

High expression of *IGFBP3* was found to be common to all the sensitive cell lines. To confirm whether *IGFBP3* could mediate sensitivity to PI3K inhibition, cell viability was assessed after combined treatment with si-*IGFBP3* and PI3K inhibitors in YCC1 (moderate expression of IGFBP3). As shown in Figure 5.4 A, si-IGFBP3 treatment resulted in significant knockdown of IGFBP3 as assessed by western blot. A trend of decrease in drug sensitivity to PI3K inhibitors was observed in IGFBP3 knockdown cells although the IC_{50} values of GDC-0941 (YCC1-si-Neg, IC_{50} =1210±155nM; YCC1-si-IGFBP3, IC_{50}=2900±1561nM, p=0.135) and BKM120 (YCC1-si-Neg, IC_{50}=2096±587nM; YCC1-si-IGFBP3, IC_{50}= 3552±127nM, p=0.076) in these cells did not differ significantly from the parental cells.

As this observation was found in a transient model, further investigation of the effect of IGFBP3 in mediating drug sensitivity in stable cells with overexpression of IGFBP3 was undertaken. Stable isogenic cell lines with overexpression of IGFBP3 were established using YCC1 (Figure 5.5A). Parental cells (YCC1-GFP) and cells with IGFBP3 overexpression (YCC1-IGFBP3) were further treated with GDC-0941 and BKM120. As shown in Figure 5.5B, YCC1-IGFBP3 cells were more responsive to the PI3K inhibitors compared to the parental cells. The IC_{50} values of GDC-0941 (YCC1-GFP, IC_{50} =2609±991nM; YCC1-IGFBP3, IC_{50}=780±325nM, p=0.013) and BKM120 (YCC1-GFP, IC_{50} =2337±159nM; YCC1-IGFBP3, IC_{50}=1431±257, p=0.007) were significantly lower in the cells with IGFBP3 overexpression than the parental cells. Taken

together, these results confirmed that IGFBP3 modulates drug sensitivity to PI3K inhibitors.

IGFBP3 binds to IGF-1, preventing the binding of IGF-1 to its receptor IGF-1R. This leads to the inactivation of PI3K signalling pathway (Cortes-Sempere *et al.*, 2013). IGFBP3 was highly expressed in the sensitive cell lines compared to the resistant cell lines, it can therefore be hypothesized that high levels of IGFBP3 sequesters IGF-1, preventing activation of the PI3K pathway. This means that less PI3K inhibitors are needed to inactivate the pathway, rendering the cells sensitive to the PI3K drugs. To test this hypothesis, western blot analysis was performed to assess the phosphorylation level of IGF-1R and downstream of PI3K pathway in response to PI3K inhibitors. As shown in Figure 5.5C, overexpression of IGFBP3 alone induced a decrease in pIGF-1R, pAKT and pS6 expression, compared to the parental cells. In the presence of 10nM and 100nM of GDC-0941, lower expression of pAKT and pS6 were observed in YCC1-IGFBP3 than in YCC1-GFP. This finding indicated that less amount of PI3K inhibitor is needed to downregulate the PI3K/AKT pathway in cells with high expression of IGFBP3. Taken together, this supported our hypothesis that the PI3K pathway is less active in the presence of high IGFBP3.

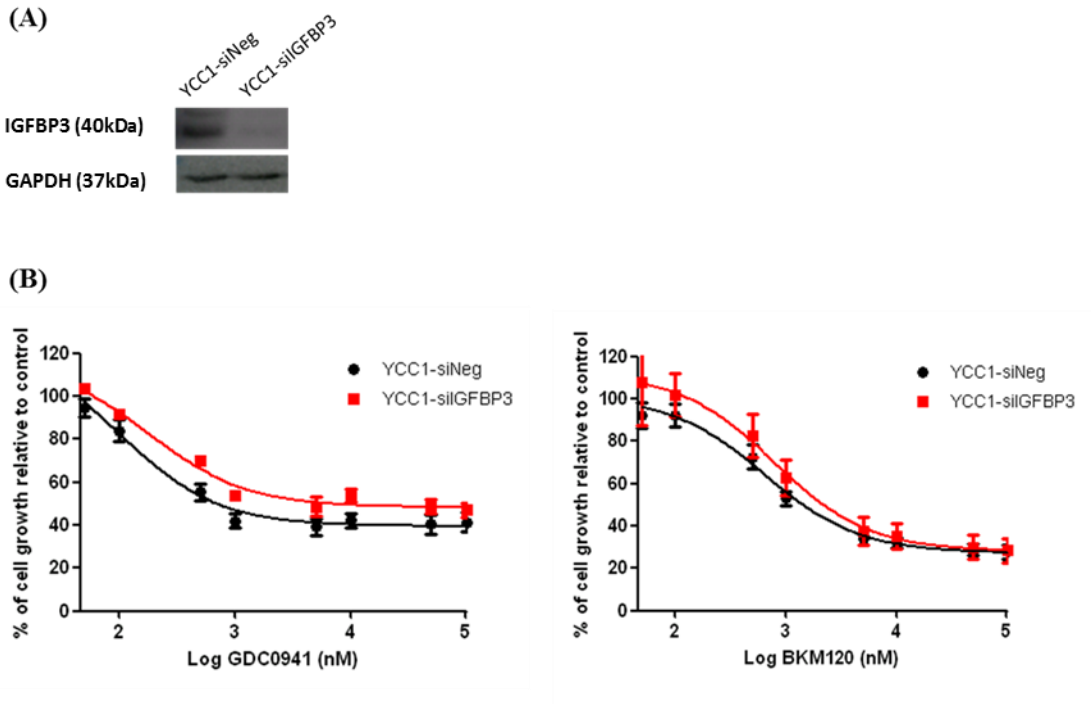

Figure 5.4. Effect of *IGFBP3* silencing on drug sensitivity. (A) Silencing efficiency of *IGFBP3* siRNA treatment in YCC1 cells as shown by western blot. (B) IC_{50} values for GDC-0941 and BKM120 treatment of YCC1 in the presence of si-*IGFBP3*. The IC_{50} response curves were obtained from the average value of three independent experiments. Each experiment was performed in three technical replicates. For the IC_{50} response curve of si-scramble (plotted as a black line), the percentages of cell viability at each drug concentration were obtained by comparing the absorbance with the si-scramble control without drug treatment (DMSO treated). For the IC_{50} response curve of si-IGFBP3 (indicated as red line), the percentages of cell viability at each drug concentration were obtained by comparing the absorbance with the si-IGFBP3 control without drug treatment (DMSO treated).

Fig.5.5 (Legend over page)

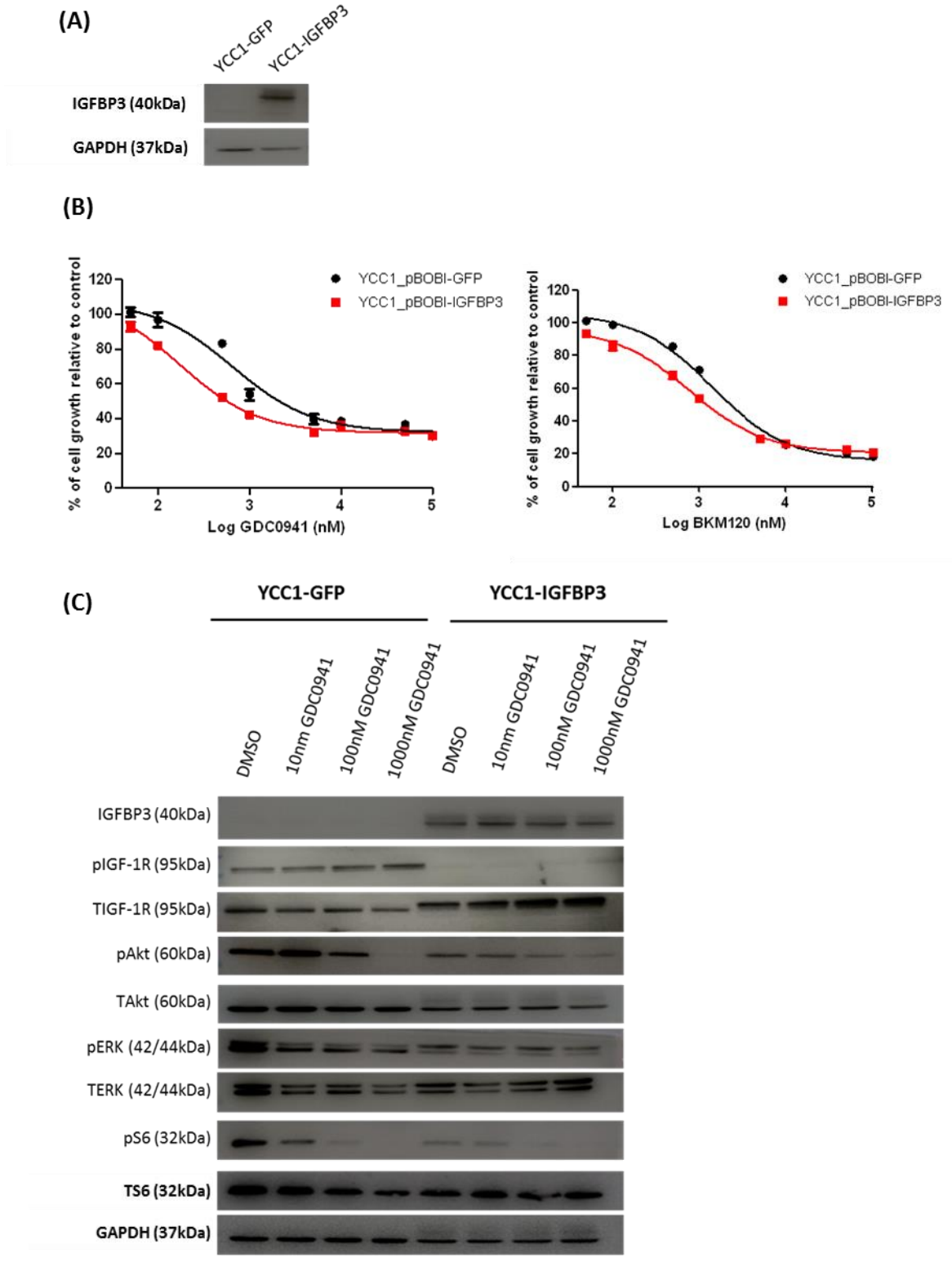

Figure 5.5. Effect of *IGFBP3* overexpression on drug sensitivity and PI3K pathway signalling. (A) Overexpression of IGFBP3 in YCC1 cells as shown by western blot. (B) IC_{50} values for GDC-0941 and BKM120 treatment of YCC1 in the isogenic cell lines. The IC_{50} response curves were obtained from the average value of three independent experiments. Each experiment was performed in three technical replicates. For the IC_{50} response curve of YCC1-GFP (plotted as a black line), the percentages of cell viability at each drug concentration were obtained by comparing the absorbance with the YCC1-GFP cells without drug treatment (DMSO treated). For the IC_{50} response curve of YCC1-IGFBP3 (indicated as red line), the percentages of cell viability at each drug concentration were obtained by comparing the absorbance with the YCC1-IGFBP3 cells without drug treatment (DMSO treated). (C) Effect of PI3K inhibition and IGFBP3 overexpression on p-IGF1R (Tyr1161), p-ERK (Thr202/Tyr204), p-AKT (Ser473) and pS6 (Ser235/236) protein expression in the isogenic cell lines. Representative data from two independent experiments is shown.

5.2 Discussion

Previous *in vitro* studies have shown significant correlation between specific mutations and treatment response, however the negative predictive value of these mutations is often poor and not all sensitive cancers are identified by single mutations or single gene panels. For instance, *PIK3CA* mutations showed excellent specificity and high positive predictive value in predicting the response to GDC-0941, but relatively low sensitivity and a poor negative predictive value in predicting drug responsiveness in the breast cell line panel which were wildtype for *PIK3CA* (O'Brien *et al.*, 2010). A number of GC cell lines without *PIK3CA* mutations were shown here to be sensitive to PI3K inhibitors, suggesting the need for additional biomarkers to identify subpopulations of *PIK3CA* wildtype patients who may respond to these drugs. With the exception of *PIK3CA* mutations, predictive biomarkers for PI3K inhibitors have so far not been well established. Therefore, a high throughput method such as RNA-sequencing was used here to identify novel biomarkers in *PIK3CA* wildtype GC cell lines in an unbiased manner.

Using RNA-sequencing, *IGFBP3* was one of the most significantly upregulated gene in the sensitive cell lines. *IGFBP3* was selected for further functional validation due to its involvement in IGF signalling (Perks and Holly, 2008). Interestingly, high expression of *IGFBP3* was found to mediate sensitivity to PI3K inhibitors (Figure 5.5). Moreover, knockdown of IGFBP3 counteracted the effect of PI3K inhibitor in reducing the pAKT level. GC cell lines with low

IGFBP3 expression were resistant to PI3K inhibitor, possibly due to the need of higher dose to downregulate the pAKT level (see Figure 5.6).

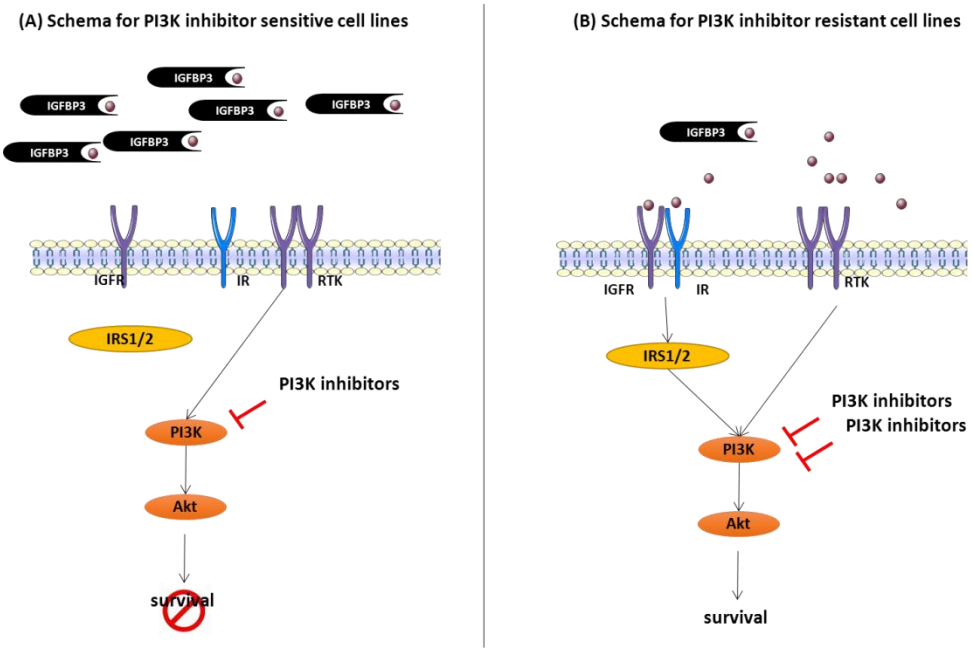

Figure 5.6. Schematic representation of the different status of the IGF1R/PI3K/AKT pathway proposed for (A) PI3K inhibitor-sensitive, or (B) -resistant cell lines according to their IGFBP3 expression.

One of the major mechanisms of action of IGFBP3 is to bind IGF-I, thus preventing the interaction of IGF-I with the insulin-like growth factor-I receptor (IGF-IR) (Perks and Holly, 2008). The expression level of IGFBP3 has been correlated with sensitivity to trastuzumab in breast cancer cells (Dokmanovic *et al.*, 2011). Moreover, *IGFBP3* methylation status together with AKT activity, IGF-IR and EGFR were able to predict the response of NSCLC patients to cisplatin (Cortes-Sempere *et al.*, 2013). The finding that elevated expression of *IGFBP3* correlates with sensitivity of GC cells to PI3K inhibition may help to

identify clinically useful predictive biomarkers for patients with wildtype *PIK3CA*. This observation provides a basis for future clinical trials to test whether GC tumours with high IGFBP3 expression are more responsive to PI3K inhibitors than tumours with low expression.

Pathway enrichment analysis showed that DNA replication and mismatch repair were associated with sensitivity to PI3K inhibitors (Table 5.3). Resistant cell lines showed high expression of *RFC5* and *RFC1 w*hich encode replication factor C subunit 5 and replication factor C subunit 1, respectively. It has been reported that treatment of human cancer cells with wortmannin could lead to reduced expression of genes of the Rad3-related protein (ATR)-checkpoint kinase 1 (CHK1) pathway, such as *RFC5*, *RFC2* and *RFC3 (Pal et al., 2012).* Moreover, overexpression of DNA repair genes has been shown to enhance the invasive behavior of tumour cells (Seedhouse *et al.*, 2006). This also suggests that high expression of DNA repair genes could contribute to the drug-resistant phenotype. Therefore, further investigation to determine whether inhibition of *RFC5* or *RFC1* may reverse the drug-resistant phenotype is warranted.

6 Chapter Six: General Discussion

6.1 Summary of major findings

In Chapter 3, knowledge on the frequency and associations of prominent candidate markers of response to PI3K inhibitors for GC and CRC was consolidated through comprehensive literature review and meta-analysis. The analyses uncovered inter-ethnic and cancer type differences in the frequencies of PI3K pathway aberrations. Co-occurrence analysis established that more than 86% of GC and CRC have at least one aberration in the PI3K pathway. These aberrations occurred primarily in a mutually exclusive pattern. The current findings support the potential use of PI3K inhibitors in GC and CRC patients, subject to validation of the role of biomarkers in tumour samples from clinical trials.

Using preclinical models in Chapter 4, several potential biomarkers for PI3K pathway inhibitors were identified for GC and CRC. Consistent with previous findings, *PIK3CA* mutation was found to be a biomarker for response of GC and CRC cell lines to PI3K inhibition. In CRC, a subtype of *KRAS* mutation, G12V, was significantly associated with higher IC_{50} value in response to PI3K inhibitor. This finding suggests that G12V could help stratify CRC patients to improve the efficacy to treatment with PI3K inhibitors.

In GC cell lines with wildtype *PIK3CA* status, this study found for the first time that high expression of *IGFBP3* was associated with sensitivity to PI3K inhibitors. This finding is important as it could help to identify *PIK3CA* wildtype

patients who will be responsive to PI3K inhibitors. However, studies on tissue samples from clinical trials are again required to confirm this observation. The current results point to a potential combination therapy in GC patients involving PI3K inhibitors and IGF-1R inhibitor. It will be interesting to further investigate the expression patterns of IGFBP3 in GC patients to determine whether they can be confirmed as biomarkers for PI3K inhibitor therapy in GC.

6.2 Recent developments in the identification of biomarkers for PI3K inhibitors

6.2.1 PIK3CA mutation

As mentioned previously, the association between *PIK3CA* mutations and the sensitivity to PI3K inhibitors was inconsistent as shown in several studies. A possible reason for these discrepancies is that different cell types have different genetic determinants to drug sensitivity. For example, the *BRAF* mutation hotspot V600E is a strong predictive biomarker for response to vemurafenib in melanoma, but not for the response of CRC patients to this BRAF inhibitor (Prahallad *et al.*, 2012) .

To my knowledge, this is the largest panel of GC cancer cell lines screened to date and highlights the potential use of *PIK3CA* mutation as pre-selection criteria in clinical trials. The meta-analyses indicated the frequencies of mutations in *PIK3CA* exons 9 and 20 in GC differ significantly between East Asians and Caucasians (Chapter 3). This suggests that the response rate of East

Asian patients might be lower than Caucasian patients to PI3K inhibitors. Nevertheless, the full clinical potential of this biomarker remains to be confirmed through clinical trials.

6.2.2 High expression of IGFBP3

High expression of IGFBP3 was associated with higher sensitivity to PI3K inhibitors in GC cell lines with *PIK3CA* wildtype (Chapter 5). IGFBP3 binds to circulating IGF-I, thus preventing activation of the IGF signaling pathway (Phillips *et al.*, 1998). Recently, overexpression of IGF-IR was identified as one of the major mediators of resistance in four cancer cell lines with acquired resistance to ZSTK474, a PI3K inhibitor (Isoyama *et al.*, 2012). In line with the present study, this finding implicates the IGF signaling pathway in mediating sensitivity to PI3K inhibitors. Aberrant DNA methylation and histone acetylation have been shown to play an important role in the silencing of IGFBP3 expression in several human cancers, including GC and CRC (Tomii *et al.*, 2007). IGFBP3 expression is significantly up-regulated by 5-aza-CdR treatment in gastric cancer cell lines (Yamashita *et al.*, 2006), providing further evidence that IGFBP3 expression is regulated by DNA methylation. Moreover, a common polymorphism in the *IGFBP3* promoter region has been associated with the level of circulating IGFBP3 in breast cancer (Schernhammer *et al.*, 2003). Therefore, it will be interesting to investigate whether tumour methylation of IGFBP3 or the genetic polymorphism have predictive value as markers of response to PI3K inhibitors in GC.

6.3 *In-vitro* efficacy of different PI3K inhibitors

Fingerprints are defined as the patterns of differential drug efficacy across a panel of cell lines and have been found to reflect mechanisms of drug action (Dan *et al.*, 2010). By analyzing the fingerprints of different PI3K inhibitors across the 8 cell lines, GDC-0941 and BSP-A were found to be highly correlated (Pairwise Pearson correlation coefficient=0.88), suggesting a close similarity in the molecular mechanisms of action between each pair of compounds. It is probable that both GDC-0941 and BSP-A are p110α and p110δ isoform-specific inhibitors.

In Elkabets *et al.*'s study, BYL719 was tested in a panel of 20 *PIK3CA*-mutant and 5 *PIK3CA*-wild-type cell lines. BYL719 is known to have high potency in cell lines with *PIK3CA* mutation (Elkabets *et al.*, 2013). The majority of cell lines had low IC_{50} values (~1μM) because these sensitive cells contained *PIK3CA* mutation. However, the 8 GC cell lines that were tested with BYL719 were all *PIK3CA*-wildtype cells. According to the Elkabets *et al.* study, 4 of *PIK3CA*-wildtype cell lines (80%) showed IC_{50} values >10μM in response to BYL719. This is in line with the current finding, in which 6 out of 8 (75%) *PIK3CA*-wildtype cell lines had IC_{50} values >10μM in response to BYL719.

A detailed analysis of the fingerprint of BKM120 with those of other PI3K inhibitors showed a relatively poor correlation, suggesting that perhaps BKM120 has a similar efficacy in inhibiting all four p110 subunits or it could mean that these are off-target effects. Previous published data showed that the IC_{50} values of BKM120 ranged from approximately 800 to 3000nM in a panel of 11 GC cell lines (Park *et al.*, 2012), and this is consistent with my finding.

6.4 Limitations of this study and future directions

The meta-analyses indicated that East Asians and Caucasians differ significantly in terms of the frequencies of *PIK3CA* mutation, *PTEN* deletion and PTEN loss in GC, and of PTEN loss in CRC. However, considerable heterogeneity was observed for all aberrations, with the exception of *PIK3CA* mutations in both GC and CRC. Comparison of the present study cohort (East Asian) with tumour samples from a Caucasian cohort should provide valuable information regarding the possibility of ethnic-specific aberrations in the PI3K pathway.

In the current study, *PIK3CA* amplification was found to be one of the major genetic aberrations in GC and the frequency was consistent with previous reports on Asian patients (Byun *et al.*, 2003; Shi *et al.*, 2012). In contrast, Kiyose *et al.* reported a frequency of only 3% for *PIK3CA* amplification in Asian GC patients (Kiyose *et al.*, 2012). It should be noted that the assay methods used in my study and in the Byun *et al.* and Shi *et al.* studies were PCR-based, whereas the method used by Kiyose was fluorescent *in situ* hybridization (FISH)-based. Thus, the large discrepancy in reported frequencies between different could be due to different techniques and thresholds. It appears that different assay methods such as FISH and qPCR can lead to different amplification frequencies even in the same patient cohort (Zaczek *et al.*, 2012). *PIK3CA* amplification has been used as inclusion criteria for the p110α-specific inhibitor BYL719 in advanced stage GC (NCT01613950), hence accurate determination of *PIK3CA* amplification in GC patients is essential. It will be important to assess the

concordance between FISH and qPCR in future studies so that the best method can be used to routinely evaluate *PIK3CA* amplification.

Two major PI3K aberration subtypes were identified in clinical samples of GC (PTEN loss alone and *PIK3CA* amplification/PTEN loss) and CRC (PTEN loss alone and PTEN loss/high pAKT) (Figure 3.3). However, the effects of PI3K inhibitors in these subtypes have not been addressed using preclinical models. This will be an interesting area for future investigation with PI3K inhibitors.

BSP-A and BSP-B are proprietary drugs provided by Bayer pharmaceuticals and their *in vitro* kinase activities are not publicly available. The sensitivity profile between the two drugs was not identical. A possible explanation for this could be differences in the mechanism of action. For instance, GSK2636771 (p110β-isoform specific inhibitor) is currently being tested in a clinical trial of PTEN-deficient malignancies following observations in preclinical models that suggested PTEN deficient cancers may depend on signaling via p110β rather than p110α (Jia *et al.*, 2008; Wee *et al.*, 2008). Therefore, knowledge of the *in vitro* kinase activities of these PI3K inhibitors may help to shed more light on the differences between BSP-A and BSP-B with respect to their regulation of GC cell growth. Unfortunate, this information was unavailable due to confidentially issues.

High expression of *IGFBP3* was found in this study to be associated with higher sensitivity to PI3K inhibitors. Knockdown of IGFBP3 using siRNA was used to confirm the role of IGFBP3 in mediating drug sensitivity in YCC1 . I

hypothesize that overexpression of IGFBP3 in resistant cell lines can reverse the effect of PI3K inhibition from resistant to sensitive. Experiments such as the overexpression of IGFBP3 in resistant cell lines could be used to further investigate this potential mechanism of resistance to PI3K inhibitors. This provides a rationale for combining IGF-1R and PI3K inhibitors for the treatment of GC. However, this combination effect still remains to be elucidated.

6.5 Future perspectives

Based on previous studies, the majority of *PIK3CA* mutations occur in exon 9 and exon 20 which encodes the helical and kinase domain, respectively (Kong *et al.*, 2014). A meta-analysis demonstrated a higher frequency of *PIK3CA* mutation in exons 9 and 20 were found in Caucasians rather than in East Asian populations. Further study is necessary to validate this finding independently.. Apart from hot spot mutations, whole exome sequencing analysis has also identified other non-hot spot *PIK3CA* mutations in GC (Cancer Genome Atlas Research, 2014). Only hot spot *PIK3CA* mutations were analyzed in this study and therefore, it will be interesting to know if other *PIK3CA* mutations can be used to predict the sensitivity of PI3K inhibitors. The current findings from this study suggest that high expression of *IGFBP3* is a potential biomarker for the efficacy of the use of PI3K inhibitors in *PIK3CA* wildtype cell lines , however, this finding should be further validated in clinical samples. Furthermore, it would also be worth exploring if overexpression of *IGFBP3* is the result of copy number aberration. It is important to understand the relationship between *PIK3CA* mutation and

overexpression of *IGFBP3* in GC patients because it would assist in prioritization during biomarker screening.

Overexpression of *IGFBP3* increased the sensitivity of GC cells to PI3K inhibitor and decreased the activity of IGF-/PI3K/AKT signaling. However, it will also be interesting to investigate if the extracellular priming of IGF-1 or knockdown of IGFBP3 in the YCC1-IGFBP3 (IGFBP overexpression) cells will reverse the effects of IGFBP3 on drug sensitivity. A previous study has reported that exogenous IGF-1 stimulates the growth of SNU cells, irrespective of the status of IGFBP3 expression. These results strongly suggest that basal levels of endogenous IGFBP3 may inhibit the growth of gastric cancer either in an IGF-dependent or IGF-independent manner (Yi *et al.*, 2001). IGFBP3 overexpression and its association with decreased activity of IGF/PI3K/AKT signaling suggests the increase in drug sensitivity could be due to IGF-dependent mechanism (Figure 5.4). However, whether the IGF-independent mechanism contributes to regulation of drug sensitivity remains to be determined. Therefore, further studies are needed to determine the specific mechanism of action of IGFBP3 in GC.

To date, the use of single agent PI3K inhibitor in therapy has not been promising and this may be partially explained by a narrow therapeutic window, particularly with pan-PI3K inhibitors (Fruman and Rommel, 2014). The adverse events of PI3K inhibitors also preclude the consistent delivery of doses necessary for adequate pathway inhibition. However, combination strategies may help to reduce the toxicity (Fruman and Rommel, 2014). In the present study, knockdown of IGFBP3 was found to increase resistance to PI3K inhibitors in GC cell lines

(Figure 5.4). It is therefore plausible that combining IGF signalling pathway inhibitors and PI3K inhibitors may increase the proportion of cancers that benefit from PI3K inhibitors and delay the development of resistance in cancers that are initially responsive. PI3K inhibitors will eventually play an important role in clinical practice across multiple tumour types once more clinical trials data is collected. Future studies will likely rely heavily on patient's selection strategies and combination approaches to determine how to maximize the efficacy of these agents in the treatment of patients with cancer.

6.6 Conclusions

This study has consolidated information in the literature on the frequency of different PI3K pathway aberrations. It has also revealed ethnic differences and co-occurrence patterns for PI3K pathway aberration in GC and CRC. The results suggest that *PIK3CA* and *KRAS* (G12V) mutations could be used as biomarkers for PI3K inhibitors in GC and CRC. *PIK3CA* wildtype tumours, high expression of *IGFBP3* could be a biomarker for the selection of GC patients who respond to PI3K inhibitors. Additional mechanistic studies are required to investigate the functional significance of IGFBP3 in mediating resistance to PI3K inhibitors. A better understanding of the known and candidate biomarkers described in this study could eventually lead to improved stratification of GC and CRC patients for treatment with PI3K inhibitors.

7 References

Andjelkovic, M., Alessi, D. R., Meier, R., Fernandez, A., Lamb, N. J., Frech, M., et al. (1997). Role of translocation in the activation and function of protein kinase B. *J Biol Chem* **272**(50): 31515-24.

Askham, J. M., Platt, F., Chambers, P. A., Snowden, H., Taylor, C. F. and Knowles, M. A. (2009). AKT1 mutations in bladder cancer: identification of a novel oncogenic mutation that can co-operate with E17K. *Oncogene* **29**(1): 150-5.

Avruch, J., Khokhlatchev, A., Kyriakis, J. M., Luo, Z., Tzivion, G., Vavvas, D., et al. (2001). Ras activation of the Raf kinase: tyrosine kinase recruitment of the MAP kinase cascade. *Recent Prog Horm Res* **56**: 127-55.

Bader, A. G., Kang, S., Zhao, L. and Vogt, P. K. (2005). Oncogenic PI3K deregulates transcription and translation. *Nat Rev Cancer* **5**(12): 921-9.

Bai, Z., Ye, Y., Chen, D., Shen, D., Xu, F., Cui, Z., et al. (2007). Homeoprotein Cdx2 and nuclear PTEN expression profiles are related to gastric cancer prognosis. *APMIS* **115**(12): 1383-90.

Bartlett, D. L. and Chu, E. (2012). Can metastatic colorectal cancer be cured? *Oncology (Williston Park)* **26**(3): 266-75.

Bendell, J. C., Rodon, J., Burris, H. A., de Jonge, M., Verweij, J., Birle, D., et al. (2011). Phase I, dose-escalation study of BKM120, an oral pan-Class I PI3K inhibitor, in patients with advanced solid tumors. *J Clin Oncol* **30**(3): 282-90.

Benistant, C., Chapuis, H. and Roche, S. (2000). A specific function for phosphatidylinositol 3-kinase alpha (p85alpha-p110alpha) in cell survival and for phosphatidylinositol 3-kinase beta (p85alpha-p110beta) in de novo DNA synthesis of human colon carcinoma cells. *Oncogene* **19**(44): 5083-90.

Bhattacharya, B., Akram, M., Balasubramanian, I., Tam, K. K., Koh, K. X., Yee, M. Q., et al. (2012). Pharmacologic synergy between dual phosphoinositide-3-kinase and mammalian target of rapamycin inhibition and 5-fluorouracil in PIK3CA mutant gastric cancer cells. *Cancer Biol Ther* **13**(1): 34-42.

Billottet, C., Grandage, V. L., Gale, R. E., Quattropani, A., Rommel, C., Vanhaesebroeck, B., et al. (2006). A selective inhibitor of the p110delta isoform of PI 3-kinase inhibits AML cell proliferation and survival and increases the cytotoxic effects of VP16. *Oncogene* **25**(50): 6648-59.

Bjornsti, M. A. and Houghton, P. J. (2004). The TOR pathway: a target for cancer therapy. *Nat Rev Cancer* **4**(5): 335-48.

Brachmann, S. M., Hofmann, I., Schnell, C., Fritsch, C., Wee, S., Lane, H., et al. (2009). Specific apoptosis induction by the dual PI3K/mTor inhibitor NVP-BEZ235 in HER2 amplified and PIK3CA mutant breast cancer cells. *Proc Natl Acad Sci U S A* **106**(52): 22299-304.

Brana, I. and Siu, L. L. (2012). Clinical development of phosphatidylinositol 3-kinase inhibitors for cancer treatment. *BMC Med* **10**: 161.

Bria, E., Milella, M., Cuppone, F., Novello, S., Ceribelli, A., Vaccaro, V., et al. (2011). Outcome of advanced NSCLC patients harboring sensitizing EGFR mutations randomized to EGFR tyrosine kinase inhibitors or chemotherapy as first-line treatment: a meta-analysis. *Ann Oncol* **22**(10): 2277-85.

Bulajic, M., Stimec, B., Jesenofsky, R., Kecmanovic, D., Ceranic, M., Kostic, N., et al. (2007). Helicobacter pylori in colorectal carcinoma tissue. *Cancer Epidemiol Biomarkers Prev* **16**(3): 631-3.

Burke, A. P., Yen, T. S., Shekitka, K. M. and Sobin, L. H. (1990). Lymphoepithelial carcinoma of the stomach with Epstein-Barr virus demonstrated by polymerase chain reaction. *Mod Pathol* **3**(3): 377-80.

Byun, D. S., Cho, K., Ryu, B. K., Lee, M. G., Park, J. I., Chae, K. S., et al. (2003). Frequent monoallelic deletion of PTEN and its reciprocal associatioin with PIK3CA amplification in gastric carcinoma. *Int J Cancer* **104**(3): 318-27.

Cancer Genome Atlas Research, N. (2014). Comprehensive molecular characterization of gastric adenocarcinoma. *Nature* **513**(7517): 202-9.

Cao, P., Maira, S. M., Garcia-Echeverria, C. and Hedley, D. W. (2009). Activity of a novel, dual PI3-kinase/mTor inhibitor NVP-BEZ235 against primary human pancreatic cancers grown as orthotopic xenografts. *Br J Cancer* **100**(8): 1267-76.

Cardone, M. H., Roy, N., Stennicke, H. R., Salvesen, G. S., Franke, T. F., Stanbridge, E., et al. (1998). Regulation of cell death protease caspase-9 by phosphorylation. *Science* **282**(5392): 1318-21.

Carpten, J. D., Faber, A. L., Horn, C., Donoho, G. P., Briggs, S. L., Robbins, C. M., et al. (2007). A transforming mutation in the pleckstrin homology domain of AKT1 in cancer. *Nature* **448**(7152): 439-44.

Cespedes, M. V., Sancho, F. J., Guerrero, S., Parreno, M., Casanova, I., Pavon, M. A., et al. (2006). K-ras Asp12 mutant neither interacts with Raf, nor

signals through Erk and is less tumorigenic than K-ras Val12. *Carcinogenesis* **27**(11): 2190-200.

Chalhoub, N. and Baker, S. J. (2009). PTEN and the PI3-kinase pathway in cancer. *Annu Rev Pathol* **4**: 127-50.

Chan, D. S., Twine, C. P. and Lewis, W. G. (2012). Systematic review and meta-analysis of the influence of HER2 expression and amplification in operable oesophageal cancer. *J Gastrointest Surg* **16**(10): 1821-9.

Christian Rommel, B. V., Peter K. Vogt (2011). Phosphoinositide 3-kinase in Health and Disease, Springer.

Cortes-Sempere, M., de Miguel, M. P., Pernia, O., Rodriguez, C., de Castro Carpeno, J., Nistal, M., et al. (2013). IGFBP-3 methylation-derived deficiency mediates the resistance to cisplatin through the activation of the IGFIR/Akt pathway in non-small cell lung cancer. *Oncogene* **32**(10): 1274-83.

Crews, C. M. and Erikson, R. L. (1993). Extracellular signals and reversible protein phosphorylation: what to Mek of it all. *Cell* **74**(2): 215-7.

Cully, M., You, H., Levine, A. J. and Mak, T. W. (2006). Beyond PTEN mutations: the PI3K pathway as an integrator of multiple inputs during tumorigenesis. *Nat Rev Cancer* **6**(3): 184-92.

Dan, S., Okamura, M., Seki, M., Yamazaki, K., Sugita, H., Okui, M., et al. (2010). Correlating phosphatidylinositol 3-kinase inhibitor efficacy with signaling pathway status: in silico and biological evaluations. *Cancer Res* **70**(12): 4982-94.

Dancey, J. and Sausville, E. A. (2003). Issues and progress with protein kinase inhibitors for cancer treatment. *Nat Rev Drug Discov* **2**(4): 296-313.

Das, K., Mohd Omar, M. F., Ong, C. W., Bin Abdul Rashid, S., Peh, B. K., Putti, T. C., et al. (2008). TRARESA: a tissue microarray-based hospital system for biomarker validation and discovery. *Pathology* **40**(5): 441-9.

Datta, S. R., Dudek, H., Tao, X., Masters, S., Fu, H., Gotoh, Y., et al. (1997). Akt phosphorylation of BAD couples survival signals to the cell-intrinsic death machinery. *Cell* **91**(2): 231-41.

Davies, S. P., Reddy, H., Caivano, M. and Cohen, P. (2000). Specificity and mechanism of action of some commonly used protein kinase inhibitors. *Biochem J* **351**(Pt 1): 95-105.

de Groot, R. P., Auwerx, J., Bourouis, M. and Sassone-Corsi, P. (1993). Negative regulation of Jun/AP-1: conserved function of glycogen synthase kinase 3 and the Drosophila kinase shaggy. *Oncogene* **8**(4): 841-7.

De Roock, W., Jonker, D. J., Di Nicolantonio, F., Sartore-Bianchi, A., Tu, D., Siena, S., et al. (2010). Association of KRAS p.G13D mutation with outcome in patients with chemotherapy-refractory metastatic colorectal cancer treated with cetuximab. *JAMA* **304**(16): 1812-20.

De Vita, F., Giuliani, F., Silvestris, N., Rossetti, S., Pizzolorusso, A., Santabarbara, G., et al. (2012). Current status of targeted therapies in advanced gastric cancer. *Expert Opin Ther Targets* **16 Suppl 2**: S29-34.

Deng, N., Goh, L. K., Wang, H., Das, K., Tao, J., Tan, I. B., et al. (2012). A comprehensive survey of genomic alterations in gastric cancer reveals systematic patterns of molecular exclusivity and co-occurrence among distinct therapeutic targets. *Gut* **61**(5): 673-84.

Des Guetz, G., Schischmanoff, O., Nicolas, P., Perret, G. Y., Morere, J. F. and Uzzan, B. (2009). Does microsatellite instability predict the efficacy of adjuvant chemotherapy in colorectal cancer? A systematic review with meta-analysis. *Eur J Cancer* **45**(10): 1890-6.

Di Nicolantonio, F., Arena, S., Tabernero, J., Grosso, S., Molinari, F., Macarulla, T., et al. (2010). Deregulation of the PI3K and KRAS signaling pathways in human cancer cells determines their response to everolimus. *J Clin Invest* **120**(8): 2858-66.

Di Nicolantonio, F., Martini, M., Molinari, F., Sartore-Bianchi, A., Arena, S., Saletti, P., et al. (2008). Wild-type BRAF is required for response to panitumumab or cetuximab in metastatic colorectal cancer. *J Clin Oncol* **26**(35): 5705-12.

Dokmanovic, M., Shen, Y., Bonacci, T. M., Hirsch, D. S. and Wu, W. J. (2011). Trastuzumab regulates IGFBP-2 and IGFBP-3 to mediate growth inhibition: implications for the development of predictive biomarkers for trastuzumab resistance. *Mol Cancer Ther* **10**(6): 917-28.

Downward, J. (2003). Targeting RAS signalling pathways in cancer therapy. *Nat Rev Cancer* **3**(1): 11-22.

Dufort, S., Richard, M. J. and de Fraipont, F. (2009). Pyrosequencing method to detect KRAS mutation in formalin-fixed and paraffin-embedded tumor tissues. *Anal Biochem* **391**(2): 166-8.

Elkabets, M., Vora, S., Juric, D., Morse, N., Mino-Kenudson, M., Muranen, T., et al. (2013). mTORC1 inhibition is required for sensitivity to PI3K

p110alpha inhibitors in PIK3CA-mutant breast cancer. *Sci Transl Med* **5**(196): 196ra99.

Engelman, J. A. (2009). Targeting PI3K signalling in cancer: opportunities, challenges and limitations. *Nat Rev Cancer* **9**(8): 550-62.

Engelman, J. A., Chen, L., Tan, X., Crosby, K., Guimaraes, A. R., Upadhyay, R., et al. (2008). Effective use of PI3K and MEK inhibitors to treat mutant Kras G12D and PIK3CA H1047R murine lung cancers. *Nat Med* **14**(12): 1351-6.

Esteva, F. J., Valero, V., Booser, D., Guerra, L. T., Murray, J. L., Pusztai, L., et al. (2002). Phase II study of weekly docetaxel and trastuzumab for patients with HER-2-overexpressing metastatic breast cancer. *J Clin Oncol* **20**(7): 1800-8.

Fabian, J. R., Vojtek, A. B., Cooper, J. A. and Morrison, D. K. (1994). A single amino acid change in Raf-1 inhibits Ras binding and alters Raf-1 function. *Proc Natl Acad Sci U S A* **91**(13): 5982-6.

Finan, P. M. and Thomas, M. J. (2004). PI 3-kinase inhibition: a therapeutic target for respiratory disease. *Biochem Soc Trans* **32**(Pt 2): 378-82.

Folkes, A. J., Ahmadi, K., Alderton, W. K., Alix, S., Baker, S. J., Box, G., et al. (2008). The identification of 2-(1H-indazol-4-yl)-6-(4-methanesulfonyl-piperazin-1-ylmethyl)-4-morpholin-4-yl-t hieno[3,2-d]pyrimidine (GDC-0941) as a potent, selective, orally bioavailable inhibitor of class I PI3 kinase for the treatment of cancer. *J Med Chem* **51**(18): 5522-32.

Foukas, L. C., Claret, M., Pearce, W., Okkenhaug, K., Meek, S., Peskett, E., et al. (2006). Critical role for the p110alpha phosphoinositide-3-OH kinase in growth and metabolic regulation. *Nature* **441**(7091): 366-70.

Foukas, L. C. and Shepherd, P. R. (2004). Phosphoinositide 3-kinase: the protein kinase that time forgot. *Biochem Soc Trans* **32**(Pt 2): 330-1.

Frattini, M., Saletti, P., Romagnani, E., Martin, V., Molinari, F., Ghisletta, M., et al. (2007). PTEN loss of expression predicts cetuximab efficacy in metastatic colorectal cancer patients. *Br J Cancer* **97**(8): 1139-45.

Fruman, D. A. and Rommel, C. (2014). PI3K and cancer: lessons, challenges and opportunities. *Nat Rev Drug Discov* **13**(2): 140-56.

Gadzicki, D., von Neuhoff, N., Steinemann, D., Just, M., Busche, G., Kreipe, H., et al. (2005). BCR-ABL gene amplification and overexpression in a patient with chronic myeloid leukemia treated with imatinib. *Cancer Genet Cytogenet* **159**(2): 164-7.

Galizia, G., Lieto, E., Orditura, M., Castellano, P., Mura, A. L., Imperatore, V., et al. (2007). Epidermal growth factor receptor (EGFR) expression is associated with a worse prognosis in gastric cancer patients undergoing curative surgery. *World J Surg* **31**(7): 1458-68.

Garassino, M. C., Marabese, M., Rusconi, P., Rulli, E., Martelli, O., Farina, G., et al. (2011). Different types of K-Ras mutations could affect drug sensitivity and tumour behaviour in non-small-cell lung cancer. *Ann Oncol* **22**(1): 235-7.

Garlich, J. R., De, P., Dey, N., Su, J. D., Peng, X., Miller, A., et al. (2008). A vascular targeted pan phosphoinositide 3-kinase inhibitor prodrug, SF1126, with antitumor and antiangiogenic activity. *Cancer Res* **68**(1): 206-15.

Garnett, M. J., Edelman, E. J., Heidorn, S. J., Greenman, C. D., Dastur, A., Lau, K. W., et al. (2012). Systematic identification of genomic markers of drug sensitivity in cancer cells. *Nature* **483**(7391): 570-5.

Gianni, L., Dafni, U., Gelber, R. D., Azambuja, E., Muehlbauer, S., Goldhirsch, A., et al. (2011). Treatment with trastuzumab for 1 year after adjuvant chemotherapy in patients with HER2-positive early breast cancer: a 4-year follow-up of a randomised controlled trial. *Lancet Oncol* **12**(3): 236-44.

Goel, A., Arnold, C. N., Niedzwiecki, D., Carethers, J. M., Dowell, J. M., Wasserman, L., et al. (2004). Frequent inactivation of PTEN by promoter hypermethylation in microsatellite instability-high sporadic colorectal cancers. *Cancer Res* **64**(9): 3014-21.

Grahn, N., Hmani-Aifa, M., Fransen, K., Soderkvist, P. and Monstein, H. J. (2005). Molecular identification of Helicobacter DNA present in human colorectal adenocarcinomas by 16S rDNA PCR amplification and pyrosequencing analysis. *J Med Microbiol* **54**(Pt 11): 1031-5.

Gregory, M. A., Qi, Y. and Hann, S. R. (2003). Phosphorylation by glycogen synthase kinase-3 controls c-myc proteolysis and subnuclear localization. *J Biol Chem* **278**(51): 51606-12.

Helicobacter and Cancer Collaborative, G. (2001). Gastric cancer and Helicobacter pylori: a combined analysis of 12 case control studies nested within prospective cohorts. *Gut* **49**(3): 347-53.

Herman, S. E., Gordon, A. L., Wagner, A. J., Heerema, N. A., Zhao, W., Flynn, J. M., et al. (2010). Phosphatidylinositol 3-kinase-delta inhibitor CAL-101 shows promising preclinical activity in chronic lymphocytic leukemia by antagonizing intrinsic and extrinsic cellular survival signals. *Blood* **116**(12): 2078-88.

Hermsen, M., Postma, C., Baak, J., Weiss, M., Rapallo, A., Sciutto, A., et al. (2002). Colorectal adenoma to carcinoma progression follows multiple pathways of chromosomal instability. *Gastroenterology* **123**(4): 1109-19.

Hong, D. S., Bowles, D. W., Falchook, G. S., Messersmith, W. A., George, G. C., O'Bryant, C. L., et al. (2012). A multicenter phase I trial of PX-866, an oral irreversible phosphatidylinositol 3-kinase inhibitor, in patients with advanced solid tumors. *Clin Cancer Res* **18**(15): 4173-82.

Hsieh, L. L., Lin, P. J., Chen, T. C. and Ou, J. T. (1998). Frequency of Epstein-Barr virus-associated gastric adenocarcinoma in Taiwan. *Cancer Lett* **129**(2): 125-9.

Ihle, N. T., Lemos, R., Jr., Wipf, P., Yacoub, A., Mitchell, C., Siwak, D., et al. (2009). Mutations in the phosphatidylinositol-3-kinase pathway predict for antitumor activity of the inhibitor PX-866 whereas oncogenic Ras is a dominant predictor for resistance. *Cancer Res* **69**(1): 143-50.

Ihle, N. T., Williams, R., Chow, S., Chew, W., Berggren, M. I., Paine-Murrieta, G., et al. (2004). Molecular pharmacology and antitumor activity of PX-866, a novel inhibitor of phosphoinositide-3-kinase signaling. *Mol Cancer Ther* **3**(7): 763-72.

Isoyama, S., Dan, S., Nishimura, Y., Nakamura, N., Kajiwara, G., Seki, M., et al. (2012). Establishment of phosphatidylinositol 3-kinase inhibitor-resistant cancer cell lines and therapeutic strategies for overcoming the resistance. *Cancer Sci* **103**(11): 1955-60.

Israel, D. A. and Peek, R. M. (2010). Surreptitious manipulation of the human host by Helicobacter pylori. *Gut Microbes* **1**(2): 119-127.

Issa, J. P. (2004). CpG island methylator phenotype in cancer. *Nat Rev Cancer* **4**(12): 988-93.

Iverson, C., Larson, G., Lai, C., Yeh, L. T., Dadson, C., Weingarten, P., et al. (2009). RDEA119/BAY 869766: a potent, selective, allosteric inhibitor of MEK1/2 for the treatment of cancer. *Cancer Res* **69**(17): 6839-47.

Jackson, S. P., Schoenwaelder, S. M., Goncalves, I., Nesbitt, W. S., Yap, C. L., Wright, C. E., et al. (2005). PI 3-kinase p110beta: a new target for antithrombotic therapy. *Nat Med* **11**(5): 507-14.

Jaiswal, B. S., Janakiraman, V., Kljavin, N. M., Chaudhuri, S., Stern, H. M., Wang, W., et al. (2009). Somatic mutations in p85alpha promote tumorigenesis through class IA PI3K activation. *Cancer Cell* **16**(6): 463-74.

Janku, F., Wheler, J. J., Westin, S. N., Moulder, S. L., Naing, A., Tsimberidou, A. M., et al. (2012). PI3K/AKT/mTOR inhibitors in patients with breast and gynecologic malignancies harboring PIK3CA mutations. *J Clin Oncol* **30**(8): 777-82.

Jerome, L., Alami, N., Belanger, S., Page, V., Yu, Q., Paterson, J., et al. (2006). Recombinant human insulin-like growth factor binding protein 3 inhibits growth of human epidermal growth factor receptor-2-overexpressing breast tumors and potentiates herceptin activity in vivo. *Cancer Res* **66**(14): 7245-52.

Jia, S., Liu, Z., Zhang, S., Liu, P., Zhang, L., Lee, S. H., et al. (2008). Essential roles of PI(3)K-p110beta in cell growth, metabolism and tumorigenesis. *Nature* **454**(7205): 776-9.

Jiang, X., Chen, S., Asara, J. M. and Balk, S. P. (2010). Phosphoinositide 3-kinase pathway activation in phosphate and tensin homolog (PTEN)-deficient prostate cancer cells is independent of receptor tyrosine kinases and mediated by the p110beta and p110delta catalytic subunits. *J Biol Chem* **285**(20): 14980-9.

Jones, M., Helliwell, P., Pritchard, C., Tharakan, J. and Mathew, J. (2007). Helicobacter pylori in colorectal neoplasms: is there an aetiological relationship? *World J Surg Oncol* **5**: 51.

Juric D, R. J., Gonzalez-Angulo AM, Burris HA, Bendell J, Berlin JD, Middleton MR, Bottle D, Boehm M, Schmitt A, Rouyre N, Quadt C, Baselga J (2012). BYL719, a next generation PI3K alpha specific inhibitor: Preliminary safety, PK, and efficacy results from the first-in-human study [abstract]. Proceedings of the 103rd Annual Meeting of the American Association for Cancer Research: March 31-April 4 2012; Chicago, IL Philadelphia, PA: American Association for Cancer Research; 2012, Abstract CT-01.

Kang, S., Bader, A. G. and Vogt, P. K. (2005). Phosphatidylinositol 3-kinase mutations identified in human cancer are oncogenic. *Proc Natl Acad Sci U S A* **102**(3): 802-7.

Kang, S., Denley, A., Vanhaesebroeck, B. and Vogt, P. K. (2006). Oncogenic transformation induced by the p110beta, -gamma, and -delta isoforms of class I phosphoinositide 3-kinase. *Proc Natl Acad Sci U S A* **103**(5): 1289-94.

Karakas, B., Bachman, K. E. and Park, B. H. (2006). Mutation of the PIK3CA oncogene in human cancers. *Br J Cancer* **94**(4): 455-9.

Katso, R., Okkenhaug, K., Ahmadi, K., White, S., Timms, J. and Waterfield, M. D. (2001). Cellular function of phosphoinositide 3-kinases: implications

for development, homeostasis, and cancer. *Annu Rev Cell Dev Biol* **17**: 615-75.

Keniry, M. and Parsons, R. (2008). The role of PTEN signaling perturbations in cancer and in targeted therapy. *Oncogene* **27**(41): 5477-85.

Khokhlatchev, A. V., Canagarajah, B., Wilsbacher, J., Robinson, M., Atkinson, M., Goldsmith, E., et al. (1998). Phosphorylation of the MAP kinase ERK2 promotes its homodimerization and nuclear translocation. *Cell* **93**(4): 605-15.

Kim, M. S., Jeong, E. G., Yoo, N. J. and Lee, S. H. (2008). Mutational analysis of oncogenic AKT E17K mutation in common solid cancers and acute leukaemias. *Br J Cancer* **98**(9): 1533-5.

Kiyose, S., Nagura, K., Tao, H., Igarashi, H., Yamada, H., Goto, M., et al. (2012). Detection of kinase amplifications in gastric cancer archives using fluorescence in situ hybridization. *Pathol Int* **62**(7): 477-84.

Knight, Z. A., Chiang, G. G., Alaimo, P. J., Kenski, D. M., Ho, C. B., Coan, K., et al. (2004). Isoform-specific phosphoinositide 3-kinase inhibitors from an arylmorpholine scaffold. *Bioorg Med Chem* **12**(17): 4749-59.

Kong, D., Yamori, T., Yamazaki, K. and Dan, S. (2014). In vitro multifaceted activities of a specific group of novel phosphatidylinositol 3-kinase inhibitors on hotspot mutant PIK3CA. *Invest New Drugs*.

Kovacina, K. S., Park, G. Y., Bae, S. S., Guzzetta, A. W., Schaefer, E., Birnbaum, M. J., et al. (2003). Identification of a proline-rich Akt substrate as a 14-3-3 binding partner. *J Biol Chem* **278**(12): 10189-94.

Kubo, H., Hazeki, K., Takasuga, S. and Hazeki, O. (2005). Specific role for p85/p110beta in GTP-binding-protein-mediated activation of Akt. *Biochem J* **392**(Pt 3): 607-14.

Lee, J., Xu, Y., Lu, L., Bergman, B., Leitner, J. W., Greyson, C., et al. (2010). Multiple abnormalities of myocardial insulin signaling in a porcine model of diet-induced obesity. *Am J Physiol Heart Circ Physiol* **298**(2): H310-9.

Lehmann, B. D., Bauer, J. A., Chen, X., Sanders, M. E., Chakravarthy, A. B., Shyr, Y., et al. (2011). Identification of human triple-negative breast cancer subtypes and preclinical models for selection of targeted therapies. *J Clin Invest* **121**(7): 2750-67.

Lengauer, C., Kinzler, K. W. and Vogelstein, B. (1997). Genetic instability in colorectal cancers. *Nature* **386**(6625): 623-7.

Li, H. and Durbin, R. (2010). Fast and accurate long-read alignment with Burrows-Wheeler transform. *Bioinformatics* **26**(5): 589-95.

Li, V. S., Wong, C. W., Chan, T. L., Chan, A. S., Zhao, W., Chu, K. M., et al. (2005). Mutations of PIK3CA in gastric adenocarcinoma. *BMC Cancer* **5**: 29.

Li, Y., Tanaka, Y., Tada, M., Hua, R., Seto, M., Asaoka, Y., et al. (2008). Absence of the AKT1 pleckstrin homology domain mutation in Japanese gastrointestinal and liver cancer patients. *APMIS* **116**(10): 931-3.

Liu, Q., Ohshima, K., Masuda, Y. and Kikuchi, M. (1995). Detection of the Epstein-Barr virus in primary gastric lymphoma by in situ hybridization. *Pathol Int* **45**(2): 131-6.

Liu, T. J., Koul, D., LaFortune, T., Tiao, N., Shen, R. J., Maira, S. M., et al. (2009). NVP-BEZ235, a novel dual phosphatidylinositol 3-kinase/mammalian target of rapamycin inhibitor, elicits multifaceted antitumor activities in human gliomas. *Mol Cancer Ther* **8**(8): 2204-10.

Loh, M., Chua, D., Yao, Y., Soo, R. A., Garrett, K., Zeps, N., et al. (2012). Can population differences in chemotherapy outcomes be inferred from differences in pharmacogenetic frequencies? *Pharmacogenomics J*.

Lothe, R. A. (1997). Microsatellite instability in human solid tumors. *Mol Med Today* **3**(2): 61-8.

Loupakis, F., Pollina, L., Stasi, I., Ruzzo, A., Scartozzi, M., Santini, D., et al. (2009). PTEN expression and KRAS mutations on primary tumors and metastases in the prediction of benefit from cetuximab plus irinotecan for patients with metastatic colorectal cancer. *J Clin Oncol* **27**(16): 2622-9.

Maira, S. M., Stauffer, F., Brueggen, J., Furet, P., Schnell, C., Fritsch, C., et al. (2008). Identification and characterization of NVP-BEZ235, a new orally available dual phosphatidylinositol 3-kinase/mammalian target of rapamycin inhibitor with potent in vivo antitumor activity. *Mol Cancer Ther* **7**(7): 1851-63.

Mao, M., Tian, F., Mariadason, J. M., Tsao, C. C., Lemos, R., Jr., Dayyani, F., et al. (2013). Resistance to BRAF inhibition in BRAF-mutant colon cancer can be overcome with PI3K inhibition or demethylating agents. *Clin Cancer Res* **19**(3): 657-67.

Marais, R., Light, Y., Paterson, H. F. and Marshall, C. J. (1995). Ras recruits Raf-1 to the plasma membrane for activation by tyrosine phosphorylation. *EMBO J* **14**(13): 3136-45.

Marais, R., Wynne, J. and Treisman, R. (1993). The SRF accessory protein Elk-1 contains a growth factor-regulated transcriptional activation domain. *Cell* **73**(2): 381-93.

Marion, F., Williams, D. E., Patrick, B. O., Hollander, I., Mallon, R., Kim, S. C., et al. (2006). Liphagal, a Selective inhibitor of PI3 kinase alpha isolated from the sponge akacoralliphaga: structure elucidation and biomimetic synthesis. *Org Lett* **8**(2): 321-4.

Marone, R., Erhart, D., Mertz, A. C., Bohnacker, T., Schnell, C., Cmiljanovic, V., et al. (2009). Targeting melanoma with dual phosphoinositide 3-kinase/mammalian target of rapamycin inhibitors. *Mol Cancer Res* **7**(4): 601-13.

Martini, M., Vecchione, L., Siena, S., Tejpar, S. and Bardelli, A. (2011). Targeted therapies: how personal should we go? *Nat Rev Clin Oncol* **9**(2): 87-97.

McCubrey, J. A., Steelman, L. S., Chappell, W. H., Abrams, S. L., Wong, E. W., Chang, F., et al. (2007). Roles of the Raf/MEK/ERK pathway in cell growth, malignant transformation and drug resistance. *Biochim Biophys Acta* **1773**(8): 1263-84.

Meili, R., Ellsworth, C., Lee, S., Reddy, T. B., Ma, H. and Firtel, R. A. (1999). Chemoattractant-mediated transient activation and membrane localization of Akt/PKB is required for efficient chemotaxis to cAMP in Dictyostelium. *EMBO J* **18**(8): 2092-105.

Miyahara, R., Niwa, Y., Matsuura, T., Maeda, O., Ando, T., Ohmiya, N., et al. (2007). Prevalence and prognosis of gastric cancer detected by screening in a large Japanese population: data from a single institute over 30 years. *J Gastroenterol Hepatol* **22**(9): 1435-42.

Morewaya, J., Koriyama, C., Akiba, S., Shan, D., Itoh, T. and Eizuru, Y. (2004). Epstein-Barr virus-associated gastric carcinoma in Papua New Guinea. *Oncol Rep* **12**(5): 1093-8.

Morrison, D. (1994). 14-3-3: modulators of signaling proteins? *Science* **266**(5182): 56-7.

Nassif, N. T., Lobo, G. P., Wu, X., Henderson, C. J., Morrison, C. D., Eng, C., et al. (2004). PTEN mutations are common in sporadic microsatellite stable colorectal cancer. *Oncogene* **23**(2): 617-28.

Ni, J., Liu, Q., Xie, S., Carlson, C., Von, T., Vogel, K., et al. (2012). Functional characterization of an isoform-selective inhibitor of PI3K-p110beta as a potential anticancer agent. *Cancer Discov* **2**(5): 425-33.

Nikolakaki, E., Coffer, P. J., Hemelsoet, R., Woodgett, J. R. and Defize, L. H. (1993). Glycogen synthase kinase 3 phosphorylates Jun family members in vitro and negatively regulates their transactivating potential in intact cells. *Oncogene* **8**(4): 833-40.

Nowak, M. A., Komarova, N. L., Sengupta, A., Jallepalli, P. V., Shih Ie, M., Vogelstein, B., et al. (2002). The role of chromosomal instability in tumor initiation. *Proc Natl Acad Sci U S A* **99**(25): 16226-31.

O'Brien, C., Wallin, J. J., Sampath, D., GuhaThakurta, D., Savage, H., Punnoose, E. A., et al. (2010). Predictive biomarkers of sensitivity to the phosphatidylinositol 3' kinase inhibitor GDC-0941 in breast cancer preclinical models. *Clin Cancer Res* **16**(14): 3670-83.

Oki, E., Baba, H., Tokunaga, E., Nakamura, T., Ueda, N., Futatsugi, M., et al. (2005). Akt phosphorylation associates with LOH of PTEN and leads to chemoresistance for gastric cancer. *Int J Cancer* **117**(3): 376-80.

Ozbay, T., Durden, D. L., Liu, T., O'Regan, R. M. and Nahta, R. (2009). In vitro evaluation of pan-PI3-kinase inhibitor SF1126 in trastuzumab-sensitive and trastuzumab-resistant HER2-over-expressing breast cancer cells. *Cancer Chemother Pharmacol* **65**(4): 697-706.

Paez, J. G., Janne, P. A., Lee, J. C., Tracy, S., Greulich, H., Gabriel, S., et al. (2004). EGFR mutations in lung cancer: correlation with clinical response to gefitinib therapy. *Science* **304**(5676): 1497-500.

Pal, J., Fulciniti, M., Nanjappa, P., Buon, L., Tai, Y. T., Tassone, P., et al. (2012). Targeting PI3K and RAD51 in Barrett's adenocarcinoma: impact on DNA damage checkpoints, expression profile and tumor growth. *Cancer Genomics Proteomics* **9**(2): 55-66.

Parang, K. and Sun, G. (2004). Design strategies for protein kinase inhibitors. *Curr Opin Drug Discov Devel* **7**(5): 617-29.

Park, E., Park, J., Han, S. W., Im, S. A., Kim, T. Y., Oh, D. Y., et al. (2012). NVP-BKM120, a novel PI3K inhibitor, shows synergism with a STAT3 inhibitor in human gastric cancer cells harboring KRAS mutations. *Int J Oncol* **40**(4): 1259-66.

Perks, C. M. and Holly, J. M. (2008). IGF binding proteins (IGFBPs) and regulation of breast cancer biology. *J Mammary Gland Biol Neoplasia* **13**(4): 455-69.

Phillips, L. S., Pao, C. I. and Villafuerte, B. C. (1998). Molecular regulation of insulin-like growth factor-I and its principal binding protein, IGFBP-3. *Prog Nucleic Acid Res Mol Biol* **60**: 195-265.

Philp, A. J., Campbell, I. G., Leet, C., Vincan, E., Rockman, S. P., Whitehead, R. H., et al. (2001). The phosphatidylinositol 3'-kinase p85alpha gene is an oncogene in human ovarian and colon tumors. *Cancer Res* **61**(20): 7426-9.

Prahallad, A., Sun, C., Huang, S., Di Nicolantonio, F., Salazar, R., Zecchin, D., et al. (2012). Unresponsiveness of colon cancer to BRAF(V600E) inhibition through feedback activation of EGFR. *Nature* **483**(7387): 100-3.

Press, M. F., Bernstein, L., Thomas, P. A., Meisner, L. F., Zhou, J. Y., Ma, Y., et al. (1997). HER-2/neu gene amplification characterized by fluorescence in situ hybridization: poor prognosis in node-negative breast carcinomas. *J Clin Oncol* **15**(8): 2894-904.

Raynaud, F. I., Eccles, S. A., Patel, S., Alix, S., Box, G., Chuckowree, I., et al. (2009). Biological properties of potent inhibitors of class I phosphatidylinositide 3-kinases: from PI-103 through PI-540, PI-620 to the oral agent GDC-0941. *Mol Cancer Ther* **8**(7): 1725-38.

Ren, J., Li, G., Ge, J., Li, X. and Zhao, Y. (2012). Is K-ras gene mutation a prognostic factor for colorectal cancer: a systematic review and meta-analysis. *Dis Colon Rectum* **55**(8): 913-23.

Rodriguez-Viciana, P., Warne, P. H., Dhand, R., Vanhaesebroeck, B., Gout, I., Fry, M. J., et al. (1994). Phosphatidylinositol-3-OH kinase as a direct target of Ras. *Nature* **370**(6490): 527-32.

Rossig, L., Badorff, C., Holzmann, Y., Zeiher, A. M. and Dimmeler, S. (2002). Glycogen synthase kinase-3 couples AKT-dependent signaling to the regulation of p21Cip1 degradation. *J Biol Chem* **277**(12): 9684-9.

Ruggero, D. and Pandolfi, P. P. (2003). Does the ribosome translate cancer? *Nat Rev Cancer* **3**(3): 179-92.

Salmena, L., Carracedo, A. and Pandolfi, P. P. (2008). Tenets of PTEN tumor suppression. *Cell* **133**(3): 403-14.

Samuels, Y. and Velculescu, V. E. (2004). Oncogenic mutations of PIK3CA in human cancers. *Cell Cycle* **3**(10): 1221-4.

Samuels, Y., Wang, Z., Bardelli, A., Silliman, N., Ptak, J., Szabo, S., et al. (2004). High frequency of mutations of the PIK3CA gene in human cancers. *Science* **304**(5670): 554.

Sanchez, C. G., Ma, C. X., Crowder, R. J., Guintoli, T., Phommaly, C., Gao, F., et al. (2011). Preclinical modeling of combined phosphatidylinositol-3-kinase inhibition with endocrine therapy for estrogen receptor-positive breast cancer. *Breast Cancer Res* **13**(2): R21.

Santiskulvong, C., Konecny, G. E., Fekete, M., Chen, K. Y., Karam, A., Mulholland, D., et al. (2011). Dual targeting of phosphoinositide 3-kinase and mammalian target of rapamycin using NVP-BEZ235 as a novel therapeutic approach in human ovarian carcinoma. *Clin Cancer Res* **17**(8): 2373-84.

Sarbassov, D. D., Guertin, D. A., Ali, S. M. and Sabatini, D. M. (2005). Phosphorylation and regulation of Akt/PKB by the rictor-mTOR complex. *Science* **307**(5712): 1098-101.

Schernhammer, E. S., Hankinson, S. E., Hunter, D. J., Blouin, M. J. and Pollak, M. N. (2003). Polymorphic variation at the -202 locus in IGFBP3: Influence on serum levels of insulin-like growth factors, interaction with plasma retinol and vitamin D and breast cancer risk. *Int J Cancer* **107**(1): 60-4.

Schnell, C. R., Stauffer, F., Allegrini, P. R., O'Reilly, T., McSheehy, P. M., Dartois, C., et al. (2008). Effects of the dual phosphatidylinositol 3-kinase/mammalian target of rapamycin inhibitor NVP-BEZ235 on the tumor vasculature: implications for clinical imaging. *Cancer Res* **68**(16): 6598-607.

Sears, R., Nuckolls, F., Haura, E., Taya, Y., Tamai, K. and Nevins, J. R. (2000). Multiple Ras-dependent phosphorylation pathways regulate Myc protein stability. *Genes Dev* **14**(19): 2501-14.

Seedhouse, C. H., Hunter, H. M., Lloyd-Lewis, B., Massip, A. M., Pallis, M., Carter, G. I., et al. (2006). DNA repair contributes to the drug-resistant phenotype of primary acute myeloid leukaemia cells with FLT3 internal tandem duplications and is reversed by the FLT3 inhibitor PKC412. *Leukemia* **20**(12): 2130-6.

Selvaggi, G., Novello, S., Torri, V., Leonardo, E., De Giuli, P., Borasio, P., et al. (2004). Epidermal growth factor receptor overexpression correlates with a poor prognosis in completely resected non-small-cell lung cancer. *Ann Oncol* **15**(1): 28-32.

Serra, V., Markman, B., Scaltriti, M., Eichhorn, P. J., Valero, V., Guzman, M., et al. (2008). NVP-BEZ235, a dual PI3K/mTOR inhibitor, prevents PI3K signaling and inhibits the growth of cancer cells with activating PI3K mutations. *Cancer Res* **68**(19): 8022-30.

She, Q. B., Chandarlapaty, S., Ye, Q., Lobo, J., Haskell, K. M., Leander, K. R., et al. (2008). Breast tumor cells with PI3K mutation or HER2 amplification are selectively addicted to Akt signaling. *PLoS One* **3**(8): e3065.

Shepherd, P. R. (2005). Mechanisms regulating phosphoinositide 3-kinase signalling in insulin-sensitive tissues. *Acta Physiol Scand* **183**(1): 3-12.

Shi, J., Yao, D., Liu, W., Wang, N., Lv, H., Zhang, G., et al. (2012). Highly frequent PIK3CA amplification is associated with poor prognosis in gastric cancer. *BMC Cancer* **12**: 50.

Shibata, D., Peinado, M. A., Ionov, Y., Malkhosyan, S. and Perucho, M. (1994). Genomic instability in repeated sequences is an early somatic event in colorectal tumorigenesis that persists after transformation. *Nat Genet* **6**(3): 273-81.

Shibata, D. and Weiss, L. M. (1992). Epstein-Barr virus-associated gastric adenocarcinoma. *Am J Pathol* **140**(4): 769-74.

Smith, I., Procter, M., Gelber, R. D., Guillaume, S., Feyereislova, A., Dowsett, M., et al. (2007). 2-year follow-up of trastuzumab after adjuvant chemotherapy in HER2-positive breast cancer: a randomised controlled trial. *Lancet* **369**(9555): 29-36.

Soong, R. and Iacopetta, B. J. (1997). A rapid and nonisotopic method for the screening and sequencing of p53 gene mutations in formalin-fixed, paraffin-embedded tumors. *Mod Pathol* **10**(3): 252-8.

Soussi, T., Asselain, B., Hamroun, D., Kato, S., Ishioka, C., Claustres, M., et al. (2006). Meta-analysis of the p53 mutation database for mutant p53 biological activity reveals a methodologic bias in mutation detection. *Clin Cancer Res* **12**(1): 62-9.

Spano, J. P., Lagorce, C., Atlan, D., Milano, G., Domont, J., Benamouzig, R., et al. (2005). Impact of EGFR expression on colorectal cancer patient prognosis and survival. *Ann Oncol* **16**(1): 102-8.

Stauffer, F., Holzer, P. and Garcia-Echeverria, C. (2005). Blocking the PI3K/PKB pathway in tumor cells. *Curr Med Chem Anticancer Agents* **5**(5): 449-62.

Stein, R. C. and Waterfield, M. D. (2000). PI3-kinase inhibition: a target for drug development? *Mol Med Today* **6**(9): 347-57.

Stokoe, D. (2005). The phosphoinositide 3-kinase pathway and cancer. *Expert Rev Mol Med* **7**(10): 1-22.

Sujobert, P., Bardet, V., Cornillet-Lefebvre, P., Hayflick, J. S., Prie, N., Verdier, F., et al. (2005). Essential role for the p110delta isoform in phosphoinositide 3-kinase activation and cell proliferation in acute myeloid leukemia. *Blood* **106**(3): 1063-6.

Tanaka, H., Yoshida, M., Tanimura, H., Fujii, T., Sakata, K., Tachibana, Y., et al. (2011). The selective class I PI3K inhibitor CH5132799 targets human cancers harboring oncogenic PIK3CA mutations. *Clin Cancer Res* **17**(10): 3272-81.

Tanner, M., Hollmen, M., Junttila, T. T., Kapanen, A. I., Tommola, S., Soini, Y., et al. (2005). Amplification of HER-2 in gastric carcinoma: association with Topoisomerase IIalpha gene amplification, intestinal type, poor prognosis and sensitivity to trastuzumab. *Ann Oncol* **16**(2): 273-8.

Tomii, K., Tsukuda, K., Toyooka, S., Dote, H., Hanafusa, T., Asano, H., et al. (2007). Aberrant promoter methylation of insulin-like growth factor binding protein-3 gene in human cancers. *Int J Cancer* **120**(3): 566-73.

Treisman, R. (1996). Regulation of transcription by MAP kinase cascades. *Curr Opin Cell Biol* **8**(2): 205-15.

Vanhaesebroeck, B., Leevers, S. J., Ahmadi, K., Timms, J., Katso, R., Driscoll, P. C., et al. (2001). Synthesis and function of 3-phosphorylated inositol lipids. *Annu Rev Biochem* **70**: 535-602.

Vasudevan, K. M., Barbie, D. A., Davies, M. A., Rabinovsky, R., McNear, C. J., Kim, J. J., et al. (2009). AKT-independent signaling downstream of oncogenic PIK3CA mutations in human cancer. *Cancer Cell* **16**(1): 21-32.

Velho, S., Oliveira, C., Ferreira, A., Ferreira, A. C., Suriano, G., Schwartz, S., Jr., et al. (2005). The prevalence of PIK3CA mutations in gastric and colon cancer. *Eur J Cancer* **41**(11): 1649-54.

Walker, E. H., Pacold, M. E., Perisic, O., Stephens, L., Hawkins, P. T., Wymann, M. P., et al. (2000). Structural determinants of phosphoinositide 3-kinase inhibition by wortmannin, LY294002, quercetin, myricetin, and staurosporine. *Mol Cell* **6**(4): 909-19.

Walker, E. H., Perisic, O., Ried, C., Stephens, L. and Williams, R. L. (1999). Structural insights into phosphoinositide 3-kinase catalysis and signalling. *Nature* **402**(6759): 313-20.

Wee, S., Wiederschain, D., Maira, S. M., Loo, A., Miller, C., deBeaumont, R., et al. (2008). PTEN-deficient cancers depend on PIK3CB. *Proc Natl Acad Sci U S A* **105**(35): 13057-62.

Wei, W., Jin, J., Schlisio, S., Harper, J. W. and Kaelin, W. G., Jr. (2005). The v-Jun point mutation allows c-Jun to escape GSK3-dependent recognition and destruction by the Fbw7 ubiquitin ligase. *Cancer Cell* **8**(1): 25-33.

Weigelt, B. and Downward, J. (2012). Genomic Determinants of PI3K Pathway Inhibitor Response in Cancer. *Front Oncol* **2**: 109.

Williams, R., Berndt, A., Miller, S., Hon, W. C. and Zhang, X. (2009). Form and flexibility in phosphoinositide 3-kinases. *Biochem Soc Trans* **37**(Pt 4): 615-26.

Wong, H. and Yau, T. (2012). Targeted therapy in the management of advanced gastric cancer: are we making progress in the era of personalized medicine? *Oncologist* **17**(3): 346-58.

Wong, H. and Yau, T. (2013). Molecular targeted therapies in advanced gastric cancer: does tumor histology matter? *Therap Adv Gastroenterol* **6**(1): 15-31.

Wu, H., Shekar, S. C., Flinn, R. J., El-Sibai, M., Jaiswal, B. S., Sen, K. I., et al. (2009). Regulation of Class IA PI 3-kinases: C2 domain-iSH2 domain contacts inhibit p85/p110alpha and are disrupted in oncogenic p85 mutants. *Proc Natl Acad Sci U S A* **106**(48): 20258-63.

Yakirevich, E. and Resnick, M. B. (2013). Pathology of gastric cancer and its precursor lesions. *Gastroenterol Clin North Am* **42**(2): 261-84.

Yamashita-Kashima, Y., Iijima, S., Yorozu, K., Furugaki, K., Kurasawa, M., Ohta, M., et al. (2011). Pertuzumab in combination with trastuzumab shows significantly enhanced antitumor activity in HER2-positive human gastric cancer xenograft models. *Clin Cancer Res* **17**(15): 5060-70.

Yamashita, K., Sakuramoto, S., Katada, N., Futawatari, N., Moriya, H., Hirai, K., et al. (2009). Diffuse type advanced gastric cancer showing dismal prognosis is characterized by deeper invasion and emerging peritoneal cancer cell: the latest comparative study to intestinal advanced gastric cancer. *Hepatogastroenterology* **56**(89): 276-81.

Yamashita, S., Tsujino, Y., Moriguchi, K., Tatematsu, M. and Ushijima, T. (2006). Chemical genomic screening for methylation-silenced genes in gastric cancer cell lines using 5-aza-2'-deoxycytidine treatment and oligonucleotide microarray. *Cancer Sci* **97**(1): 64-71.

Yi, H. K., Hwang, P. H., Yang, D. H., Kang, C. W. and Lee, D. Y. (2001). Expression of the insulin-like growth factors (IGFs) and the IGF-binding proteins (IGFBPs) in human gastric cancer cells. *Eur J Cancer* **37**(17): 2257-63.

Zaczek, A., Markiewicz, A., Supernat, A., Bednarz-Knoll, N., Brandt, B., Seroczynska, B., et al. (2012). Prognostic value of TOP2A gene amplification and chromosome 17 polysomy in early breast cancer. *Pathol Oncol Res* **18**(4): 885-94.

Zhang, H., Liu, G., Dziubinski, M., Yang, Z., Ethier, S. P. and Wu, G. (2008). Comprehensive analysis of oncogenic effects of PIK3CA mutations in human mammary epithelial cells. *Breast Cancer Res Treat* **112**(2): 217-27.

Zhang, J., Roberts, T. M. and Shivdasani, R. A. (2011). Targeting PI3K signaling as a therapeutic approach for colorectal cancer. *Gastroenterology* **141**(1): 50-61.

Zhao, L. and Vogt, P. K. (2008). Helical domain and kinase domain mutations in p110alpha of phosphatidylinositol 3-kinase induce gain of function by different mechanisms. *Proc Natl Acad Sci U S A* **105**(7): 2652-7.

Zhu, X., Qin, X., Fei, M., Hou, W., Greshock, J., Bachman, K. E., et al. (2012). Combined Phosphatase and Tensin Homolog (PTEN) Loss and Fatty Acid Synthase (FAS) Overexpression Worsens the Prognosis of Chinese Patients with Hepatocellular Carcinoma. *Int J Mol Sci* **13**(8): 9980-91.

Zhukov, N. V. and Tjulandin, S. A. (2008). Targeted therapy in the treatment of solid tumors: practice contradicts theory. *Biochemistry (Mosc)* **73**(5): 605-18.

8 Appendix

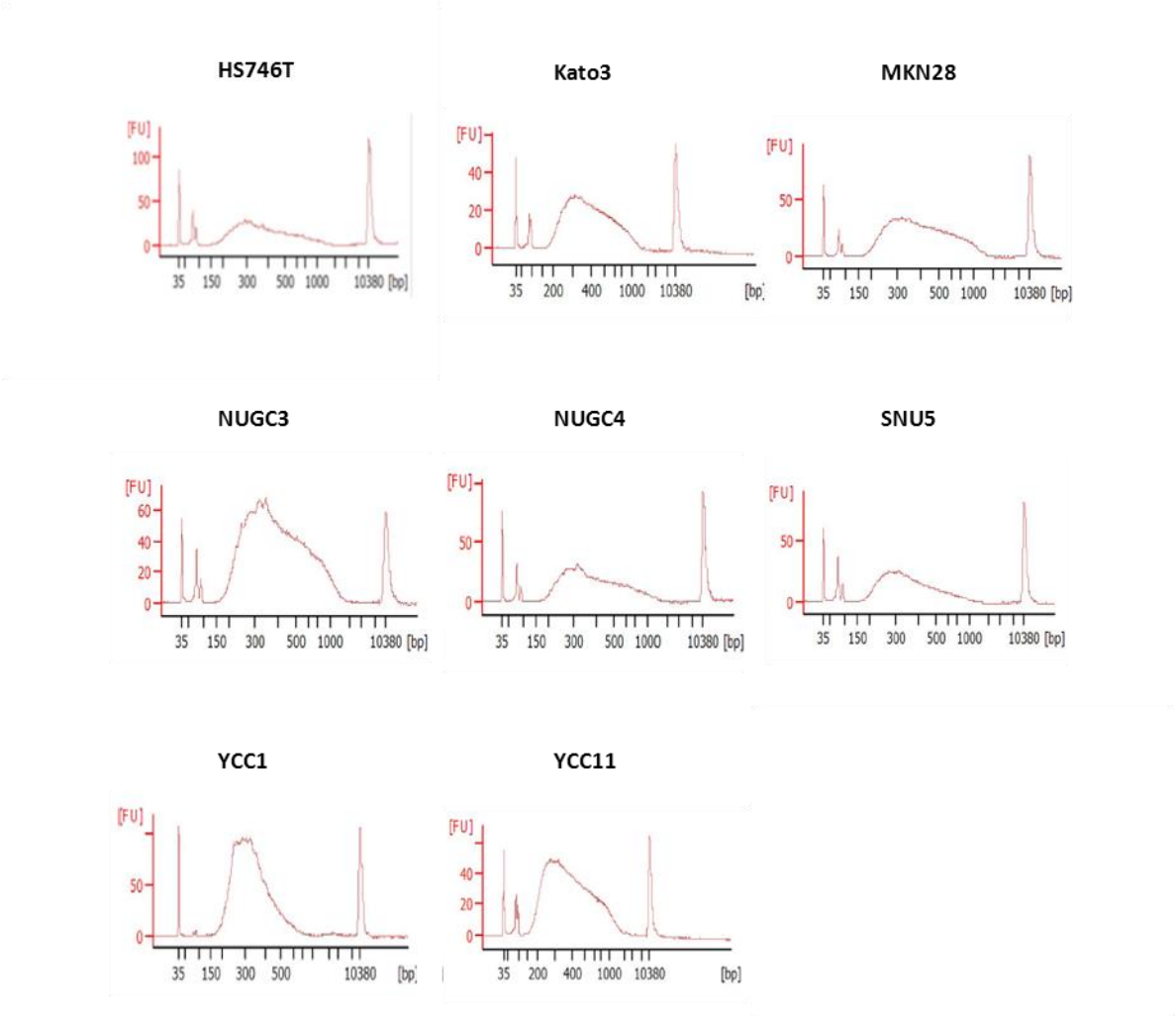

Appendix Figure 1. cDNA quality analysis using Agilent Bioanalyzer. cDNA was converted from rRNA-depleted RNA using ScriptSeq™ v2 mRNA-Seq Library Preparation Kit. The Bioanalyzer showed optimal cDNA fragmentation in the range of 200-500 bp.

Appendix Fig.2 (Legend over page)

A. HS746T

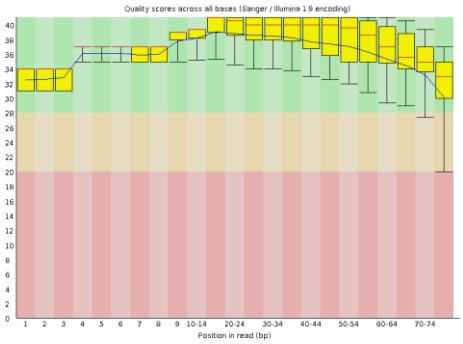

Per base sequence quality_R1

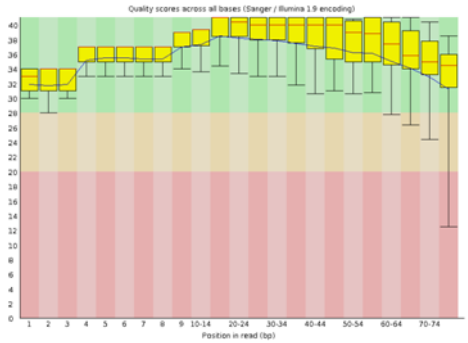

Per base sequence quality_R2

B. Kato3

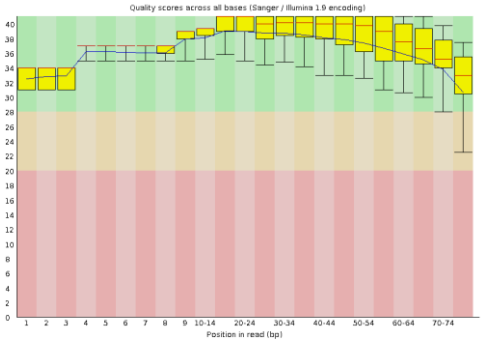

Per base sequence quality_R1

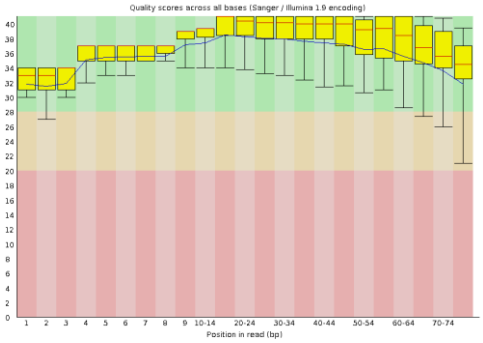

Per base sequence quality_R2

C. MKN28

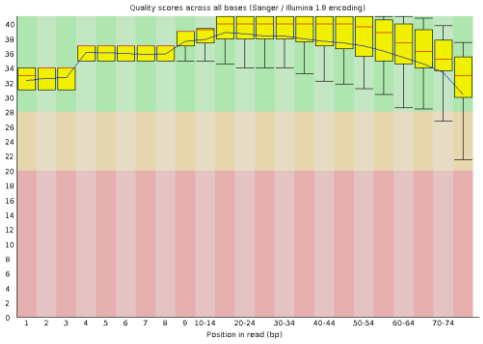

Per base sequence quality_R1

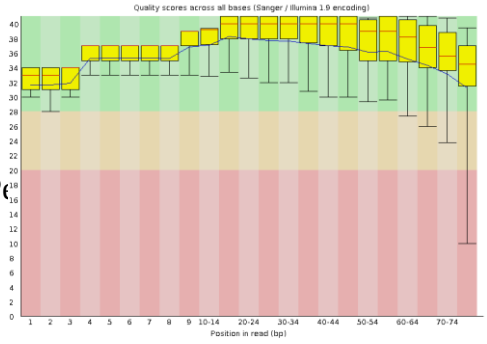

Per base sequence quality_R2

Appendix Fig.2 (Legend over page)

D. NUGC3

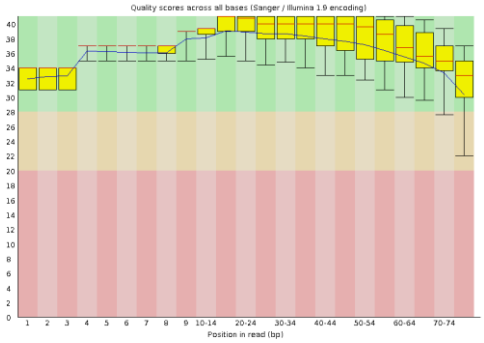

Per base sequence quality_R1

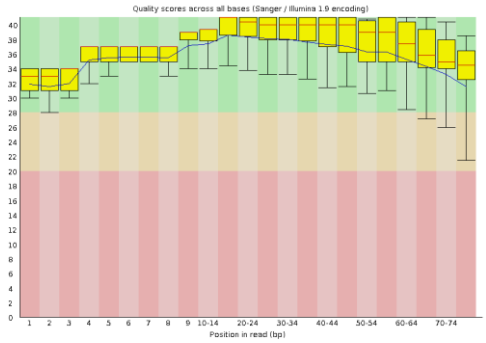

Per base sequence quality_R2

E. NUGC4

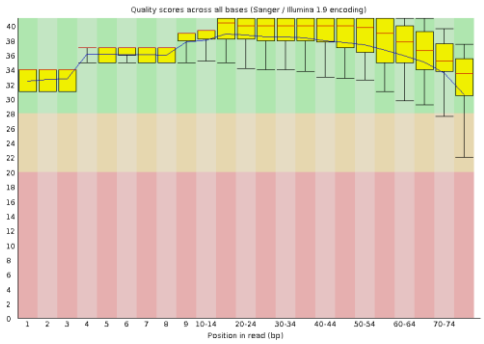

Per base sequence quality_R1

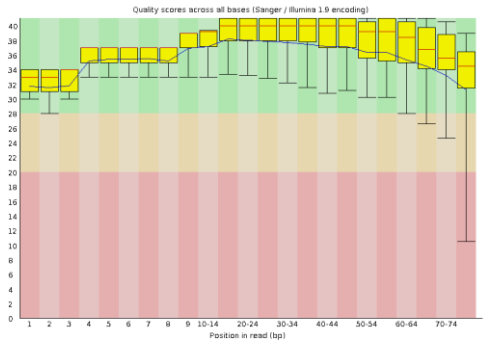

Per base sequence quality_R2

F. SNU5

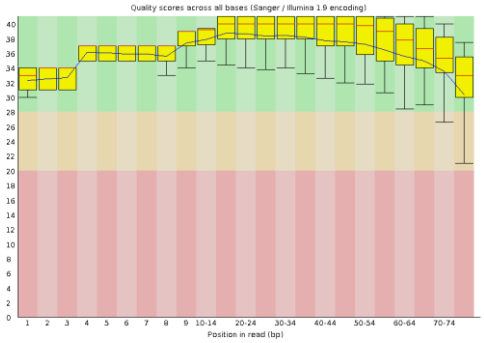

Per base sequence quality_R1

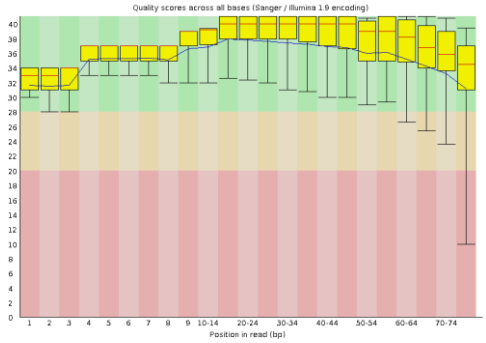

Per base sequence quality_R2

Appendix Fig.2

G. YCC1

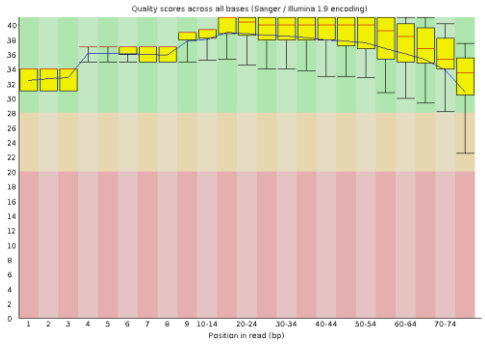

Per base sequence quality_R1

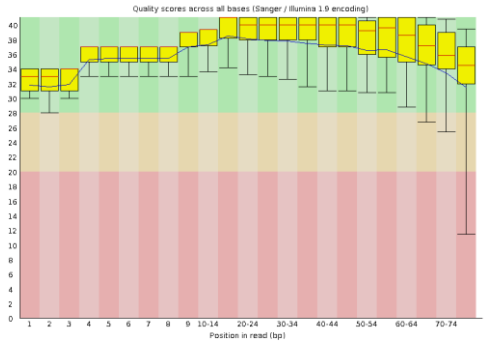

Per base sequence quality_R2

H. YCC11

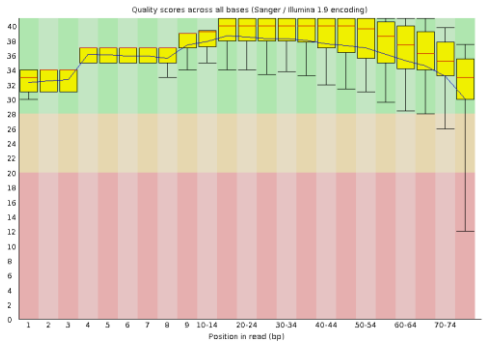

Per base sequence quality_R1

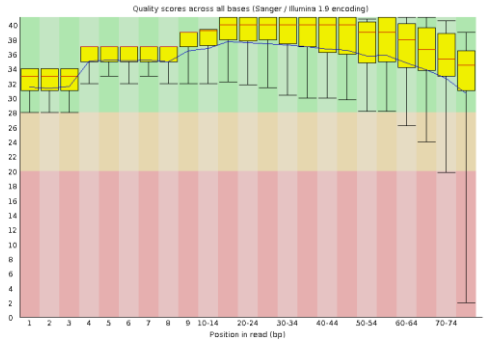

Per base sequence quality_R2

Appendix Figure 2. Per base sequence quality of 8 GC cell lines (RNA-sequencing). The y-axis on the graph shows the quality scores. The higher the score the better the base call. The background of the graph divides the y axis into very good quality calls (green), calls of reasonable quality (orange), and calls of poor quality (red).The central red line is the median value. The yellow box represents the inter-quartile range (25-75%). The upper and lower whiskers represent the 10% and 90% points. The blue line represents the mean quality.

Appendix Table 1. Total sequences and aligned reads obtained from RNA-sequencing.

Cell lines	Total reads	Aligned reads
HS746T	57528536	54000777
Kato3	79409139	63896235
MKN28	103674181	74139979
NUGC3	61965021	43856415
NUGC4	82924921	59710746
SNU5	89097623	66913289
YCC1	83076193	40317541
YCC11	81886491	73318968